Design of Electrical Energy Network Based on Power Packetization

Shinya Nawata

2017

Abstract

Electric power has been considered as a continuous flow based on circuit theory. Recently, however, wide-bandgap power semiconductor devices, which provide the potential for handling high-power and high-frequency electricity, enable us to digitize power through power packetization. Power packets are directly and physically tagged as their voltage waveforms. The power packet dispatching system consists of network lines and routers, which store and forward power packets according to the tags' information. Here, power packet is defined as a unit of electric power transferred by a power pulse with an information tag.

This dissertation addresses to design electrical energy networks based on power packetization. Our goal is to design the network, which meets intermittent and spatially distributed supply and demand, by processing power according to the number of power packets in a digitized manner. To this end, we establish packet-centric framework, in which power is digitized and quantized. In Shannon's information theory, messages are represented by symbol sequences in a digitized manner. Referring to this formulation, we define symbol in power packetization as a minimum unit of power transferred by a tagged pulse. Then, power packetization is a simultaneous representation of messages and energy with symbol sequences.

Prior to discussing power packetization in networks, we clarify router's operation in the physical layer, presenting two studies. The first study discusses power packet transfer under asynchronous conditions. Synchronization is the key to detect the tag's information at the receiving router. The second study investigates power dispatching at router with density modulation of power packets in transmission.

Then, we consider the packet-centric framework, introducing symbol as a minimum unit of electric power. Here, energy of each symbol is uniquely determined as a positive

real number. Energy representation for a finite duration is considered with a set of symbol sequences, which represent energy as the total amount of energy of symbols. First, we clarify the condition for existence of energy representation. Then, we mathematically prove an asymptotic property. This property shows that, as the represented energy becomes infinite, the frequency of occurrences of a symbol in almost all sequences can be approximated by the probability determined from the energy of symbols.

Next, we consider packetized power in networks for a finite duration. Here, symbols and their energies are given to the network. A network structure is defined using a graph, whose nodes represent routers, sources, and destinations. As a representation of packetized power, we introduce symbol propagation matrix (SPM), in which symbols are transferred at links during unit times. Packetized power is described as network flow in a spatio-temporal structure. First, we consider the problem of selecting a SPM in terms of transferability, that is, the possibility to represent given energies at sources and destinations for the finite duration. We formulate the problem of selecting packetized power as M-convex submodular flow problem, which is known as generalization of the minimum cost flow problem and it is solvable. Then, we consider the discrete dynamics of energy transfer by designing the router's operation for matching supply and demand. The network is designed to separately and individually manage the up-stream dispatching of required power from destinations and the down-stream dispatching of supplied power from sources at the symbol level in a decentralized manner.

At last, we take a glance at the corresponding continuous dynamics for future work. Here, power packet transfer is considered as wave propagation by averaging in time.

Acknowledgments

First of all, I would like to express my deepest gratitude to Professor Takashi Hikihara of Kyoto University, for his patient guidance and constant encouragement as my supervisor throughout this work. I also would like to express my sincere gratitude to Professor Shinji Doi of Kyoto University, and Professor Ken Umeno of Kyoto University, for providing me with valuable suggestions and taking part in my dissertation committee. I would also like to appreciate Associate Professor Tomohiko Mitani of Kyoto University, for his helpful suggestions and serving on my pre-defense committee.

I wish to express my sincere gratitude to Associate Professor Atsuto Maki of Kungliga Tekniska Högskolan (KTH), for his kindness and valuable suggestions, particularly in the mathematical formulation of symbol propagation matrix in Chapter 4. I also wish to express my sincere gratitude to Professor Mikio Hasegawa of Tokyo University of Science, for his kindness and valuable suggestions on communication networks. I wish to express my gratitude to Assistant Professor Ryo Takahashi of Kyoto University, for his supports and suggestions.

I would like to appreciate Professor Darryl Holm of Imperial College London, Professor Andrew Davison of Imperial College London, Professor Nobuo Satoh of Chiba Institute of Technology, Associate Professor Yoshihiko Susuki of Osaka Prefecture University, Ms. Keiko Saitoh, and Assistant Professor Takafumi Okuda of Kyoto University for their discussions and supports. I also would like to appreciate all the current and former members of the Hikihara laboratory, the Robotics, Perception and Learning laboratory of KTH, and the Hasegawa laboratory of Tokyo University of Science.

I also thank Dr. Yanzi Zhou, Mr. Takuya Kajiyama, Mr. Naoaki Fujii, Mr. Masateru Tanimoto, and Mr. Masayuki Matsushima for collaboration in this research. I'm especially grateful for the official assistance given by Ms. Yoshiko Deguchi.

Parts of this dissertation were financially supported by Kyoto University, SIP project funded by NEDO, and Super Cluster Program (Kyoto) funded by JST.

I thank everyone who helped and supported me while completing this dissertation.

Notation

$\mathbb{R}$	set of real numbers
$\mathbb{R}_{>0}$	set of positive real numbers
$\mathbb{Z}$	set of integer numbers
$\mathbb{Z}_{\geq 0}$	set of non-negative integers
$\mathbb{Z}_{\geq 1}$	set of positive integers
$\emptyset$	empty set
2^X	set of all subsets of set X, i.e. power set of X
$\lvert X \rvert$	number of elements of a finite set X
$[x, y)$	interval defined as $\{z \in \mathbb{R} \mid z \geq x \wedge z < y\}$
$(x, y]$	interval defined as $\{z \in \mathbb{R} \mid z > x \wedge z \leq y\}$
$[x, y]$	interval defined as $\{z \in \mathbb{R} \mid z \geq x \wedge z \leq y\}$
$\lfloor x \rfloor$	largest integer not exceeding a real number x
$\lceil x \rceil$	smallest integer not less than a real number x
$\langle x \rangle$	fractional part of a real number x, i.e. $\langle x \rangle = x - \lfloor x \rfloor$
$\operatorname{dom} f$	effective domain of function f
Σ, Σ_{T}	set of symbols (symbol is a minimum unit of electric power)
$\mathcal{E} : \Sigma \to \mathbb{R}_{>0}$	energy of symbols Σ
$G = (V, A)$	directed graph with node set V and link set A
$\partial^+ a$	initial node of link a
$\partial^- a$	terminal node of link a
$\delta^+ v$	set of links leaving node v
$\delta^- v$	set of links entering node v
$\partial \xi$	boundary of flow ξ

Contents

Chapter 1

Introduction

Shannon shows in his seminal work [1] that "all technical communications are essentially digital; more precisely, that all technical communications are equivalent to the generation, transmission, and reception, of random binary digits" [2]. Sampling theorem explains that a continuous band-limited signal can be represented as a discrete-time signal without loss of generality [1, 3]. Communication networks have been developed in a digitized manner by utilizing packet switching, which breaks messages into smaller pieces named "packets", for dynamic assignment of network resources [4]. Until now, design frameworks of these networks have been presented with protocol hierarchies from the physical layer to the application layer [5].

Conversely, electric power has been considered as a continuous flow based on circuit theory, in which power flow is governed by Kirchhoff laws and Tellegen's theorem [6]. The circuit theory is generalized as network thermodynamics [7]. Power is expressed as a product of a variable and its covariable, which are voltage difference and current in electrical network, force and velocity in mechanics, and so on. Various nonlinear complex systems can be represented as circuits in the system topology with energy dissipation and energy storage. Even when different types of energy are converted from one type to another, all energy flows can be handled on an equal footing with bond graphs [7]. Here, energy flow is handled in a continuous manner under the conservation of energy.

Although information transfer is digital while electric energy has been transferred as continuous flow, there exists a close relationship between energy and information. As Shannon discussed channel capacity with a power limitation [1], information is trans-

ferred with energy in practical systems. Information theory can include source coding with cost functions, in which the cost of symbols, such as energy, is minimized [1, 8]. Simultaneous transfer of information and energy has been also performed in power line communication, radio frequency identification, radio-frequency-based energy harvesting, and so on, and tradeoffs between transferred energy and information rate are theoretically derived in several settings [9–11]. From a viewpoint of physics, the notion of information attaches to the notion of entropy in statistical mechanics and has brought to our attention the second law of thermodynamics [1, 12, 13].

Recently, wide-bandgap power semiconductor devices, which provide the potential for handling high-power and high-frequency electricity, enable us to digitize power through power packetization [14, 15]. Introducing a power packet as a unit of electric power transferred by a power pulse with an information tag, the dissertation addresses the design of electrical energy networks based on power packetization.

1.1 Electrical Energy Networks and Power Management

Electrical energy network is an electrical circuit connecting sources and loads, which is designed to transfer energy between the sources and the loads and to match supply and demand. Electric power supply system has been widely spread among various applications, such as vehicles [16, 17], aircrafts [18, 19], and robots [20], besides conventional power systems [21]. In addition, more and more electrical energy generators and storage have been introduced into these systems. For example, vehicles have been equipped with battery, supercapacitor, photovoltaic cell, regenerative breaking, and so on [16]. Utilization of these multiple energy sources leads to optimal energy operation while satisfying the vehicle's performances [17]. In an aircraft, the distributed power system, which brings the flexibility to generate and distribute power efficiently near to where it is being consumed, is expected to save significant weight and volume and reduce the power rating of the main conductors [18, 19]. In legged robots, since legged locomotion involves alternating positive and negative work, passive dynamics and elastic elements provide "mechanical energy capacitors" that can store kinetic or elastic potential energy

and return the same without itself consuming a significant amount of energy [20]. The introduction of these potential energy sources highlights the necessity to manage the intermittent and spatially distributed supply and demand in electrical energy networks.

On the other hand, information and communication technology is coming into the spotlight for managing power systems with control and monitoring [22]. For saving energy in each household, home energy management systems have been developed [23, 24]. The proposed HEMS calls attention to the possibility of saving energy by visualizing power usage in real time, and it also controls air conditioning and lighting automatically to suppress energy consumption based on information from sensors in rooms. Recently, on-demand home energy networking has been proposed with a hierarchical protocol, which composed of the request/response layer, the path control layer, and the physical layer [25, 26]. In the request/response layer, each powered device decides how much power it requests, and each power source decides how much it offers in response [26]. The rules for managing energy can be automatically generated based on the priorities of appliances [27]. These studies show the possibility of adjusting the best match between supply and demand by integrating information and communication technologies into electrical energy networks.

The concept of power packet was proposed in 1990s to manage complicated power flows in power systems caused by various power transactions after deregulation [28]. In the proposal, electric energy routers, which include energy storage devices, were installed into the electrical energy networks. The router manipulates its own storage device according to the flow control data transferred with the power packet so as to compensate for the difference between the generation schedule and the demand schedule. Referring to this work, power packet transactions was proposed for an electric power distribution system [29]. He *et al.* proposed an electric power architecture, rooted in lessons learned from the Internet and microgrids, to produce a grid network designed for distributed renewable energy, prevalent energy storage, and stable autonomous systems [30]. "Energy packet networks" were also proposed to provide energy on demand to Cloud Computing servers [31]. There is a proposal for controllable-delivery power grid, in which electrical power is delivered through discrete power levels directly to customers [32]. In the physical layer, a universal power router is designed and evaluated for residential applications [33]. On the other hand, in most of these proposals, electric energy and information

are separately transferred or the physical design is not mentioned. It has been difficult to realize the practical hardware to deal with electric power in the same way as information, because energy has been transferred with high-power and low-frequency electricity while information has been transferred with low-power and high-frequency electricity [14, 15]. For ensuring consistency between the physical layer and the logical layer, the synchrony between energy and information is crucial for managing power.

In the physical layer, wide-bandgap power semiconductors, such as Silicon Carbide (SiC) and Gallium Nitride (GaN), have shown material properties enabling power device operation at potentially higher temperatures, voltages, and switching speeds than the current Si technology [34, 35]. High-speed gate drive circuits have been developed to achieve high frequency switching over 1 MHz [36, 37]. This work enables us to handle high-power and high-frequency electricity and physically develop AC power routing systems and power packet dispatching systems [14, 15]. The AC power routing has been realized by circuit exchanges and is applicable to both single-phase systems and three-phase systems [14, 15, 38–40]. To keep the consistency between the physical and the logical layer, information for managing power flow is superimposed on power waveforms by utilizing power line communication (PLC) in these propositions. In the next section, we introduce the power packet dispatching systems in which power is transferred by power pulses tagged with their voltage waveform.

1.2 Power Packet Dispatching Systems

In this section, we introduce power packet dispatching systems. In the system, power packets are directly and physically tagged with their voltage waveforms [14, 15]. Thus, energy and information are integrated at an individual packet level. A power packet consists of a header, a payload, and a footer as shown in Fig. 1.1. The waveform of a packet is not necessarily rectangular and can be designed suitable for power line channels [41]. The payload brings power, while the header and the footer carry the information as the packet's tag. The information tag identifies the different kinds of power due to different sources, destinations, voltages, control command, and so on.

Power packet is processed by routers with multiple input ports, multiple output ports, and multiple energy storage. The router has been empirically designed as schematically

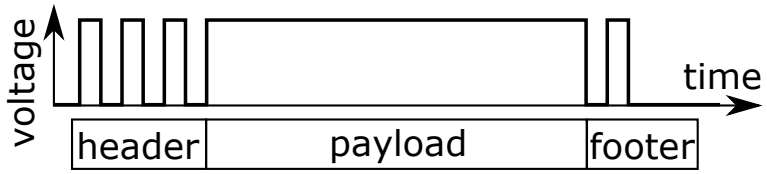

Figure 1.1: The concept of power packet.

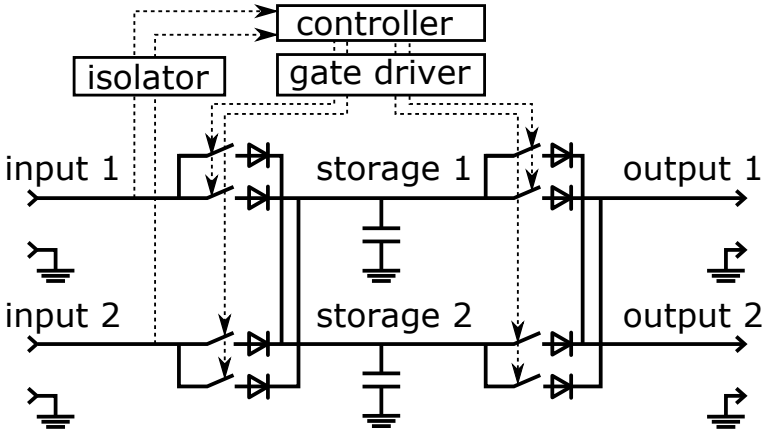

Figure 1.2: Schematic configuration of a router with two inputs, two outputs, and two storage units [42].

shown in Fig. 1.2 [42]. Energy storage consists of capacitors implemented between input and output ports. To detect the information provided by the tags, the voltage waveform of every packet is sampled with the router's internal clock. Here, the packet itself can contain the preamble for recognizing the sent information, fixing the clock of the receiving router with phase-locked loop [43, 44]. According to the detected information, the receiving router stores the energy of the packet to its internal storage and forwards the packet attaching the tag to the packet again. The forwarding of power packets has been experimentally achieved in several network topologies [42, 45].

Power demand can be satisfied through density modulation of power packets. Power regulation algorithm is proposed to realize the desired dynamical behavior of the objective loads by extending the optimal dynamic quantizer, which is investigated in the context of control with a discrete-valued signal [46]. The trajectory control of the manipulator has been numerically and experimentally verified in the power packet dispatching system [47]. This work demonstrates that power can be supplied to loads in a discrete

form.

1.3 Network Design Based on Power Packetization

In sharing energy between sources and destinations in an electrical energy network, there exist up-stream dispatching of required power from destinations to sources and down-stream dispatching of supplied power from sources to destinations[1] [48]. The required power from destinations should be met to satisfy the desired behavior of the system, while the amount of supplied power from sources is restricted at each source. If electrical energy networks can be designed to connect numerous sources and loads and allow them to generate and consume energy as needed, it will lead to saving of a significant amount of energy by utilizing potential energy sources (e.g. regenerative energy from all motors in a robot) whose energy would otherwise be dissipated as heat.

On the other hand, power supply systems have usually been assumed to have a sufficiently high inertia. In these systems, multiple sources have been connected in parallel and stabilized so as to utilize them as a single bus. However, with physically coupled multiple sources and multiple loads, it seems to be difficult to realize the desired supply and desired demand simultaneously. Thus, the key is to directly and physically process the power in the network through power packetization.

Now, the design of electric energy networks is considered based on physically developed power packet dispatching systems. Our goal is to design the network, which matches the intermittent and spatially distributed supply and demand, by processing power according to the number of power packets in a digitized manner. With power packetization, the up-stream dispatching and the down-stream dispatching can be separately and individually managed in a single network. A schematic of power packet dispatching network is shown in Fig. 1.3. The system consists of routers and network lines. When we send the packets in the network using time-division multiplexing (TDM), it becomes possible to distinguish the power at each line by using the information tag as an index. In the router, the different kinds of power are identified by multiple storage units installed in the router. In the network, power is given by the density of power

[1]The up-stream dispatching and down-stream dispatching were discussed in conventional power systems to trace the flow of electricity to sources and to destinations respectively [48].

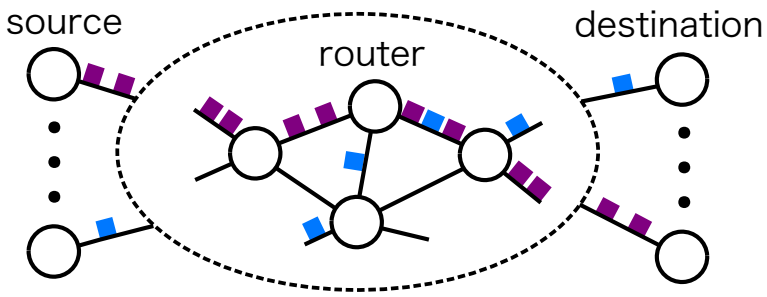

Figure 1.3: A schematic of power packet dispatching network.

packets. Here, power is digitized and quantized.

The main part of this dissertation presents and investigates packet-centric framework of energy transfer for network design. Here, power packet is defined as a unit of electric power transferred by a power pulse with an information tag. In Shannon's information theory, messages are represented by symbol sequences in a digitized manner. Referring to this formulation, we define symbol in power packetization as a minimum unit of power transferred by a tagged pulse. Then, power packetization is a simultaneous representation of messages and energy with symbol sequences. Power packetization may change power distribution completely different from the conventional.

1.4 Outline

The dissertation addresses the design of electrical energy network based on power packetization. The structure of the dissertation is shown in Fig. 1.4. In Chapter 2, the router's operation in the physical layer is clarified through complementing studies mentioned in Sect. 1.2. Next, in Chapters 3, 4, and 5, the packet-centric framework is considered in networks with defining symbol as a minimum unit of power: In Chapter 3, energy representation with symbols is investigated; In Chapters 4 and 5, transmission of symbols in networks is considered. Finally, we take a glance at the corresponding continuous dynamics in Chapter 5. The contents in each chapter are summarized below:

- **Chapter 2: Router's Operation in Physical Layer**

  Two studies on the router's operations in the physical layer are presented to com-

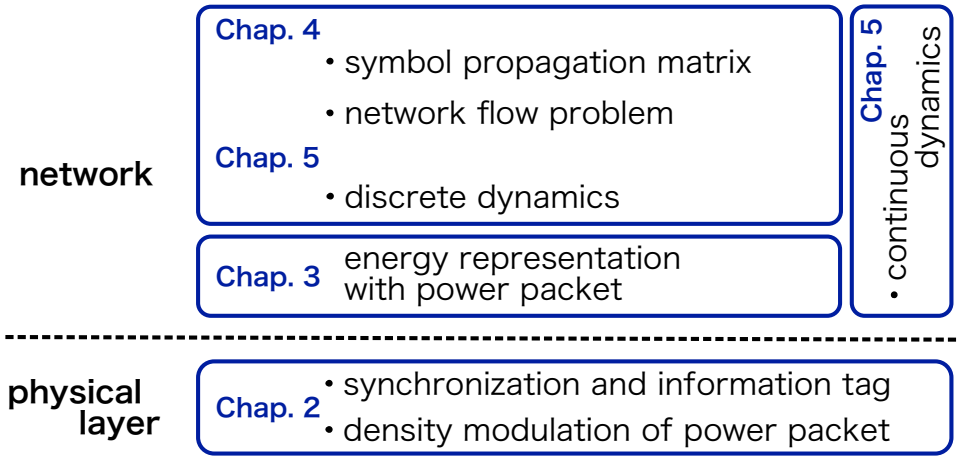

Figure 1.4: The structure of the dissertation. Chapter 2 covers the physical layer. Chapters 3, 4, and 5 mostly consider the packet-centric framework in networks, defining symbol as a minimum unit of power. Finally, we take a glance at the corresponding continuous dynamics in Chapter 5.

plement studies on power packet dispatching systems mentioned in Sect. 1.2. The first study investigates the reception of information tags at the receiving router under asynchronous conditions. By analyzing the asynchronous sampling at the receiving router, we describe the effect of detection errors on the density of power packets. The second study investigates the up-stream dispatching of power at a router with the density modulation of power packets in transmission. It is analyzed by the averaging method and is numerically verified. Through this chapter, the router's operations are clarified in the physical layer.

- **Chapter 3: Energy Representation with Power Packet**

  This chapter introduces symbol as a minimum unit of power and theoretically investigates energy representation with symbols. Energy of each symbol is uniquely determined as a positive real number. Energy representation for a finite duration is formulated as a set of symbol sequences, which represent energy as the total amount of energy of symbols. First, we mathematically clarify the condition for existence of energy representation. This shows the limit on accuracy with which all sufficiently large energies can be represented. Then, we prove an asymptotic property which shows that, as the represented energy becomes infinite, the fre-

quency of occurrences of a symbol in almost all sequences can be approximated by the probability determined from the energy of symbols. Finally, this asymptotic property is numerically verified in the representation of finite energy.

- **Chapter 4: Symbol Propagation in Networks**

  This chapter considers packetized power in networks for a finite duration. Here, symbols and their energies are given to the network. A network structure is defined using a graph, whose nodes represent routers, sources, and destinations. First, we introduce symbol propagation matrix (SPM), in which symbols are transferred at links during unit times. Packetized power is described as network flow in a spatio-temporal structure. Then, we consider the problem of selecting a SPM in terms of transferability, that is, the possibility to represent given energies at sources and destinations for the finite duration. To select packetized power as a network flow problem, we weight the supplied energy from the sources and the supplied energy to the destinations (V1), transferred energy at each link during each unit time (V2), and change of stored energy in each router (V3). The problem is formulated as M-convex submodular flow problem which is known as generalization of the minimum cost flow problem and it is solvable. At last, through examples, we verify that this formulation provides reasonable packetized power.

- **Chapter 5: Dynamics of Energy Transfer**

  This chapter considers the dynamics of energy transfer with power packets, in networks, based on the conservation of energy. In the formulation of symbol propagation matrix introduced in Chapter 4, we mainly consider the discrete dynamics of energy transfer by designing the operation of nodes. Unlike Chapter 4 which selects packetized power by globally optimizing the power flow, here, transferred symbols are determined by exchanging information between adjacent nodes in a decentralized manner. The exchanged information is the up-stream requests to get symbols from adjacent nodes and down-stream requests to give symbols to adjacent nodes. The up-stream dispatching of required power and the down-stream dispatching of supplied power are simultaneously managed in a single network at the symbol level. At the router, stored energy is kept within a given capacity. It

is numerically verified that supply and demand can be met in the designed network. At last, we take a glance at corresponding continuous dynamics for future work. Here, power packet transfer is considered as wave propagation by averaging in time.

- **Chapter 6: Conclusion and Future Work**

  The results are summarized and future work is discussed.

Chapter 2

Router's Operation in Physical Layer

In this chapter, two studies on router's operations in the physical layer are presented to complement the studies on power packet dispatching systems mentioned in Sect. 1.2. The first one investigates the reception of information tags at the receiving router under asynchronous conditions. By analyzing the asynchronous sampling at the receiving router, we describe the effect of detection errors on the density of power packets. The other one investigates the up-stream dispatching of the required power from loads to sources with the density modulation of power packets in transmission. It is analyzed by averaging method and is numerically verified.

2.1 Power Packet Transfer under Asynchronous Conditions

In this section, the operation of the receiving router is investigated under the condition that there is no synchronization between packets and the receiving router, so that the received tags are asynchronously sampled. In communication systems, asynchronous sampling introduces insertions and deletions of symbols, i.e. synchronization errors, for the recipient [49,50]. Synchronization errors also appear in detecting the tags of packets. In packetized power, however, it is impossible to drop or copy packets to deal with the

errors as in information transfer, because energy, which is the payload of a packet, is the conserved physical quantity. In the following, we first explain the operation of a receiving router mentioned in Sect. 1.2 in detail. Then, asynchronous sampling is analyzed at the receiving router. Finally, we discuss the effect of synchronization errors on the density of power packets.

2.1.1 Power Packet and Receiving Router

Power packet is a unit of power tagged with its voltage waveform. The information tag precedes the power pulse and identifies kinds of power due to different sources, destinations, voltages, control command and so on. At each router, power packets are processed according to the information provided by the tags. The voltage tag is sampled with a router's internal clock and the tag is received as a symbol sequence[1]. Here, the packet itself can contain the preamble for recognizing the tag's information by fixing the clock of receiving router with phase-locked loop [43, 44]. According to the received information, the router stores the energy of the packet to its internal storage and forwards the packet attaching the tag to the packet again[2].

If the received tag is asynchronously sampled, some symbols in the tag can be duplicated or deleted, that is, synchronization errors occur. Then, the packet is processed as if the packet had a different tag and forwarded with the tag different from the original one. In other words, the packet is exchanged for a different one at the receiving router.

2.1.2 Analysis of Asynchronous Sampling

Here, we analyze the asynchronous sampling at the receiving router. In the following, for a real number $x \in \mathbb{R}$, $\lfloor x \rfloor$ denotes the largest integer not greater than x, $\lceil x \rceil$ denotes the smallest integer not less than x, and $\langle x \rangle$ denotes the fractional part of x, i.e. $x - \lfloor x \rfloor$.

First, we describe the system model. The receiver samples the voltage of the received packets with fixed sampling period $T_\mathrm{c} \in \mathbb{R}_{>0}$ at $t \in T_\mathrm{c}\mathbb{Z} := \{T_\mathrm{c} j \mid j \in \mathbb{Z}\}$. Symbols in

[1] To detect a tag, the receiving router needs to know a symbol from which each tag begins. However, unlike the word synchronization problem in communication systems [49], power pulses are always inserted between successive tags and can be used to find the beginning of the tags in power packetization.

[2] In addition, there is a possibility that the router does not receive the packet by opening the circuit of the input port. In this case, energy of the packet remains in the sending router.

each tag are set to have the same duration $T_\mathrm{b} \in \mathbb{R}_{>0}$. The tag i is received from $\tau_i \in \mathbb{R}$, where $i \in \mathbb{Z}$ is indexed to all tags, and hence to all packets, in time order. The k-th symbol of the tag i is detected if the tag is sampled during a time $[T_\mathrm{b}k+\tau_i, T_\mathrm{b}(k+1)+\tau_i)$ ($k \in \{0, 1, \cdots, K_i - 1\}$). Focusing on the periodic sampling $T_\mathrm{c}\mathbb{Z}$, we define

$$\langle \tau \rangle_{\overline{\mathrm{c}}} := \langle -\tau / T_\mathrm{c} \rangle \quad (\tau \in \mathbb{R}). \tag{2.1}$$

For a timing $\tau \in \mathbb{R}$, $T_\mathrm{c}\langle \tau \rangle_{\overline{\mathrm{c}}}$ is equal to the time difference between the timing τ and the first sampling point after τ; more precisely, we have the following equation (see Appendix A.1):

$$T_\mathrm{c}\langle \tau \rangle_{\overline{\mathrm{c}}} = \min\{T_\mathrm{c}j - \tau \mid j \in \mathbb{Z} \wedge T_\mathrm{c}j \geq \tau\}. \tag{2.2}$$

In the following, we consider $\langle \tau_i \rangle_{\overline{\mathrm{c}}}$ as the phase of the packet i.

Then, we consider the detection of the tag i[3]. The received symbol sequence from the tag i is determined by the number of times the k-th symbol is sampled ($k \in \{0, \cdots, K_i - 1\}$), which is derived as follows (see Appendix A.2):

$$\begin{aligned} &|[T_\mathrm{b}k + \tau_i, T_\mathrm{b}(k+1) + \tau_i) \cap T_\mathrm{c}\mathbb{Z}| \\ &\quad = \begin{cases} \lfloor T_\mathrm{b}/T_\mathrm{c} \rfloor & \langle \langle \tau_i \rangle_{\overline{\mathrm{c}}} - k \langle T_\mathrm{b}/T_\mathrm{c} \rangle \rangle \geq \langle T_\mathrm{b}/T_\mathrm{c} \rangle , \\ \lfloor T_\mathrm{b}/T_\mathrm{c} \rfloor + 1 & \langle \langle \tau_i \rangle_{\overline{\mathrm{c}}} - k \langle T_\mathrm{b}/T_\mathrm{c} \rangle \rangle < \langle T_\mathrm{b}/T_\mathrm{c} \rangle . \end{cases} \end{aligned} \tag{2.3}$$

In the case of $\langle T_\mathrm{b}/T_\mathrm{c} \rangle = 0$, every symbol is sampled $\lfloor T_\mathrm{b}/T_\mathrm{c} \rfloor$ times, so that the received symbol sequence is determined by the fixed value $\lfloor T_\mathrm{b}/T_\mathrm{c} \rfloor$. In the case of $\langle T_\mathrm{b}/T_\mathrm{c} \rangle \neq 0$, each symbol is sampled $\lfloor T_\mathrm{b}/T_\mathrm{c} \rfloor$ times or $\lfloor T_\mathrm{b}/T_\mathrm{c} \rfloor + 1$ times depending on the phase of the packet i, i.e. $\langle \tau_i \rangle_{\overline{\mathrm{c}}}$, so that the received symbol sequence is determined by the set of symbols sampled $\lfloor T_\mathrm{b}/T_\mathrm{c} \rfloor$ times or equivalently by the set of symbols sampled $\lfloor T_\mathrm{b}/T_\mathrm{c} \rfloor + 1$ times. As derived in Appendix A.3, the former set is represented as

$$\{\iota_l(\langle \tau_i \rangle_{\overline{\mathrm{c}}}) \mid 0 \leq \iota_l(\langle \tau_i \rangle_{\overline{\mathrm{c}}}) < K_i \wedge l \in \{0, 1, \cdots\}\}, \tag{2.4}$$

[3]Note that the length of the received symbol sequence from a tag changes depending on the number of duplicated symbols and deleted symbols.

where

$$\iota_l(\phi) := \left\lceil \frac{1}{1-\langle T_\mathrm{b}/T_\mathrm{c}\rangle}(l+1-\phi) \right\rceil - 1 \quad (\phi \in [0,1), l \in \mathbb{Z}), \tag{2.5}$$

and the later set is represented as

$$\{\kappa_l(\langle\tau_i\rangle_{\overline{c}}) \mid 0 \leq \kappa_l(\langle\tau_i\rangle_{\overline{c}}) < K_i \wedge l \in \{0,1,\cdots\}\}, \tag{2.6}$$

where

$$\kappa_l(\phi) := \left\lfloor \frac{1}{\langle T_\mathrm{b}/T_\mathrm{c}\rangle}(l+\phi) \right\rfloor \quad (\phi \in [0,1), l \in \mathbb{Z}). \tag{2.7}$$

Obviously, we have $\iota_{-1}(\phi) < 0 \leq \iota_0(\phi)$ and $\iota_{l+1}(\phi) \geq \iota_l(\phi) + 1$, and $\kappa_{-1}(\phi) < 0 \leq \kappa_0(\phi)$ and $\kappa_{l+1}(\phi) \geq \kappa_l(\phi) + 1$. Both ι_l and κ_l designate a received symbol sequence as a function of the phase of the packet. In other words, every possible packet exchange corresponds to a subset of the space of phase variable $\phi \in [0,1)$.

Finally, we consider a sequence of packets, setting that the same packets are periodically transferred with period T_p, i.e. $\tau_{i+1} = \tau_i + T_\mathrm{p}$. In this case, the phase of packets is described as

$$\langle\tau_{i+1}\rangle_{\overline{c}} = \langle\langle\tau_i\rangle_{\overline{c}} + \langle T_\mathrm{p}\rangle_{\overline{c}}\rangle\,, \tag{2.8}$$

which represents the rotation of the circle [51]. Thus, the phase is periodically changed when T_p is rationally related with T_c, and the phase is uniformly distributed when T_p is irrationally related with T_c [51]. In both the cases, packets are exchanged with a constant rate by asynchronous sampling. On the other hand, the rate is determined depending on the initial phase $\langle\tau_0\rangle_{\overline{c}}$ in the former case, while the rate is determined independently of $\langle\tau_0\rangle_{\overline{c}}$ in the latter case.

2.1.3 Discussion with Example

In this section, we discuss power packet transfer with a simple example system. The rate of packet exchange is investigated both analytically and numerically. Here, the rate of packet exchange is the key to handle power with the density of power packets.

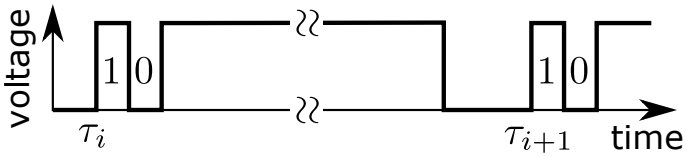

Figure 2.1: Voltage waveform of power packet. Each tag represents "10", i.e. packet α. The payload is accompanied with the current.

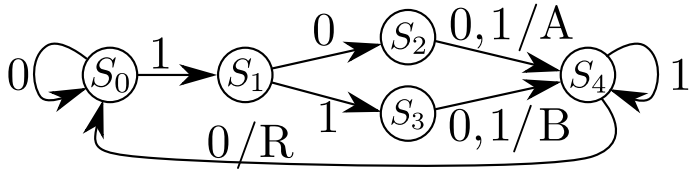

Figure 2.2: A state machine for router's operation driven by the received binary sequences. A and B are commands to process a packet as α and β respectively. R is a command to open the circuit of the input port.

Simple Example System

First, we provide a simple example of a power packet dispatching system referring to experimental settings in [14,15,42]. The system has two distinct tags, and hence has the two varieties of packets called packet α and packet β. Theses packets are generated from DC power supplies as shown in Fig. 2.1. Each tag represents a binary sequence with two bits whose head is "1", which represents a start signal. The second bit identifies the packet; "0" and "1" denote the packet α and β respectively. The power pulse has a rectangular voltage waveform, which is detected as "1" at the receiving router, and takes a much longer time than the tag. In order to reset the router, a zero-voltage interval is inserted between the power pulse and the successive tag.

Fig. 2.2 shows a state machine for router's operation. The state machine is driven by the received binary sequences. A and B are commands to process a packet as α and β respectively. R is a command to open the circuit of the input port. Thus, power is brought at the state S_4. In the following, we assume that the zero-voltage interval preceding each tag is sufficiently long, so that the state machine is reset to S_0 before each tag.

The packet α can be exchanged for the packet β by asynchronous sampling. For

example, if the first bit "1" is sampled twice and the second bit "0" is sampled once, the packet α is exchanged for the packet β. On the other hand, packet β is not exchanged for packet α by asynchronous sampling in this example system.

Packet Exchange and Phase

In the example system, we demonstrate that a packet is exchanged according to its phase with the following cases of the sampling period T_c and the symbol duration T_b: (C1) $1/2 \leq T_\mathrm{b}/T_\mathrm{c} < 1$, in which case $\iota_1(\phi) \geq 2$ holds for all $\phi \in [0, 1)$, and hence at most one symbol is deleted in each tag; (C2) $1 < T_\mathrm{b}/T_\mathrm{c} \leq 3/2$, in which case $\kappa_1(\phi) \geq 2$ holds for all $\phi \in [0, 1)$, and hence at most one symbol is sampled twice in each tag; (C3) $T_\mathrm{b} = T_\mathrm{c}$.

The packet i is received as packet α. Then, in the case of (C1), the head of the received symbol sequence after τ_i becomes (i) "0111" when $\iota_0(\langle \tau_i \rangle_{\bar{c}}) = 0$ holds, (ii) "1111" when $\iota_0(\langle \tau_i \rangle_{\bar{c}}) = 1$ holds, and (iii) "1011" when $\iota_0(\langle \tau_i \rangle_{\bar{c}}) \geq 2$ holds. According to the state machine in Fig. 2.2, the packet i becomes α in the case of (iii) and β in the case of (i) and (ii). Therefore, noting that $\iota_0^{-1}(\{2, 3, \cdots\}) = [0, 2\langle T_\mathrm{b}/T_\mathrm{c} \rangle - 1)$ and $\iota_0^{-1}(\{0, 1\}) = [2\langle T_\mathrm{b}/T_\mathrm{c} \rangle - 1, 1)$, we find that the packet i becomes

$$\begin{cases} \alpha & \langle \tau_i \rangle_{\bar{c}} \in [0, 2\langle T_\mathrm{b}/T_\mathrm{c} \rangle - 1), \\ \beta & \langle \tau_i \rangle_{\bar{c}} \in [2\langle T_\mathrm{b}/T_\mathrm{c} \rangle - 1, 1). \end{cases} \tag{2.9}$$

Eq. (2.9) shows that the packet i changes from α to β when $\langle \tau_i \rangle_{\bar{c}} \in [2\langle T_\mathrm{b}/T_\mathrm{c} \rangle - 1, 1)$ holds. Thus, if the phase is uniformly distributed, packet α is exchanged for packet β with the probability of $2(1 - \langle T_\mathrm{b}/T_\mathrm{c} \rangle)$.

Similarly, in the case of (C2), the head of a received symbol sequence after τ_i becomes (i) "1101" when $\kappa_0(\langle \tau_i \rangle_{\bar{c}}) = 0$ holds, (ii) "1001" when $\kappa_0(\langle \tau_i \rangle_{\bar{c}}) = 1$ holds, and (iii) "1011" when $\kappa_0(\langle \tau_i \rangle_{\bar{c}}) \geq 2$ holds. According to the state machine in Fig. 2.2, the packet i becomes α in the case of (ii) and (iii) and β in the case of (i). Therefore, noting that $\kappa_0^{-1}(\{1, 2, \cdots\}) = [\langle T_\mathrm{b}/T_\mathrm{c} \rangle, 1)$ and $\kappa_0^{-1}(\{0\}) = [0, \langle T_\mathrm{b}/T_\mathrm{c} \rangle)$, we find that the packet i becomes

$$\begin{cases} \alpha & \langle \tau_i \rangle_{\bar{c}} \in [\langle T_\mathrm{b}/T_\mathrm{c} \rangle, 1), \\ \beta & \langle \tau_i \rangle_{\bar{c}} \in [0, \langle T_\mathrm{b}/T_\mathrm{c} \rangle). \end{cases} \tag{2.10}$$

Eq. (2.10) shows that the packet i changes from α to β when $\langle \tau_i \rangle_{\bar{c}} \in [0, \langle T_\mathrm{b}/T_\mathrm{c} \rangle)$ holds. Thus, if the phase is uniformly distributed, packet α is exchanged for packet β with the probability of $\langle T_\mathrm{b}/T_\mathrm{c} \rangle$.

In the case of (C3), packets are not exchanged.

Rate of Packet Exchange in Periodic Transfer

Finally, we numerically investigate the rate of packet exchange in periodic transfer of packet α with period T_p. Here, the rate determines the density of packet α and packet β. The rate of packet β is evaluated as the proportion of packet β in the sequence of the packet 0 to the packet 99. We consider the case of (C1), i.e. $T_\mathrm{c}/2 \leq T_\mathrm{b} < T_\mathrm{c}$. The sending router sets the period as $T_\mathrm{p} = 100 T_\mathrm{b}$.

Then, with Eq. (2.9), the rate of packet β is calculated in various settings of the ratio $T_\mathrm{b}/T_\mathrm{c} = \langle T_\mathrm{b}/T_\mathrm{c} \rangle$ and the initial phase $\langle \tau_0 \rangle_{\bar{c}}$. In the simulation, the ratio $T_\mathrm{b}/T_\mathrm{c}$ is uniformly distributed from 1/2 to 1 and the initial phase $\langle \tau_0 \rangle_{\bar{c}}$ is uniformly distributed form 0 to 1. The results for 10,000 trials are plotted in Figs. 2.3 and 2.4. Figure 2.3 shows that, in almost all trials, the rate of packet β is given by the probability $2(1 - \langle T_\mathrm{b}/T_\mathrm{c} \rangle)$ induced from Eq. (2.9) by the phase with uniform distribution.

As shown in Fig. 2.4, the difference between the rate of packet β and the probability $2(1 - \langle T_\mathrm{b}/T_\mathrm{c} \rangle)$ becomes large when $\langle T_\mathrm{p} \rangle_{\bar{c}}$ is close to a value such as 0, 1/2, 1/3, and 2/3, which induces a periodic rotation with a short period. To explain this, we demonstrate that the difference becomes large when $\langle T_\mathrm{p} \rangle_{\bar{c}}$ is close to 1/2. If $\langle T_\mathrm{p} \rangle_{\bar{c}} = 1/2$, the sequence of exchanged packets becomes a repetition of $\alpha\alpha$, $\alpha\beta$, $\beta\alpha$, or $\beta\beta$ depending on the initial phase and the boundary point $2 \langle T_\mathrm{b}/T_\mathrm{c} \rangle - 1$ in Eq. (2.9), so that the rate of packet β is discretized to 0, 0.5[4], or 1. If $\langle T_\mathrm{p} \rangle_{\bar{c}}$ is close but not equal to 1/2, the rate of packet β takes a value between 0.5 and 1 in the case of $2 \langle T_\mathrm{b}/T_\mathrm{c} \rangle - 1 < 1/2$ and between 0 and 0.5 in the case of $2 \langle T_\mathrm{b}/T_\mathrm{c} \rangle - 1 > 1/2$ as an average. Thus, the difference becomes large when $\langle T_\mathrm{p} \rangle_{\bar{c}} \approx 1/2$ holds.

[4]If the rate of packet β is evaluated as the proportion in an odd-number of packets, the rate of packet β slightly changes from 0.5 depending on whether the sequence is a repetition of $\alpha\beta$ or $\beta\alpha$.

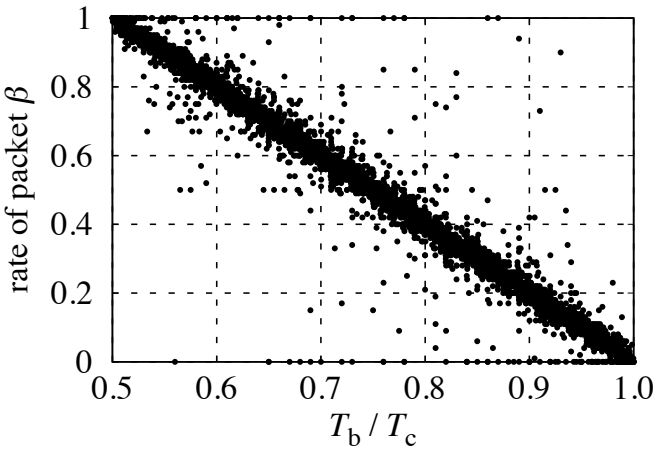

Figure 2.3: Relationship between the ratio T_b/T_c and the rate of packet β in 10,000 trials.

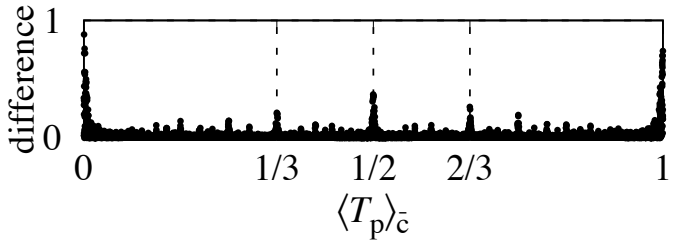

Figure 2.4: Relationship between $\langle T_p \rangle_{\bar{c}}$ and the difference between the rate of packet β and the probability $2(1 - \langle T_b/T_c \rangle)$ in 10,000 trials.

2.2 Up-stream Dispatching of Power at Router

The up-stream and down-stream dispatching of power can be dynamically realized by routing power according to the tags of packets as mentioned in Sect. 1.3. Here, power is given by the density of power packets. Up till now, the method for generating power packets is proposed to realize the desired dynamical behavior of the objective loads by extending the dynamic quantizer for a discrete-valued signal [46, 47]. The aim of down-stream dispatching is to transfer the amount of supplied power to multiple destinations. On the other hand, the aim of up-stream dispatching is to allocate the desired amount of required power to multiple sources.

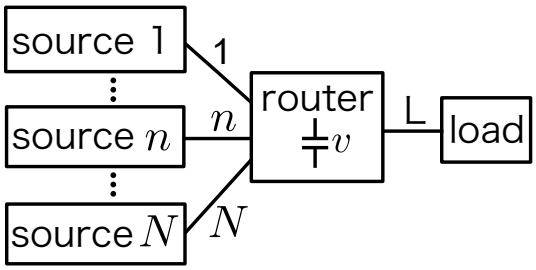

Figure 2.5: Schematic diagram of the system to investigate up-stream dispatching of power at router.

In this section, we focus on the up-stream dispatching of the required power from destinations to sources with density modulation of power packets in transmission. The up-stream dispatching is discussed at a router, i.e. a unit element of the network which dispatches power packets spatially and temporally based on information tags. Here, assuming the router developed physically as shown in Fig. 1.2, we show the relationship between transferred power into the router and the density of packets being sent. The relationship is analyzed by the averaging method [52], and then is numerically verified by simulating the dynamics of the storage in the router.

2.2.1 Problem Settings

Handling power as a continuous flow by averaging, we focus on up-stream dispatching of power packets stored at a same storage in each router. Power packets are physically coupled if they are stored at a same storage. Except that, there is no coupling. In the up-stream dispatching, at a router, the required power from the load is supplied by multiple sources and through multiple paths.

The up-stream dispatching is investigated in the setting shown in Fig. 2.5. In the system, power packets are asynchronously transferred to the same storage through multiple inputs. The input ports are indexed by a finite set $I = \{1, 2, \cdots, N\}$ and the output port is indexed by "L". The power packet transferred via the port $n \in I$ to the storage is called packet n and power packets transferred via the port L from the storage is called packet L.

For a finite duration, u_n denotes the average power transferred by packet n for

$n \in I \cup \{\mathrm{L}\}$. D_n denotes the density of packet n, i.e. the proportion of the payload of packet n. For a time series x, $\overline{x}$ denotes the average of x. For a packet n with non-empty payload, $\overline{\vec{x}}^{n}$ denotes the average of x over the payload of the packet n. Considering a stationary state, we investigate the problem of up-stream dispatching by the proportion of power transferred via each input port $n \in I$, i.e. u_n, in the total supplied power $\sum_{n \in I} u_n$.

Finally, the operation of the system is explained as follows. For $n \in I$, the source of the packet n is treated as a Thévenin equivalent circuit with the open-circuit voltage $e_n \geq 0$ and resistance r_n. The support of e_n corresponds to the payload of packet n. Noting that D_n is the proportion of the support of e_n, we have $\overline{e_n} = D_n \overline{\vec{e}_n}^{n}$. The storage capacitance in the router is set as C and the voltage across the storage is denoted by v. A diode is placed at each switch of the router to protect the reverse current as shown in Fig. 1.2. Thus, the reverse current is prevented at the time of $e_n < v$ for each $n \in I$. The router regenerates the packet L with the voltage v of the storage. With PFC circuits, the load is treated as a resistance R, which requires energy $u_{\mathrm{R}} = D_{\mathrm{L}} E_0^2 / R$, where E_0 is a base value according to which voltage of packets is determined[5].

2.2.2 Analysis by Averaging Method

Here, we analyze the relationship between transferred power into the router and the density of packets being sent. In the analysis, we assume a small ripple fluctuation of the voltage v. According to the averaging method [52], we approximate $v \approx \overline{v}$.

First, we consider a small ripple fluctuation of e_n for $n \in I$ and a small difference between $\{e_n\}_{n \in I}$ enough to have $e_n > v$ for all $n \in I$. The packet n transfers power approximated by

$$u_n \approx D_n \overline{v} \frac{\overline{\vec{e}_n}^{n} - \overline{v}}{r_n}. \tag{2.11}$$

In addition, the following equation is led by averaging the constraint equation of the Kirchhoff's current law at the router's storage in a stationary state:

$$\sum_{n \in I} D_n \frac{\overline{\vec{e}_n}^{n} - \overline{v}}{r_n} \approx D_{\mathrm{L}} \frac{\overline{v}}{R}, \tag{2.12}$$

[5]In the whole network, the base value of voltage can be different depending on the varieties of power identified by tags and multiple storage [42].

or

$$\overline{v} \approx \frac{\sum_{n\in I} \frac{D_n}{r_n} \bar{e}_n^{-n-}}{\sum_{n\in I} \frac{D_n}{r_n} + \frac{D_\mathrm{L}}{R}}. \tag{2.13}$$

Using Eqs. (2.11) and (2.13), we can derive the proportion of the transferred power by packet m for each $m \in I$:

$$\frac{u_m}{\sum_{n\in I} u_n} \approx \frac{\frac{D_m}{r_m} \bar{e}_m^{-m-} + \sum_{n\in I} \frac{R}{D_\mathrm{L}} \frac{D_m}{r_m} \frac{D_n}{r_n} (\bar{e}_m^{-m-} - \bar{e}_n^{-n-})}{\sum_{n\in I} \frac{D_n}{r_n} \bar{e}_n^{-n-}}. \tag{2.14}$$

If differences at source sides are negligible, the densities of power packets give the proportion of each transferred power. In other words, if $\bar{e}_n^{-n-} = \bar{e}_m^{-m-}$ and $r_n = r_m$ for all $n, m \in I$, the proportion can be written as

$$\frac{u_m}{\sum_{n\in I} u_n} \approx \frac{D_m}{\sum_{n\in I} D_n}. \tag{2.15}$$

This relationship shows the possibility of dynamical adjustment of the up-stream dispatching of power at routers in a network through density modulation of power packets.

Finally, we briefly discuss the case $e_n < v$ for some $n \in I$. During $e_n < v$, no power is transferred by packet n, because the diode at link n prevents reverse instantaneous power [44]. Therefore, the effect of the diodes should be considered by using power density at port n[6] instead of D_n which is the proportion of the payload of packet n.

2.2.3 Numerical Verification

The analytical results in Sect. 2.2.2 are obtained with a small ripple fluctuation of the voltage v across the capacitor. Here, the relationship between transferred powers and packet densities is numerically verified by simulating the dynamics of the voltage v. For simplicity, we consider the case in which the number of inputs are two, i.e. $I = \{1, 2\}$. As an example, the basis of the system is set by $E_0 = 12$ V and $u_\mathrm{R} = 1$ W. Each packet is periodically transmitted with the period from 0.5 ms to 5 ms[7]. The payload of packet

[6]Power density at port n is the proportion of support of instantaneous power at port n, which is included in the payload of packet n. The power density at port n takes a value between 0 to D_n.

[7]In this simulation, the time series of packet L is assumed to be independent from the time series of inputted packets. In our developed router, the packet L can be regenerated based on the time series of inputted packets by router's algorithms [42].

1 and packet 2 has rectangular waveform of voltage, i.e. $e_n = \bar{e}_n$ on the payload for $n \in \{1, 2\}$. We set $C = 1000$ μF and $r_1 = r_2 = 1$ Ω. The average powers u_1 and u_2 are defined in a duration of 100 ms.

In the following, the transferred powers $\{u_n\}_{n \in I}$ are calculated in various settings of densities $\{D_n\}_{n \in I}$ in the both cases of $\bar{e}_1 = \bar{e}_2$ and $\bar{e}_1 \neq \bar{e}_2$. The period and the phase of each packet are uniformly distributed. The density D_{L} is uniformly distributed from 0 to 1, and then the resistance of the load is decided as $R = D_{\mathrm{L}} \cdot E_0^2 / u_{\mathrm{R}} = D_{\mathrm{L}} \cdot 144$ Ω. The switches and diodes in the router are ideal in the simulation.

In Case of $\bar{e}_1 = \bar{e}_2$

First, we discuss the case of $\bar{e}_1 = \bar{e}_2 = E_0$. The relationship between transferred powers and the packet densities is examined in the simulation by uniformly distributing D_1 and D_2 from 0 to 1. The results for 10,000 trials are plotted in Figs. 2.6 and 2.7. Figure 2.6 shows that, almost regardless of the dynamics, the densities of power packets give the proportion of each transferred power as in Eq. (2.15).

Figure 2.7 shows that the total required power is satisfied with a sufficiently large sum of densities, but is not satisfied with a small sum of densities. Here, by using Eq. (2.13), the total transferred power can be approximated by averaging method as

$$u_1 + u_2 \approx \frac{\overline{v}^2}{R} = \left(\frac{D_1 + D_2}{D_1 + D_2 + 0.0069} \right)^2 \text{ W}. \tag{2.16}$$

This relationship, shown in Fig. 2.7 as a solid line, approximates the simulated results well. Thus, the sum of densities should be set sufficiently large in order to keep the voltage across the capacitor close to E_0, i.e. to keep energy stored in the router at a constant level. Then, sufficient power can be supplied to the next step.

In Case of $\bar{e}_1 \neq \bar{e}_2$

Next, we discuss the case of $\bar{e}_1 \neq \bar{e}_2$. As an example, we set $\bar{e}_1 = 12.5$ V and $\bar{e}_2 = 12$ V. The relationship between transferred powers and packet densities is numerically examined again by uniformly distributing D_1 and D_2 from 0 to 1. The simulation was repeated 10,000 times and the results were drawn in Figs. 2.8 and 2.9. In Fig. 2.9, to

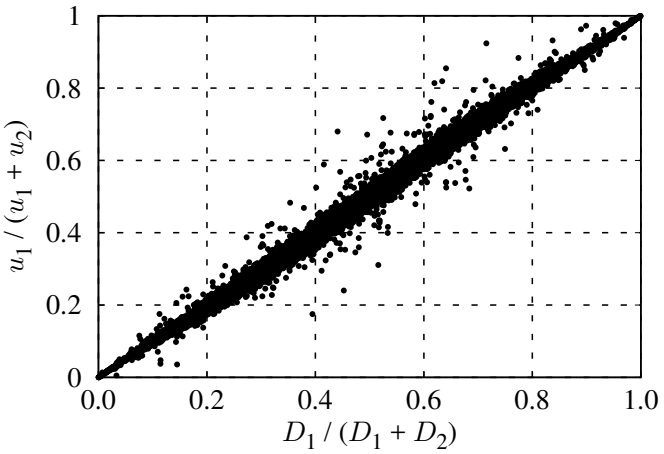

Figure 2.6: Relationship between proportion of transferred power by packet 1 and packet densities in the case of $\bar{e_1} = \bar{e_2} = E_0$.

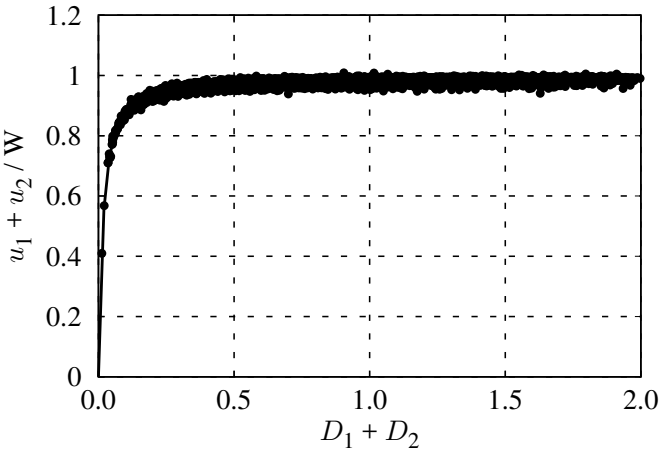

Figure 2.7: Relationship between total amount of transferred power and packet densities in the case of $\bar{e_1} = \bar{e_2} = E_0$. The solid line shows the relationship of Eq. (2.16).

ignore the effect of the voltage drop, only the results with the sufficiently large sum of densities are plotted.

Figure 2.8 shows no power is transferred by packet 2 if D_1 is not small. This means the power density at link 2 becomes 0 for all possible values of D_2 if packet 1 is frequently transmitted. Fig. 2.8, however, also shows the proportion of power transferred by packet 2 ranges from 0 to 1 if D_1 is sufficiently small. In addition, Fig. 2.9 shows, if the sum

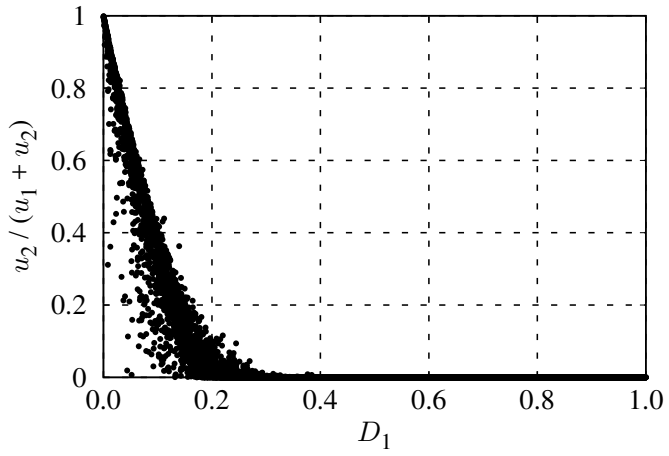

Figure 2.8: Relationship between proportion of transferred power by packet 2 and density of packet 1 in the case of $\bar{e}_1^{1-} > \bar{e}_2^{2-}$.

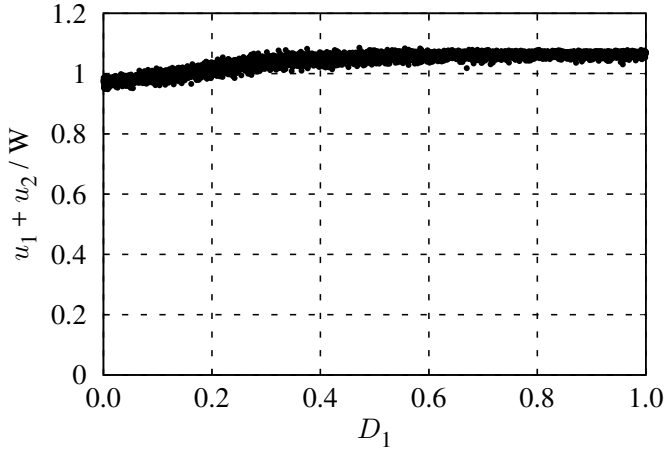

Figure 2.9: Relationship between total amount of transferred power and density of packet 1 in the case of $\bar{e}_1^{1-} > \bar{e}_2^{2-}$. Only the results which satisfy $D_1 + D_2 > 0.3$ are plotted to ignore the voltage drop across the capacitor.

of densities is sufficiently large, i.e. $D_1 + D_2 > 0.3$ in this case, the required power is met[8]. These results imply that, even if the differences between source voltages are not negligible, we can adjust the proportion of input power by setting the densities of packets with high voltage to be small.

[8]The transferred power slightly decreases when D_1 is small. This result implies that the supplied voltage varies from $\bar{e}_1^{1-}$ to $\bar{e}_2^{2-}$.

Using 10 different seeds for the random number generator, we obtained similar simulation results with Figs. 2.6, 2.7, 2.8, and 2.9, which ensure the consistency of the results.

2.3 Summary

2.3.1 Summary of Sect. 2.1

In Sect. 2.1, we investigated power packet transfer under asynchronous conditions by analyzing the detection of tags at the receiving router. If the received tag is asynchronously sampled, some symbols in the tag can be duplicated or deleted, that is, synchronization errors occur, so that the packet is exchanged for a different one at the receiving router. We analyze that, at the receiving router, symbol sequences are detected from the tags according to the phase of the packet arrival times, which is described by a rotation dynamics. In a simple example system, numerical simulation demonstrates that the rate of packet exchange is determined by a ratio of the symbol duration and the sampling period, except for the case of the periodic rotation with a small period. These discussions provide a possibility for handling synchronization errors in the density of power packets via the rotation dynamics.

2.3.2 Summary of Sect. 2.2

In Sect. 2.2, we demonstrated the possibility of realizing the up-stream dispatching of required power to the sources by density modulation of power packets. The up-stream dispatching is adjustable at a router with power packets transferred through multiple inputs to the storage. The averaging method reveals the relationship between density of power packets and average power transferred by the packets. By numerically simulating the dynamics of the router's storage, it is verified that the up-stream dispatching can be realized if energy stored in the router is kept at a constant level. Simulated results clearly show that even if the differences between voltages of packets are not negligible, the dispatching is realized by reducing the densities of packets with high voltage. These discussions provide a method for realizing desired supplies and demands by processing power with density modulation of power packets in electrical energy networks.

Chapter 3

Energy Representation with Power Packet

In the following chapters, we provide the packet-centric framework of energy transfer. Power packet is defined as a unit of electric power transferred by a pulse with an information tag. In Shannon's information theory, messages are represented by symbol sequences in a digitized manner [1]. Referring to this formulation, we define symbol in power packetization as a minimum unit of power transferred by a tagged pulse. Then, power packetization is a simultaneous representation of messages and energy with symbol sequences. Here, power is digitized and quantized.

In information theory, the representation of messages is treated as a coding problem, in which the goal is to minimize cost such as the length of codewords. In power packetization, however, it is important to represent the given energy as the total amount of energy of symbols. Thus, energy representation is a problem unique to power packetization and is important to generally understand power packetization.

This chapter considers energy representation with a set of symbol sequences, which represent energy as the total amount. For a finite duration, given energy can be represented with a variety of symbol sequences as the total amount. In this chapter, after introducing symbols and energy representation, we mathematically clarify the condition for existence of energy representation. Then, an asymptotic property of energy representation is theoretically proved. Finally, this asymptotic property is numerically confirmed in the representation of finite energy.

3.1 Symbols and Energy Representation

We introduce symbol as a minimum unit of power and formulate energy representation[1]. Here, a load is treated as resistive with PFC circuit, and power is discussed in real numbers without lack of generality. Then, information tags are set to specify the energy as a real number. Symbol is a tagged pulse with uniquely determined energy[2]. Power packetization is given as the simultaneous representation of messages and energy with a sequence of the symbols. We call the symbol sequence which represents the given energy as codeword. Energy representation is investigated with symbols whose energy is uniquely determined in real numbers.

Σ denotes a finite set of symbols, and W denotes a set of finite sequences of elements of Σ with length greater than or equal to one. W represents a set of codewords. $\mu_w(\Sigma')$ denotes the number of occurrences of elements of $\Sigma' \subset \Sigma$ in $w \in W$, where μ_w is a measure on Σ. $\mu_w(\Sigma)$ is the length of the codeword w. We introduce an equivalence relation in W defined as $w \sim w' \overset{\text{def}}{\Leftrightarrow} \mu_w = \mu_{w'}$. Codewords composed of the same number of symbols are considered equivalent with respect to this equivalence relation. The equivalence class of w is defined as $[w]:=\{w' \in W \mid \mu_{w'} = \mu_w\}$. The energy of symbols is uniquely determined as a map

$$\mathcal{E} : \Sigma \to \mathbb{R}_{>0}. \tag{3.1}$$

For convenience, we put $\mathcal{E}_* = \min_{\sigma\in\Sigma} \mathcal{E}(\sigma)$ and $\mathcal{E}^* = \max_{\sigma\in\Sigma} \mathcal{E}(\sigma)$. The energy of a codeword $w \in W$ is defined as $\sum_{\sigma\in\Sigma} \mathcal{E}(\sigma)\mu_w(\{\sigma\})$. Energy of a codeword is total energy of symbols of which the codeword is composed.

Energy representation is formulated as a set[3]

$$W_{\mathcal{E},(c-\Delta c,c]}:=\left\{ w \in W \;\middle|\; \sum_{\sigma\in\Sigma} \mathcal{E}(\sigma)\mu_w(\{\sigma\}) \in (c-\Delta c, c] \right\} \tag{3.2}$$

for $c \in \mathbb{R}_{>0}$ and $\Delta c \in \mathbb{R}_{>0}$, where the energy is represented in the interval $(c - \Delta c, c]$.

[1]Here, we ignore the details of the physical phenomenon. In the physical layer, the symbol can be transferred in a variety of ways during a unit time.

[2]In this setting, power pulses with same energy can be represented by a single symbol. The properties which symbols does not specify are treated by indexing the symbols. The index becomes important in terms of redundancy of the system.

[3]Note that energy is represented by symbol sequences with different length.

$W_{\mathcal{E},(7,8]}$

$\sigma_1\sigma_1\sigma_1\sigma_1$	$2+2+2+2 \in (7,8]$
$\sigma_1\sigma_1\sigma_2$	$2+2+4 \in (7,8]$
$\sigma_1\sigma_2\sigma_1$	$2+4+2 \in (7,8]$
$\sigma_2\sigma_1\sigma_1$	$4+2+2 \in (7,8]$
$\sigma_2\sigma_2$	$4+4 \in (7,8]$

Figure 3.1: Illustration of energy representation. Here, we set $\Sigma = \{\sigma_1, \sigma_2\}$, $\mathcal{E}(\sigma_1) = 2$, $\mathcal{E}(\sigma_2) = 4$, $c = 8$, and $\Delta c = 1$. Energy $(7, 8]$ is represented with five symbol sequences.

Fig. 3.1 illustrates energy representation. Here, because the energy of a codeword $w \in W$ is determined by μ_w, $w \in W_{\mathcal{E},(c-\Delta c,c]}$ leads to $[w] \subset W_{\mathcal{E},(c-\Delta c,c]}$. This implies that the equivalence classes $\{[w] \mid w \in W_{\mathcal{E},(c-\Delta c,c]}\}$ forms a partition of $W_{\mathcal{E},(c-\Delta c,c]}$. In the following sections, we mathematically clarify the existence condition and the asymptotic property of energy representation.

3.2 Existence Condition of Energy Representation

In this section, we investigate the condition for the existence of energy representation, i.e. $W_{\mathcal{E},(c-\Delta c,c]} \neq \emptyset$. By definition, $W_{\mathcal{E},(c-\Delta c,c]} \neq \emptyset$ implies that the intersection of the interval $(c - \Delta c, c]$ and the set of energies which can be represented with symbols Σ, i.e.

$$\left\{ \sum_{\sigma\in\Sigma} \mathcal{E}(\sigma)\mu_w(\{\sigma\}) \;\middle|\; w \in W \right\}, \tag{3.3}$$

is not empty. Fig. 3.2 shows the elements of Eq. (3.3) with two settings of Σ and $\mathcal{E}$. Here, we introduce the following definition for energy of symbols [53]:

Definition 3.1. *For $\mathcal{E} : \Sigma \to \mathbb{R}_{>0}$,*

1. *$(\mathcal{E}(\sigma))_{\sigma\in\Sigma}$ is said to be rationally related if there exists a real number Λ and positive integers $(q_\sigma)_{\sigma\in\Sigma}$ such that $\mathcal{E}(\sigma) = \Lambda q_\sigma$ holds for all $\sigma \in \Sigma$ and the greatest common divisor of $(q_\sigma)_{\sigma\in\Sigma}$ is 1. We call Λ as the greatest common divisor of $(\mathcal{E}(\sigma))_{\sigma\in\Sigma}$.*

2. *$(\mathcal{E}(\sigma))_{\sigma\in\Sigma}$ is said to be irrationally related if $(\mathcal{E}(\sigma))_{\sigma\in\Sigma}$ is not rationally related.*

(a) Representable energies with the setting $\Sigma = \{\sigma_1, \sigma_2\}$, $\mathcal{E}(\sigma_1) = 2$, and $\mathcal{E}(\sigma_2) = 4$. The greatest common divisor of $(\mathcal{E}(\sigma))_{\sigma\in\Sigma}$ is $\Lambda = 2$. All positive integer multiples of $\Lambda = 2$ are representable.

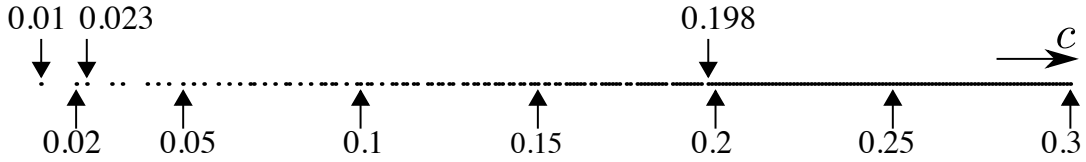

(b) Representable energies with the setting $\Sigma = \{\sigma_1, \sigma_2, \sigma_3\}$, $\mathcal{E}(\sigma_1) = 0.023$, $\mathcal{E}(\sigma_2) = 0.02$, and $\mathcal{E}(\sigma_2) = 0.01$. The greatest common divisor of $(\mathcal{E}(\sigma))_{\sigma\in\Sigma}$ is $\Lambda = 0.001$. All integer multiples of $\Lambda = 0.001$ greater than or equal to 0.198 are representable, while some integer multiples of $\Lambda = 0.001$ less than 0.198 are not representable.

Figure 3.2: Representable energies, i.e. the elements of Eq. (3.3).

We have a codeword with energy $n\mathcal{E}_*$ for all positive integers $n \in \mathbb{Z}_{\geq 1}$ because there exists a sequence of n symbols whose energy is $\mathcal{E}_*$. Thus, $\Delta c \geq \mathcal{E}_*$ implies that $W_{\mathcal{E},(c-\Delta c,c]}$ is not empty for all $c \geq \mathcal{E}_*$. In Fig. 3.2(a), we can easily find that, if $\Delta c \geq \mathcal{E}_* = 2$ holds, there is some representable energy in the interval $(c-\Delta c, c]$ for all $c \geq 2$. In this setting, the condition $\Delta c \geq \mathcal{E}_* = 2$ is also necessary to ensure that $W_{\mathcal{E},(c-\Delta c,c]}$ is not empty for all sufficiently large c because all representable energies are integer multiples of $\Lambda = 2$. In Fig. 3.2(b), however, to represent sufficiently large c, the condition $\Delta c \geq \mathcal{E}_* = 0.01$ is not necessary and $\Delta c \geq \Lambda = 0.001$ is sufficient because all integer multiples of $\Lambda = 0.001$ greater than or equal to 0.198 are representable. In the following, we prove the following theorem to show the infimum of Δc which guarantees that $W_{\mathcal{E},(c-\Delta c,c]}$ is not empty for all sufficiently large energy c.

Theorem 3.1. *The two conditions on $\mathcal{E}$ and Δc below are equivalent.*

I. There exists $c_0 \in \mathbb{R}_{>0}$ such that $W_{\mathcal{E},(c-\Delta c,c]}$ is not empty for all $c \geq c_0$.

II. If $(\mathcal{E}(\sigma))_{\sigma\in\Sigma}$ is rationally related and the greatest common divisor of $(\mathcal{E}(\sigma))_{\sigma\in\Sigma}$ is Λ, then $\Delta c \geq \Lambda$ holds. If $(\mathcal{E}(\sigma))_{\sigma\in\Sigma}$ is irrationally related, then $\Delta c > 0$ holds.

Proof that I implies II. We prove that, if II is false, then I is false. We assume II is false. First, we consider the case that $(\mathcal{E}(\sigma))_{\sigma\in\Sigma}$ is rationally related and the greatest common divisor of $(\mathcal{E}(\sigma))_{\sigma\in\Sigma}$ is Λ. Then, for every codeword $w \in W$, its energy $\sum_{\sigma\in\Sigma}\mathcal{E}(\sigma)\mu_w(\{\sigma\})$ is an integer multiple of Λ. In addition, $\Delta c < \Lambda$ follows from the assumption. Thus, we have that, for all $c_0 \in \mathbb{R}_{>0}$, there exists some real number $c \geq c_0$ such that $W_{\mathcal{E},(c-\Delta c,c]}$ is empty. Thus, I is false. Next, we consider the case that $(\mathcal{E}(\sigma))_{\sigma\in\Sigma}$ is irrationally related. In this case, $\Delta c \leq 0$ follows from the assumption. Therefore, $W_{\mathcal{E},(c-\Delta c,c]}$ is obviously empty for all $c \in \mathbb{R}_{>0}$. Thus, I is false. □

In the following, we prove that II implies I by establishing Lemma 3.1 below. Here, for a probability P on Σ, we introduce a notation

$$\overline{\mathcal{E}}(P) := \sum_{\sigma\in\Sigma}\mathcal{E}(\sigma)P(\{\sigma\}). \tag{3.4}$$

Lemma 3.1 not only implies the existence of some codeword in $W_{\mathcal{E},(c-\Delta c,c]}$ but also refers to the frequency of occurrences of symbols in the codewords. This lemma is used to prove the asymptotic property to be described in Theorem 3.2.

Lemma 3.1. *Let $\mathcal{E}$ and Δc satisfy the condition II in Theorem 3.1. Let a probability P on Σ satisfy $P(\{\sigma\}) \neq 0$ for all $\sigma \in \Sigma$. Then, there exist a positive real number c_0 and a positive integer N_0 depending on $\mathcal{E}$, $|\Sigma|$, Δc, and P such that, for all $c \geq c_0$, there exists $w \in W_{\mathcal{E},(c-\Delta c,c]}$ which satisfies*

$$\sum_{\sigma\in\Sigma}|\mu_w(\{\sigma\}) - \mu_w(\Sigma)P(\{\sigma\})| \leq N_0. \tag{3.5}$$

Proof of Lemma 3.1. First, we outline the proof. In the first step, we prove the following claim:

Claim 1: For every real number $c \geq (|\Sigma|+1)\mathcal{E}^*$, there exists some codeword $w_c \in W$ such that

$$\mu_{w_c}(\Sigma) = \left\lfloor \frac{c - |\Sigma|\,\mathcal{E}^*}{\overline{\mathcal{E}}(P)} \right\rfloor, \tag{3.6}$$

$$|\mu_{w_c}(\{\sigma\}) - \mu_{w_c}(\Sigma)P(\{\sigma\})| \leq 1 \ \text{ for } \sigma \in \Sigma, \tag{3.7}$$

and

$$\sum_{\sigma\in\Sigma}\mathcal{E}(\sigma)\mu_{w_c}(\{\sigma\}) \in \left(c-(2\,|\Sigma|+1)\mathcal{E}^*, c\right]. \tag{3.8}$$

In the next step, we prove the following:

Claim 2: There exists a positive real number $c_0 \geq (|\Sigma|+1)\mathcal{E}^*$ and a positive integer N_0' depending on $\mathcal{E}$, $|\Sigma|$, Δc, and P such that, for all $c \geq c_0$, there exist some codeword w_c satisfying Eqs. (3.6)–(3.8) and an integer tuple $(n_\sigma)_{\sigma\in\Sigma}$ such that

$$\sum_{\sigma\in\Sigma}|n_\sigma| \leq N_0', \tag{3.9}$$

$$\sum_{\sigma\in\Sigma}\mathcal{E}(\sigma)(\mu_{w_c}(\{\sigma\})+n_\sigma) \in (c-\Delta c, c], \tag{3.10}$$

and

$$\mu_{w_c}(\{\sigma\})+n_\sigma \geq 0 \ \text{ for } \sigma\in\Sigma \quad \wedge \quad \sum_{\sigma\in\Sigma}(\mu_{w_c}(\{\sigma\})+n_\sigma) \geq 1. \tag{3.11}$$

Then, from Claim 2, it follows that there exists some $w \in W_{\mathcal{E},(c-\Delta c,c]}$ such that $\mu_w(\{\sigma\}) = \mu_{w_c}(\{\sigma\})+n_\sigma$ for $\sigma\in\Sigma$ and

$$\begin{aligned}
&\sum_{\sigma\in\Sigma}|\mu_w(\{\sigma\})-\mu_w(\Sigma)P(\{\sigma\})| \\
\leq\ &\sum_{\sigma\in\Sigma}\left|\mu_{w_c}(\{\sigma\})-\mu_{w_c}(\Sigma)P(\{\sigma\})\right| + \sum_{\sigma\in\Sigma}\left|n_\sigma-\left(\sum_{\sigma\in\Sigma}n_\sigma\right)P(\{\sigma\})\right| \\
\leq\ &|\Sigma| + \sum_{\sigma\in\Sigma}|n_\sigma| + \left|\sum_{\sigma\in\Sigma}n_\sigma\right| \leq |\Sigma|+2N_0'.
\end{aligned} \tag{3.12}$$

Thus, Lemma 3.1 is proved by putting $N_0 = |\Sigma|+2N_0'$. In the following, we prove Claim 1 and Claim 2.

(Proof of Claim 1) Let $c \geq (|\Sigma|+1)\mathcal{E}^*$. Then, we have $\left\lfloor (c-|\Sigma|\,\mathcal{E}^*)/\overline{\mathcal{E}}(P)\right\rfloor \geq 1$, where, for $x\in\mathbb{R}$ in general, $\lfloor x\rfloor$ denotes the integer part of x. We denote the integer part and the fractional part of $\left\lfloor (c-|\Sigma|\,\mathcal{E}^*)/\overline{\mathcal{E}}(P)\right\rfloor P(\{\sigma\})$ as $\alpha_\sigma \in \mathbb{Z}_{\geq 0}$ and $\beta_\sigma \in [0,1)$ respectively for $\sigma\in\Sigma$. Because $\sum_{\sigma\in\Sigma}\beta_\sigma \in \{0,1,\cdots,|\Sigma|-1\}$ holds, there exists some $(\beta_\sigma')_{\sigma\in\Sigma}$ such that $\beta_\sigma' \in \{0,1\}$ for $\sigma\in\Sigma$ and $\sum_{\sigma\in\Sigma}\beta_\sigma' = \sum_{\sigma\in\Sigma}\beta_\sigma$. Here, we have

$\alpha_\sigma + \beta'_\sigma \in \mathbb{Z}_{\geq 0}$ for $\sigma \in \Sigma$ and $\sum_{\sigma\in\Sigma} \alpha_\sigma + \beta'_\sigma = \left\lfloor (c - |\Sigma|\,\mathcal{E}^*)/\overline{\mathcal{E}}(P) \right\rfloor \geq 1$, so that there exists some codeword $w_c \in W$ such that $\mu_{w_c}(\{\sigma\}) = \alpha_\sigma + \beta'_\sigma$ for $\sigma \in \Sigma$. This codeword w_c obviously satisfies Eq. (3.6). Because $|\mu_{w_c}(\{\sigma\}) - \mu_{w_c}(\Sigma)P(\{\sigma\})| = |\beta'_\sigma - \beta_\sigma| \leq 1$ holds for $\sigma \in \Sigma$, w_c also satisfies Eq. (3.7). From Eq. (3.6), we have

$$c - |\Sigma|\,\mathcal{E}^* - \overline{\mathcal{E}}(P) < \mu_{w_c}(\Sigma)\overline{\mathcal{E}}(P) \leq c - |\Sigma|\,\mathcal{E}^*. \tag{3.13}$$

In addition, from Eq. (3.7), we have

$$\begin{aligned}
\left| \sum_{\sigma\in\Sigma} \mathcal{E}(\sigma)\mu_{w_c}(\{\sigma\}) - \mu_{w_c}(\Sigma)\overline{\mathcal{E}}(P) \right| &= \left| \sum_{\sigma\in\Sigma} \mathcal{E}(\sigma)\left(\mu_{w_c}(\{\sigma\}) - \mu_{w_c}(\Sigma)P(\{\sigma\})\right) \right| \\
&\leq \sum_{\sigma\in\Sigma} \mathcal{E}(\sigma)\,|\mu_{w_c}(\{\sigma\}) - \mu_{w_c}(\Sigma)P(\{\sigma\})| \\
&\leq |\Sigma|\,\mathcal{E}^*.
\end{aligned} \tag{3.14}$$

From Eqs. (3.13) and (3.14), it follows that $c - 2\,|\Sigma|\,\mathcal{E}^* - \overline{\mathcal{E}}(P) < \mu_{w_c}(\Sigma)\overline{\mathcal{E}}(P) \leq c$. Thus, because $\overline{\mathcal{E}}(P) \leq \mathcal{E}^*$ holds, we have Eq. (3.8). This establishes Claim 1.

(Proof of Claim 2) Let $c \geq (|\Sigma|+1)\mathcal{E}^*$. Then, from Claim 1, it follows that there exists some codeword w_c which satisfies Eqs. (3.6)–(3.8). If $\sum_{\sigma\in\Sigma} \mathcal{E}(\sigma)\mu_{w_c}(\{\sigma\}) \in (c - \Delta c, c]$ holds, Claim 2 is established by setting $n_\sigma = 0$ for $\sigma \in \Sigma$. In the following, we suppose $\sum_{\sigma\in\Sigma} \mathcal{E}(\sigma)\mu_{w_c}(\{\sigma\}) \notin (c - \Delta c, c]$.

First, we consider the case that $(\mathcal{E}(\sigma))_{\sigma\in\Sigma}$ is rationally related and the greatest common divisor of $(\mathcal{E}(\sigma))_{\sigma\in\Sigma}$ is Λ. We put $q_\sigma = \mathcal{E}(\sigma)/\Lambda$ for $\sigma \in \Sigma$ and $M = \sum_{\sigma\in\Sigma} \mathcal{E}(\sigma)\mu_{w_c}(\{\sigma\})/\Lambda$. From the assumption of Lemma 3.1, it follows that $\Delta c \geq \Lambda$, and hence there exists some $M_c \in \mathbb{Z}_{\geq 0}$ such that $M_c\Lambda \in (c - \Delta c, c]$. From Eq. (3.8) and $\sum_{\sigma\in\Sigma} \mathcal{E}(\sigma)\mu_{w_c}(\{\sigma\}) \notin (c - \Delta c, c]$, it follows that

$$0 < M_c - M < (2\,|\Sigma| + 1)q_{\sigma^*}, \tag{3.15}$$

where σ^* is a symbol which satisfies $\mathcal{E}(\sigma^*) = \mathcal{E}^*$. Here, for $N \in \mathbb{Z}_{\geq 1}$, we put

$$E_N = \left\{ \sum_{\sigma\in\Sigma} q_\sigma l_\sigma \;\middle|\; l_\sigma \in \mathbb{Z} \text{ for } \sigma \in \Sigma \wedge \sum_{\sigma\in\Sigma} |l_\sigma| \leq N \right\}. \tag{3.16}$$

Noting that the greatest common divisor of $\{q_\sigma\}_{\sigma\in\Sigma}$ is 1, we find $\bigcup_{N\in\mathbb{Z}_{\geq 1}} E_N = \mathbb{Z}$. That is, there exists some N_0' such that

$$\{1, 2, \cdots, (2\,|\Sigma| + 1)q_{\sigma^*} - 1\} \subset E_{N_0'}. \tag{3.17}$$

Therefore, there exists some integer tuple $(n_\sigma)_{\sigma\in\Sigma}$ such that Eq. (3.9) and

$$\sum_{\sigma\in\Sigma} q_\sigma n_\sigma = M_c - M, \tag{3.18}$$

and hence Eq. (3.10), are satisfied.

Here, putting $p_* = \min_{\sigma\in\Sigma} P(\{\sigma\})$, we set

$$c_0 = |\Sigma|\,\mathcal{E}^* + \overline{\mathcal{E}}(P)\left(\frac{N_0' + 1}{p_*} + 1\right). \tag{3.19}$$

Obviously, $c_0 \geq (|\Sigma| + 1)\mathcal{E}^*$ is satisfied. Let $c \geq c_0$. Then, from Eq. (3.6), it follows that

$$\mu_{w_c}(\Sigma)p_* = \left\lfloor \frac{c - |\Sigma|\,\mathcal{E}^*}{\overline{\mathcal{E}}(P)} \right\rfloor p_* \geq \left\lfloor \frac{N_0' + 1}{p_*} + 1 \right\rfloor p_* > N_0' + 1. \tag{3.20}$$

From this and Eq. (3.7), we obtain for all $\sigma \in \Sigma$,

$$\begin{aligned} \mu_{w_c}(\{\sigma\}) + n_\sigma &\geq \mu_{w_c}(\{\sigma\}) - N_0' \\ &\geq \mu_{w_c}(\Sigma)P(\{\sigma\}) - 1 - N_0' \\ &\geq \mu_{w_c}(\Sigma)p_* - 1 - N_0' > 0. \end{aligned} \tag{3.21}$$

Thus, $c \geq c_0$ implies Eq. (3.11). Therefore, we find the integer tuple $(n_\sigma)_{\sigma\in\Sigma}$ which satisfies the given condition.

Finally, we consider the case that $(\mathcal{E}(\sigma))_{\sigma\in\Sigma}$ is irrationally related. From Eq. (3.8) and $\sum_{\sigma\in\Sigma} \mathcal{E}(\sigma)\mu_w(\{\sigma\}) \notin (c - \Delta c, c]$, it follows that there exists $m \in \{1, 2, \cdots, \lfloor 2(2\,|\Sigma| + 1)\mathcal{E}^*/\Delta c\rfloor\}$ such that

$$\sum_{\sigma\in\Sigma} \mathcal{E}(\sigma)\mu_{w_c}(\{\sigma\}) \in \left(c - (m+1)\frac{\Delta c}{2}, c - m\frac{\Delta c}{2}\right]. \tag{3.22}$$

Here, for $N \in \mathbb{Z}_{\geq 1}$, we put

$$F_N = \left\{ \sum_{\sigma \in \Sigma} \mathcal{E}(\sigma) l_\sigma \mod (2|\Sigma|+1)\mathcal{E}^* \;\middle|\; l_\sigma \in \mathbb{Z}_{\geq 0} \text{ for } \sigma \in \Sigma \wedge \sum_{\sigma \in \Sigma} l_\sigma \leq N \right\}. \quad (3.23)$$

Noting that there exists some $\sigma \in \Sigma$ such that $\mathcal{E}(\sigma)/(2|\Sigma|+1)\mathcal{E}^*$ is irrational, we find that $\bigcup_{N \in \mathbb{Z}_{\geq 1}} F_N$ is dense in the interval $[0, (2|\Sigma|+1)\mathcal{E}^*)$ [51]. Thus, there exists some $N_0'' \in \mathbb{Z}_{\geq 1}$ such that for all $m' \in \{1, 2, \cdots, \lfloor 2(2|\Sigma|+1)\mathcal{E}^*/\Delta c \rfloor\}$,

$$F_{N_0''} \cap \left((m'-1)\frac{\Delta c}{2}, m'\frac{\Delta c}{2} \right] \neq \emptyset. \quad (3.24)$$

Thus, there exists some non-negative integer tuple $(n'_\sigma)_{\sigma \in \Sigma}$ such that $\sum_{\sigma \in \Sigma} n'_\sigma \leq N_0''$ and

$$\Delta \in \left((m-1)\frac{\Delta c}{2}, m\frac{\Delta c}{2} \right], \quad (3.25)$$

where $\Delta = \sum_{\sigma \in \Sigma} \mathcal{E}(\sigma) n'_\sigma \mod (2|\Sigma|+1)\mathcal{E}^*$. Here, we set an integer tuple $(n_\sigma)_{\sigma \in \Sigma}$ as

$$n_\sigma = n'_\sigma \text{ for } \sigma \in \Sigma \setminus \{\sigma^*\} \quad \wedge \quad n_{\sigma^*} = n'_{\sigma^*} - \frac{\sum_{\sigma \in \Sigma} \mathcal{E}(\sigma) n'_\sigma - \Delta}{\mathcal{E}^*},$$

where σ^* is a symbol which satisfies $\mathcal{E}(\sigma^*) = \mathcal{E}^*$. Then, putting $N_0' = 2N_0''$, we have

$$\sum_{\sigma \in \Sigma} |n_\sigma| \leq \sum_{\sigma \in \Sigma} n'_\sigma + \frac{\sum_{\sigma \in \Sigma} \mathcal{E}(\sigma) n'_\sigma - \Delta}{\mathcal{E}^*} \leq 2 \sum_{\sigma \in \Sigma} n'_\sigma \leq 2N_0'' = N_0'. \quad (3.26)$$

Thus, Eq. (3.9) is satisfied. In addition, noting that $\sum_{\sigma \in \Sigma} \mathcal{E}(\sigma) n_\sigma = \Delta$, we find that Eq. (3.10) is satisfied.

Here, we set

$$c_0 = |\Sigma| \mathcal{E}^* + \overline{\mathcal{E}}(P) \left(\frac{N_0'' + 1}{P(\{\sigma^*\})} + 1 \right). \quad (3.27)$$

Obviously, $c_0 \geq (|\Sigma|+1)\mathcal{E}^*$ is satisfied. Let $c \geq c_0$. Then, from Eqs. (3.6), it follows that

$$\mu_{w_c}(\Sigma) P(\{\sigma^*\}) = \left\lfloor \frac{c - |\Sigma| \mathcal{E}^*}{\overline{\mathcal{E}}(P)} \right\rfloor P(\{\sigma^*\}) \geq \left\lfloor \frac{N_0'' + 1}{P(\{\sigma^*\})} + 1 \right\rfloor P(\{\sigma^*\}) > N_0'' + 1. \quad (3.28)$$

From this and Eq. (3.7), we obtain

$$\begin{aligned}\mu_{w_c}(\{\sigma^*\}) + n_{\sigma^*} &= \mu_{w_c}(\{\sigma^*\}) + n'_{\sigma^*} - \frac{\sum_{\sigma\in\Sigma}\mathcal{E}(\sigma)n'_\sigma - \Delta}{\mathcal{E}^*} \\ &\geq \mu_{w_c}(\{\sigma^*\}) - N''_0 \\ &\geq \mu_{w_c}(\Sigma)P(\{\sigma^*\}) - 1 - N''_0 > 0. \end{aligned} \tag{3.29}$$

In addition, we have $\mu_{w_c}(\{\sigma\}) + n_\sigma = \mu_{w_c}(\{\sigma\}) + n'_\sigma \geq 0$ for $\sigma \in \Sigma \setminus \{\sigma^*\}$. Thus, $c \geq c_0$ implies (3.11). Therefore, we find the integer tuple $(n_\sigma)_{\sigma\in\Sigma}$ which satisfies the given condition. This establishes Claim 2. □

3.3 Asymptotic Property

Asymptotic properties of the number of elements in the $W_{\mathcal{E},(c-\Delta c,c]}$ were studied as a problem of source coding with cost function [53–55]. Referring to these researches, an asymptotic property of energy representation $W_{\mathcal{E},(c-\Delta c,c]}$ is revealed.

3.3.1 Probability Maximizing Size of Equivalence Classes

Let us consider $W_{\mathcal{E},(c-\Delta c,c]}$ based on the method of types [8, 56]. For each $w \in W$, we define a probability P_w on Σ as

$$P_w(\{\sigma\}) = \frac{\mu_w(\{\sigma\})}{\mu_w(\Sigma)} \quad \text{for} \quad \sigma \in \Sigma. \tag{3.30}$$

P_w denotes the frequency of occurrences of symbols in w. We define entropy as

$$\mathcal{H}(P) := -\sum_{\sigma\in\Sigma} P(\{\sigma\}) \log P(\{\sigma\}) \tag{3.31}$$

and divergence as

$$D(P\|Q) := \sum_{\sigma\in\Sigma} P(\{\sigma\}) \log \frac{P(\{\sigma\})}{Q(\{\sigma\})}, \tag{3.32}$$

where P and Q are probabilities on Σ and log denotes natural logarithm. We have $D(P\|Q) \geq 0$, with equality only if $P = Q$. In addition, we have the following lemma on the entropy of P_w [57].

Lemma 3.2. *For all $w \in W$,*

$$\frac{\exp\left(\mu_w(\Sigma)\mathcal{H}(P_w)\right)}{(\mu_w(\Sigma)+1)^{|\Sigma|}} \leq |[w]| \leq \exp\left(\mu_w(\Sigma)\mathcal{H}(P_w)\right) \tag{3.33}$$

holds. □

Let a codeword w have energy $c \in \mathbb{R}_{>0}$. Then, $\mu_w(\Sigma) = c/\overline{\mathcal{E}}(P_w)$ holds, and hence, noting Lemma 3.2, we have

$$\frac{\exp\left(c\mathcal{H}(P_w)/\overline{\mathcal{E}}(P_w)\right)}{(\mu_w(\Sigma)+1)^{|\Sigma|}} \leq |[w]| \leq \exp\left(c\mathcal{H}(P_w)/\overline{\mathcal{E}}(P_w)\right). \tag{3.34}$$

From this inequality, the size of the equivalence class $|[w]|$ is evaluated as $\mathcal{H}(P_w)/\overline{\mathcal{E}}(P_w)$. We define probability $P_{\mathcal{E}}$ on Σ as

$$P_{\mathcal{E}}(\{\sigma\}) = \exp(-\lambda\mathcal{E}(\sigma)) \quad \text{for } \sigma \in \Sigma, \tag{3.35}$$

where λ is a positive real number uniquely determined by the normalization condition $\sum_{\sigma\in\Sigma}\exp(-\lambda\mathcal{E}(\sigma)) = 1$. Here, we have the following lemma [58]. This lemma means that $P_{\mathcal{E}}$ maximizes the size of the equivalence class $|[w]|$.

Lemma 3.3. *Let P be a probability on Σ. Then, we have*

$$\lambda \geq \frac{\mathcal{H}(P)}{\overline{\mathcal{E}}(P)}, \tag{3.36}$$

with equality only if $P = P_{\mathcal{E}}$.

Proof of Lemma 3.3. We have

$$D(P\|P_{\mathcal{E}}) = \lambda\overline{\mathcal{E}}(P) - \mathcal{H}(P). \tag{3.37}$$

Thus, $\lambda\overline{\mathcal{E}}(P) - \mathcal{H}(P) \geq 0$ holds, with equality $P = P_{\mathcal{E}}$. □

3.3.2 Asymptotic Property of Energy Representation

Here, it is proved in Theorem 3.2 that the ratio of δ-divergent sequences for $P_{\mathcal{E}}$ [59] in $W_{\mathcal{E},(c-\Delta c,c]}$ approaches 1 as c becomes infinite. This theorem ensures the asymptotic

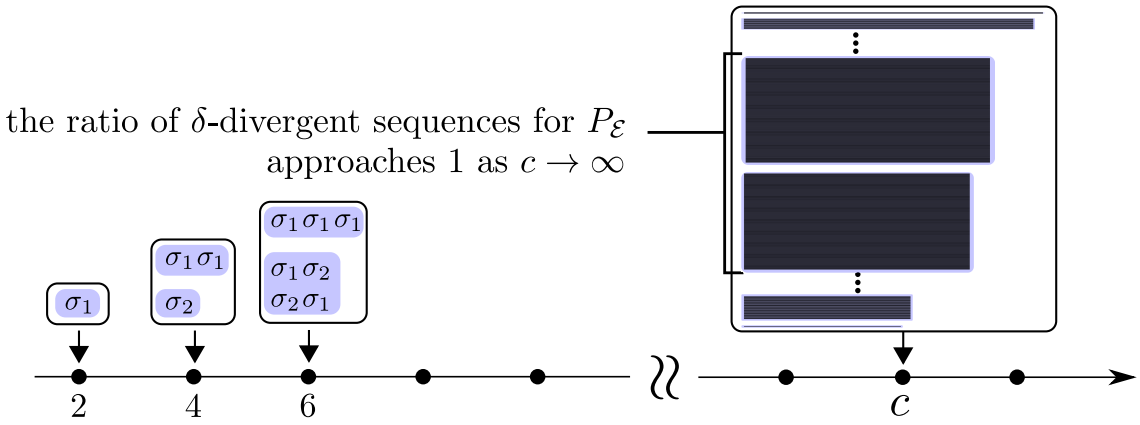

Figure 3.3: Schematic diagram showing that the ratio of δ-divergent sequences for $P_{\mathcal{E}}$ in $W_{\mathcal{E},(c-\Delta c,c]}$ approaches 1 as c becomes infinite. Here, we consider the symbols $\Sigma = \{\sigma_1, \sigma_2\}$ with energies $\mathcal{E}(\sigma_1) = 2$ and $\mathcal{E}(\sigma_2) = 4$.

property of energy representation. Fig. 3.3 illustrates the asymptotic property given in Theorem 3.2. As theoretical limits of communication are given in information theory by asymptotic properties with the length of codewords increasing to infinity, this asymptotic property has a potential to provide design principles for representing given energy with symbol sequences in power packet dispatching networks.

Theorem 3.2. *Let $\mathcal{E}$ and Δc satisfy the condition of Theorem 3.1 and let $\delta > 0$. Then, there exists $(\epsilon_c)_{c\in\mathbb{R}}$, depending on $\mathcal{E}$, $|\Sigma|$, Δc, and δ, such that $\lim_{c\to\infty} \epsilon_c = 0$ is satisfied and*

$$\frac{\left|\left\{w \in W_{\mathcal{E},(c-\Delta c,c]} \;\middle|\; D(P_w \| P_{\mathcal{E}}) > \delta\right\}\right|}{\left|W_{\mathcal{E},(c-\Delta c,c]}\right|} < \epsilon_c \tag{3.38}$$

for all $c \geq c_0$ where c_0 is a positive real number determined by $\mathcal{E}$, $|\Sigma|$, and Δc.

We have found the following upper bound

$$\epsilon_c = \frac{1}{|\Sigma|+1}\left(\frac{c}{\mathcal{E}_*}+2\right)^{|\Sigma|+1}\left(\frac{c}{\mathcal{E}_*}+1\right)^{|\Sigma|}\exp\left(\lambda\Delta c + \mathrm{e}^{\lambda\mathcal{E}^*}N_0\right)\exp\left(-\frac{\delta}{\mathcal{E}^*}c\right), \tag{3.39}$$

where $\mathcal{E}^* = \max_{\sigma\in\Sigma}\mathcal{E}(\sigma)$, $\mathcal{E}_* = \min_{\sigma\in\Sigma}\mathcal{E}(\sigma)$, and N_0 is a positive real number determined by $\mathcal{E}$, $|\Sigma|$, and Δc. Definitely, this upper bound exponentially decays as c approaches infinity.

To prove Theorem 3.2, we prepare the following lemma:

Lemma 3.4. *Let $c \in \mathbb{R}_{>0}$ and $\Delta c > 0$. Then, for all $\delta \geq 0$, we have*

$$\begin{aligned}\left|\left\{w \in W_{\mathcal{E},(c-\Delta c,c]} \;\middle|\; D(P_w \| P_{\mathcal{E}}) > \delta\right\}\right| \\ < \frac{1}{|\Sigma|+1}\left(\frac{c}{\mathcal{E}_*}+2\right)^{|\Sigma|+1} \exp\left\{c\left(\lambda - \frac{\delta}{\mathcal{E}^*}\right)\right\}.\end{aligned} \tag{3.40}$$

Proof of Lemma 3.4. Noting that $\mu_w(\{\sigma\}) \in \{0, 1, \cdots, k\}$ for all $\sigma \in \Sigma$ for $w \in W$ with length k, we have

$$|\{[w] \in W/\sim \mid \mu_w(\Sigma) = k\}| \leq (k+1)^{|\Sigma|}, \tag{3.41}$$

where $W/\sim$ is a set of equivalence classes, i.e. $\{[w] \mid w \in W\}$. $W_{\mathcal{E},(c-\Delta c,c]}/\sim$ is a set of equivalence classes included in $W_{\mathcal{E},(c-\Delta c,c]}$. i.e. $\{[w] \mid w \in W_{\mathcal{E},(c-\Delta c,c]}\}$. Then, noting that $w \in W_{\mathcal{E},(c-\Delta c,c]}$ implies $\mu_w(\Sigma) \leq \lfloor c/\mathcal{E}_* \rfloor$, we have

$$\begin{aligned}|W_{\mathcal{E},(c-\Delta c,c]}/\sim| &\leq \sum_{k=1}^{\lfloor c/\mathcal{E}_* \rfloor} (k+1)^{|\Sigma|} \\ &< \int_1^{c/\mathcal{E}_*+1} (k+1)^{|\Sigma|} dk \\ &< \frac{1}{|\Sigma|+1}\left(\frac{c}{\mathcal{E}_*}+2\right)^{|\Sigma|+1}.\end{aligned} \tag{3.42}$$

Let $w \in W_{\mathcal{E},(c-\Delta c,c]}$ satisfy $D(P_w \| P_{\mathcal{E}}) > \delta$. Then, from Lemma 3.2 and Eq. (3.37), we have

$$\begin{aligned}|[w]| &\leq \exp\left(\mu_w(\Sigma)\mathcal{H}(P_w)\right) \\ &= \exp\left\{\mu_w(\Sigma)\left(\lambda\overline{\mathcal{E}}(P_w) - D(P_w\|P_{\mathcal{E}})\right)\right\} \\ &< \exp\left\{\mu_w(\Sigma)\overline{\mathcal{E}}(P_w)\left(\lambda - \frac{\delta}{\overline{\mathcal{E}}(P_w)}\right)\right\}.\end{aligned} \tag{3.43}$$

From $\lambda - \delta/\mathcal{E}^* \geq \lambda - \delta/\overline{\mathcal{E}}(P_w) > \mathcal{H}(P_w)/\overline{\mathcal{E}}(P_w) \geq 0$ and $\mu_w(\Sigma)\overline{\mathcal{E}}(P_w) \leq c$, we have

$$|[w]| < \exp\left\{c\left(\lambda - \frac{\delta}{\mathcal{E}^*}\right)\right\}. \tag{3.44}$$

Therefore, we have

$$\begin{aligned}
&\left|\left\{w \in W_{\mathcal{E},(c-\Delta c,c]} \;\middle|\; D(P_w \| P_{\mathcal{E}}) > \delta\right\}\right| \\
&< |W_{\mathcal{E},(c-\Delta c,c]}/\sim| \exp\left\{c\left(\lambda - \frac{\delta}{\mathcal{E}^*}\right)\right\} \\
&< \frac{1}{|\Sigma|+1}\left(\frac{c}{\mathcal{E}_*}+2\right)^{|\Sigma|+1} \exp\left\{c\left(\lambda - \frac{\delta}{\mathcal{E}^*}\right)\right\}. \qquad (3.45)
\end{aligned}$$

This completes the proof. □

Proof of Theorem 3.2. First, we derive a lower bound of $\left|W_{\mathcal{E},(c-\Delta c,c]}\right|$. From Lemma 3.1, it follows that there exists a positive real number c_0 and a positive integer N_0 depending on $\mathcal{E}$, $|\Sigma|$, and Δc such that, for all $c \geq c_0$, there exists $w \in W_{\mathcal{E},(c-\Delta c,c]}$ which satisfies

$$\sum_{\sigma \in \Sigma} |\mu_w(\{\sigma\}) - \mu_w(\Sigma) P_{\mathcal{E}}(\{\sigma\})| \leq N_0. \qquad (3.46)$$

From $[w] \subset W_{\mathcal{E},(c-\Delta c,c]}$, Lemma 3.2, and Eq. (3.37), we have

$$\begin{aligned}
|W_{\mathcal{E},(c-\Delta c,c]}| &\geq |[w]| \\
&\geq \frac{1}{(\mu_w(\Sigma)+1)^{|\Sigma|}} \exp\left(\mu_w(\Sigma)\mathcal{H}(P_w)\right) \\
&= \frac{\exp\left\{\lambda \mu_w(\Sigma)\overline{\mathcal{E}}(P_w) - \mu_w(\Sigma) D(P_w||P_{\mathcal{E}})\right\}}{(\mu_w(\Sigma)+1)^{|\Sigma|}}. \qquad (3.47)
\end{aligned}$$

Noting that $w \in W_{\mathcal{E},(c-\Delta c,c]}$ implies

$$\mu_w(\Sigma)\overline{\mathcal{E}}(P_w) = \sum_{\sigma \in \Sigma} \mathcal{E}(\sigma)\mu_w(\{\sigma\}) > c - \Delta c, \qquad (3.48)$$

we have

$$|W_{\mathcal{E},(c-\Delta c,c]}| > \frac{\exp\left\{\lambda(c-\Delta c) - \mu_w(\Sigma) D(P_w||P_{\mathcal{E}})\right\}}{(c/\mathcal{E}_*+1)^{|\Sigma|}}. \qquad (3.49)$$

Here, from Eq. (3.46), we have

$$\mu_w(\Sigma) D(P_w||P_{\mathcal{E}}) = \sum_{\sigma \in \Sigma} \mu_w(\{\sigma\}) \log\left(\frac{\mu_w(\{\sigma\})/\mu_w(\Sigma)}{\mathrm{e}^{-\lambda \mathcal{E}(\sigma)}}\right)$$

$$
\begin{aligned}
&\leq \sum_{\sigma\in\Sigma} \mu_w(\{\sigma\}) \log\left(1+\left|\frac{\mu_w(\{\sigma\})/\mu_w(\Sigma)-\mathrm{e}^{-\lambda\mathcal{E}(\sigma)}}{\mathrm{e}^{-\lambda\mathcal{E}(\sigma)}}\right|\right)\\
&\leq \sum_{\sigma\in\Sigma} \mu_w(\{\sigma\}) \left|\frac{\mu_w(\{\sigma\})/\mu_w(\Sigma)-\mathrm{e}^{-\lambda\mathcal{E}(\sigma)}}{\mathrm{e}^{-\lambda\mathcal{E}(\sigma)}}\right|\\
&\leq \mathrm{e}^{\lambda\mathcal{E}^*}\sum_{\sigma\in\Sigma}\left|\mu_w(\{\sigma\})-\mu_w(\Sigma)\mathrm{e}^{-\lambda\mathcal{E}(\sigma)}\right|\\
&\leq \mathrm{e}^{\lambda\mathcal{E}^*}N_0. \qquad (3.50)
\end{aligned}
$$

Thus, from this inequality and Eq. (3.49), we have

$$
|W_{\mathcal{E},(c-\Delta c,c]}| > \frac{\exp\left(-\lambda\Delta c-\mathrm{e}^{\lambda\mathcal{E}^*}N_0\right)}{(c/\mathcal{E}_*+1)^{|\Sigma|}}\exp\left(\lambda c\right). \qquad (3.51)
$$

Therefore, from Lemma 3.4 and Eq. (3.51), when we set ϵ_c as Eq. (3.39), we have $\lim_{c\to\infty}\epsilon_c = 0$ and

$$
\frac{\left|\left\{w\in W_{\mathcal{E},(c-\Delta c,c]} \;\middle|\; D(P_w\|P_{\mathcal{E}})>\delta\right\}\right|}{\left|W_{\mathcal{E},(c-\Delta c,c]}\right|} < \epsilon_c. \qquad (3.52)
$$

This completes the proof. □

3.4 Numerical Verification of Representation of Finite Energy

Theorem 3.2 ensures the asymptotic property of $W_{\mathcal{E},(c-\Delta c,c]}$ with sufficiently large c. However, finite energy is represented with power packet in practical systems. Thus, in this section, Theorem 3.2 is numerically confirmed for finite energy by calculating the ratio of δ-divergent sequences for $P_{\mathcal{E}}$ in $W_{\mathcal{E},(c-\Delta c,c]}$.

We consider symbols $\Sigma = \{\sigma_1, \sigma_2, \sigma_3\}$. The energy is set as $\mathcal{E}(\sigma_1) = 0.023$, $\mathcal{E}(\sigma_2) = 0.02$, and $\mathcal{E}(\sigma_3) = 0.01$. Table 3.1 shows the values of $\mathcal{E}$, $P_{\mathcal{E}}$, λ, $\overline{\mathcal{E}}(P_{\mathcal{E}})$, and $\mathcal{H}(P_{\mathcal{E}})$ in this setting. We calculate the ratio of codewords w satisfying $D(P_w||P_{\mathcal{E}}) = \lambda\overline{\mathcal{E}}(P_w)-\mathcal{H}(P_w) > 0.01$ in $W_{\mathcal{E},(c-\Delta c,c]}$, i.e.

$$
r(c,\Delta c) := \frac{\left|\left\{w\in W_{\mathcal{E},(c-\Delta c,c]} \;\middle|\; D(P_w\|P_{\mathcal{E}})>0.01\right\}\right|}{\left|W_{\mathcal{E},(c-\Delta c,c]}\right|}. \qquad (3.53)
$$

The threshold is set to 0.01, which is approximately one hundredth of $\mathcal{H}(P_{\mathcal{E}})$.

3.4.1 Dependence on c

First, we set $\Delta c = 0.01$ and verify the asymptotic property. The values of $r(c, \Delta c)$ and $\log r(c, \Delta c)$ are calculated at $c \in \{0.01, 0.011, 0.012, \cdots, 10\}$ and shown in Figs. 3.4 and 3.5 respectively. Because Δc is set to be equal to $\mathcal{E}(\sigma_3)$, $W_{\mathcal{E},(c-\Delta,c]}$ is not empty, and hence $r(c, \Delta c)$ is well defined, for all $c \geq 0.01$.

Figure 3.4 shows that, at $c = 1$, approximately half of the codewords w in $W_{\mathcal{E},(c-\Delta c,c]}$ satisfy $D(P_w||P_{\mathcal{E}}) \leq 0.01$. Here, we can estimate the length of the codeword w as $c/\overline{\mathcal{E}}(P_{\mathcal{E}}) = 64.53$ at $c = 1$ assuming $P_w = P_{\mathcal{E}}$.

In addition, it is confirmed that $r(c, \Delta c)$ approaches 0 as c increases. Figure 3.5 demonstrates that $r(c, \Delta c)$ decays exponentially, or more precisely, we have $\log r(c, \Delta c) \approx -0.645c$. This verifies the asymptotic property. On the other hand, the upper bound ϵ_c in Eq. (3.39) decays with the time constant $\delta/\mathcal{E}^* = 0.4348$, which does not correctly reflect the value of the slope, i.e. -0.645, in Fig. 3.5. As the absolute value of the slope, i.e. 0.645, is roughly equal to the value of $\delta/\overline{\mathcal{E}}(P_{\mathcal{E}}) = 0.6453$, we may obtain a better upper bound than ϵ_c in Eq. (3.39).

3.4.2 Dependence on Δc

Then, we set $c = 1$ and investigate the dependence on Δc. The values of $r(c, \Delta c)$ are calculated at $\Delta c \in \{0.001, 0.002, \cdots, 0.03\}$ and shown in Fig. 3.6. This figure shows that the value of $r(c, \Delta c)$ varies at small Δc, especially at $\Delta c = 0.001$.

To clarify the reason for this, equivalence classes $[w]$ in $W_{\mathcal{E},(1-\Delta c,1]}$ are arranged in descending order of their number of elements, i.e. $|[w]|$. Tables 3.2, 3.3, and 3.4 show the largest equivalence classes in the case of $\Delta c \geq 0.03$, $\Delta c = 0.02$, and $\Delta c = 0.01$ respectively. All equivalence classes $[w]$ in Tabs. 3.2 and 3.3 satisfy $D(P_w||P_{\mathcal{E}}) \leq 0.01$, while all equivalent classes $[w]$ in Tab. 3.4 satisfies $D(P_w||P_{\mathcal{E}}) > 0.01$. In other words, $W_{\mathcal{E},(1-0.001,1]}$ does not include the equivalence classes $[w]$ in Tabs. 3.2 and 3.3, which have the larger numbers of elements and the smaller values of $D(P_w||P_{\mathcal{E}})$.

Here, because the greatest common divisor of $(\mathcal{E}(\sigma))_{\sigma\in\Sigma}$ is 0.001, energy of every codeword is an integer multiple of 0.001 in this setting. This implies that energy of

Table 3.1: The values of $\mathcal{E}$, $P_{\mathcal{E}}$, λ, $\overline{\mathcal{E}}(P_{\mathcal{E}})$, and $\mathcal{H}(P_{\mathcal{E}})$.

$\mathcal{E}(\sigma_1) = 0.023$	$P_{\mathcal{E}}(\{\sigma_1\}) = 0.2181$	$\lambda = 66.20$
$\mathcal{E}(\sigma_2) = 0.02$	$P_{\mathcal{E}}(\{\sigma_2\}) = 0.2661$	$\overline{\mathcal{E}}(P_{\mathcal{E}}) = 0.01550$
$\mathcal{E}(\sigma_3) = 0.01$	$P_{\mathcal{E}}(\{\sigma_3\}) = 0.5158$	$\mathcal{H}(P_{\mathcal{E}}) = 1.026$

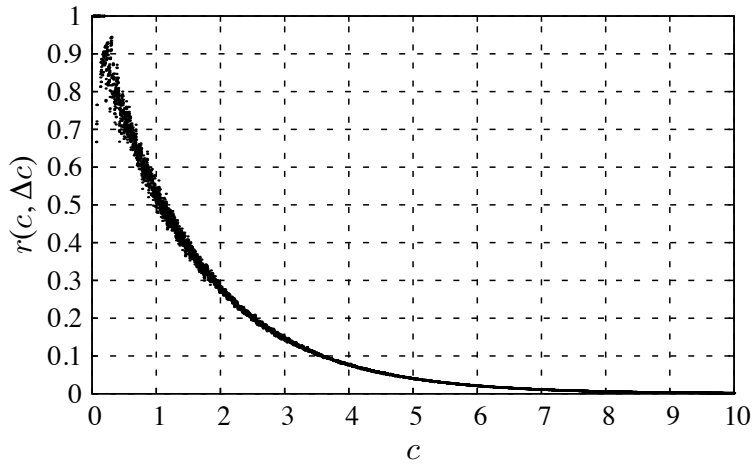

Figure 3.4: $r(c, \Delta c)$ with a change of c.

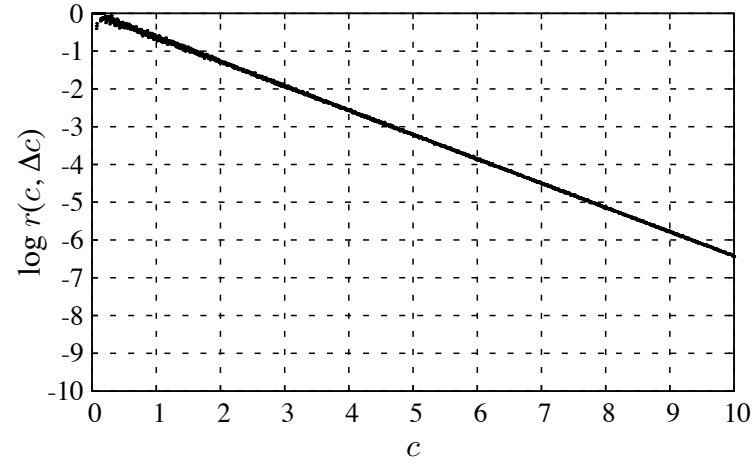

Figure 3.5: $\log r(c, \Delta c)$ with a change of c.

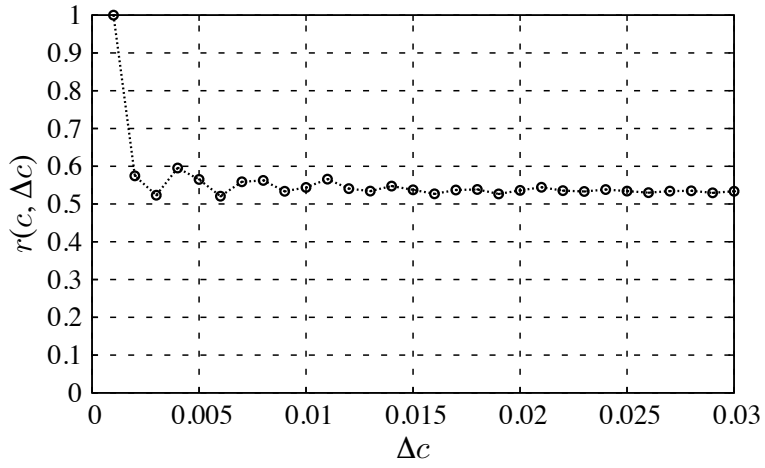

Figure 3.6: $r(c, \Delta c)$ with a change of Δc.

Table 3.2: The largest equivalence classes in the case of $\Delta c \geq 0.003$.

$\lvert[w]\rvert$	$D(P_w \lvert\rvert P_{\mathcal{E}})$	$\mu_w(\{\sigma_1\})$	$\mu_w(\{\sigma_2\})$	$\mu_w(\{\sigma_3\})$
$7.007 \cdot 10^{26}$	0.001045	13	18	34
$6.607 \cdot 10^{26}$	0.002034	13	17	36
$6.366 \cdot 10^{26}$	0.002493	13	19	32
$5.508 \cdot 10^{26}$	0.003628	16	16	31
$5.352 \cdot 10^{26}$	0.005305	13	16	38

Table 3.3: The largest equivalence classes in the case of $\Delta c = 0.002$.

$\lvert[w]\rvert$	$D(P_w \lvert\rvert P_{\mathcal{E}})$	$\mu_w(\{\sigma_1\})$	$\mu_w(\{\sigma_2\})$	$\mu_w(\{\sigma_3\})$
$7.007 \cdot 10^{26}$	0.001045	13	18	34
$6.607 \cdot 10^{26}$	0.002034	13	17	36
$6.366 \cdot 10^{26}$	0.002493	13	19	32
$5.352 \cdot 10^{26}$	0.005305	13	16	38
$4.934 \cdot 10^{26}$	0.006560	13	20	30

Table 3.4: The largest equivalence classes in the case of $\Delta c = 0.001$.

$\lvert[w]\rvert$	$D(P_w \lvert\rvert P_{\mathcal{E}})$	$\mu_w(\{\sigma_1\})$	$\mu_w(\{\sigma_2\})$	$\mu_w(\{\sigma_3\})$
$3.001 \cdot 10^{26}$	0.01540	10	20	37
$2.841 \cdot 10^{26}$	0.01641	10	21	35
$2.754 \cdot 10^{26}$	0.01654	10	19	39
$2.329 \cdot 10^{26}$	0.01970	10	22	33
$2.202 \cdot 10^{26}$	0.01968	10	18	41

every codeword in $W_{\mathcal{E},(1-0.001,1]}$ is 1. Noting this and the fact that $\mathcal{E}(\sigma_2)$ and $\mathcal{E}(\sigma_3)$ are integer multiples of 0.01 and $\mathcal{E}(\sigma_1) = 0.023$, we find that $w \in W_{\mathcal{E},(1-0.001,1]}$ implies that $\mu_w(\{\sigma_1\})$ is a multiple of 10. This explains why $W_{\mathcal{E},(1-0.001,1]}$ does not include the equivalence classes $[w]$ in Tabs. 3.2 and 3.3, whose $\mu_w(\{\sigma_1\})$ are not multiples of 10, and hence the value of $r(c, \Delta c)$ varies at $\Delta c = 0.001$. The result implies that, although Theorem 3.2 ensures the asymptotic property with sufficiently large c, the asymptotic property is not easily recognized at finite energy when Δc is small, i.e. when energy is represented with high accuracy.

3.5 Summary

In this chapter, we introduced symbol in power packetization as a minimum unit of power transferred by a tagged pulse, referring to Shannon's information theory in which messages are represented by symbol sequences in a digitized manner. Power packetization is a simultaneous representation of messages and energy with symbol sequences. Energy representation was investigated with a set of symbol sequences, which represent energy as the total amount. First, we clarified the condition for existence of energy representation. This shows the limit on accuracy with which all sufficiently large energy can be represented. Then, we proved an asymptotic property which shows that, as the represented energy becomes infinite, the frequency of occurrences of a symbol in almost all sequences can be approximated by the probability determined from the energy of symbols. This asymptotic property was numerically verified in representation of finite energy. The numerical examination shows that the asymptotic property in this theorem is not easily recognized when energy is represented with high accuracy. The study of

energy representation has a potential to provide design principles for representing given energy in power packet dispatching networks.

Chapter 4

Symbol Propagation in Networks

In the following chapters, we investigate packetized power in networks under the conservation of energy. Here, the set of symbols and their energies are given to the network. A symbol is a minimum unit of power transferred by a power pulse with an information tag, as mentioned in Chapter 3. In networks, a symbol is transferred at a link during a unit time. At each node, energy is represented with symbols sent to and received from neighboring nodes for a finite duration. In this way, packetized power is spatially and temporally transferred as symbols in a digitized and quantized manner in networks.

To mathematically represent such transmission of packetized power, we refer to the work about detecting bipedal motion using point trajectories in video sequences [60,61]. In this work, to obtain discriminative point trajectories from image sequences over a sufficiently long time period under both image noise and occlusion, probabilistic trajectories are designed by prioritizing the concept of temporal connectedness. They are extracted from directed acyclic graphs whose edges represent temporal point correspondences and are weighted with their matching probability in terms of appearance and location.

In this chapter, considering transfer of a symbol at each link during each unit time as a spatio-temporal correspondence, we introduce symbol propagation matrix (SPM) as a representation of packetized power. In power packetization, energy of the symbol is transferred as network flow at each spatio-temporal correspondence. The temporal connectedness is important in power packetization to transfer power in networks with low "strain", i.e. the spatial difference of power, which is equal to the temporal change

of energy stored in each router. Then, we consider the problem of selecting a SPM in terms of transferability, that is, the possibility to represent given energies at sources and destinations for the finite duration. To select packetized power as a network flow problem, we weight the supplied energy from the sources and the supplied energy to the destinations (V1), transferred energy at each link during each unit time (V2), and change of stored energy in each router (V3). The problem is formulated as M-convex submodular flow problem which is known as generalization of the minimum cost flow problem and it is solvable [62]. At last, through examples, we verify that the formulation provides reasonable transmission of packetized power.

4.1 Packetized Power in Networks

Here, we introduce symbol propagation matrix as a representation of packetized power transferred by symbols in a digitized and quantized manner. Via SPM, packetized power is represented as network flow in a spatio-temporal structure.

4.1.1 Symbol Propagation Matrices

The set of symbols Σ_{T} and their energies $\mathcal{E} : \Sigma_{\mathrm{T}} \to \mathbb{R}_{>0}$ are given to the network. The symbols have a partition $\{\Sigma_m\}_{m=0,1,\cdots,M-1}$, whose cell represents a distinct power flow[1]. For each distinct power flow, energy is represented as a summation of the symbol's energy. Here, symbols of a same cell can be exchanged under the conservation of energy.

The network structure is given as a directed graph $G = (\tilde{V}, A)$, where $\tilde{V}$ is a disjoint union of the set of routers V, sources V_{S}, and destinations V_{D}, and A is the set of links. Here, sources and destinations represent the external system of the network. The incidence relation is a couple of functions $\partial^+ : A \to \tilde{V}$ and $\partial^- : A \to \tilde{V}$. Other representation of the incidence relation is introduced as a couple of functions $\delta^+ : \tilde{V} \ni v \mapsto \{a \mid \partial^+ a = v\} \in 2^A$ and $\delta^- : \tilde{V} \ni v \mapsto \{a \mid \partial^- a = v\} \in 2^A$ [62–64]. As for the link, power is kept between nodes. The directions of links are assigned with power directions.

[1]In power packetization, energy is transferred with time division multiplexing (TDM) at links and stored in the corresponding storage unit in routers. Thus, power flow can be distinguished by the information tags of power packets.

Next, we set that the network is synchronized and symbols are transferred during same unit times $\overline{T} = \{\overline{t_0}, \overline{t_1}, \cdots, \overline{t_{N-1}}\}$, where N is a positive integer, $\overline{t_n} := [t_n, t_{n+1})$, and $t_0 < t_1 < \cdots < t_N$. Here, energy is transferred by N unit times. Although various power pulses can transfer the energy of same symbol during a unit time, we ignore the variety and focus on the integrated value of power during the unit time.

Now, we focus on a single cell Σ_m. At each link $a \in A$ during each unit time $\bar{t} \in \overline{T}$, there are three cases of transfer of symbols Σ_m: Case 1: a single symbol $\sigma \in \Sigma_m$ is transferred from node $\partial^+ a$ to node $\partial^- a$; Case 2: a single symbol $\sigma \in \Sigma_m$ is transferred from node $\partial^- a$ to node $\partial^+ a$; Case 3: no symbol is transferred[2]. Therefore, packetized power is given by a map, which we name symbol propagation matrix:

$$SPM_m : \overline{T} \times A \to \Sigma_m \times \{\mathrm{f}, \mathrm{b}\} \cup \{\sigma_\emptyset\}, \tag{4.1}$$

where $\sigma_\emptyset$ is an element which does not belongs to Σ_T. $SPM_m(\bar{t}, a) = (\sigma, \mathrm{f})$ and $SPM_m(\bar{t}, a) = (\sigma, \mathrm{b})$ denote that σ is transferred from node $\partial^+ a$ to node $\partial^- a$ and from node $\partial^- a$ to node $\partial^+ a$ respectively. $SPM_m(\bar{t}, a) = \sigma_\emptyset$ denotes no symbol is transferred.

4.1.2 Packetized Power as Network Flow

Here, we introduce packetized power as network flow [62–64]. First, we define a graph with spatio-temporal structure induced by the network structure G and unit times $\overline{T}$ as

$$\hat{G} = (\overline{T} \times \tilde{V}, \overline{T} \times A), \tag{4.2}$$

whose incidence relation is defined by

$$\hat{\partial}^+ : \overline{T} \times \tilde{V} \ni (\bar{t}, v) \mapsto (\bar{t}, \partial^+ v) \in \overline{T} \times A \tag{4.3}$$

and

$$\hat{\partial}^- : \overline{T} \times \tilde{V} \ni (\bar{t}, v) \mapsto (\bar{t}, \partial^- v) \in \overline{T} \times A. \tag{4.4}$$

[2]Here, because we do not care the various ways of power transfer during each unit time, more than one symbol is not transferred. For example, if twice the amount of energy of a symbol $\sigma_1 \in \Sigma_m$ is transferred, then we consider that a symbol $\sigma_2 \in \Sigma_m$ with a energy $\mathcal{E}(\sigma_2) = 2\mathcal{E}(\sigma_1)$ is transferred.

Then, packetized power is introduced as a network flow on $\hat{G}$, i.e. as

$$u : \overline{T} \times A \to \mathbb{R}, \tag{4.5}$$

and its boundary $\partial u : \overline{T} \times \tilde{V} \to \mathbb{R}$ is defined by

$$\partial u(\bar{t}, v) = \sum_{a \in \delta^+ v} u(\bar{t}, a) - \sum_{a \in \delta^- v} u(\bar{t}, a) \quad (\bar{t} \in \overline{T}, v \in \tilde{V}). \tag{4.6}$$

Each link of $\hat{G}$, i.e. $(\bar{t}, a) \in \overline{T} \times A$, represents a spatio-temporal correspondence at which each symbol is transferred. Each cell Σ_m represents packetized power $u_m : \overline{T} \times A \to \mathbb{R}$ and u_m is given by SPM_m as

$$u_m(\bar{t}, a) = \begin{cases} \mathcal{E}(\sigma) & (SPM_m(\bar{t}, a) = (\sigma, \mathrm{f})), \\ -\mathcal{E}(\sigma) & (SPM_m(\bar{t}, a) = (\sigma, \mathrm{b})), \\ 0 & (SPM_m(\bar{t}, a) = \sigma_\emptyset). \end{cases} \tag{4.7}$$

Here, we assume the conservation of energy; more precisely, we assume that all energy exchanges in each node $v \in \tilde{V}$ are represented with symbols transferred through the adjacent links $a \in \delta^+ v \cup \delta^- v$[3]. Then, $\partial u_m(\bar{t}, v)$ is equal to the increment of stored energy corresponding to Σ_m in the node $v \in \tilde{V}$ during the unit time $\bar{t} \in \overline{T}$. Packetized power is spatially and temporally transferred as symbols in the digitized and quantized form.

4.1.3 Example of Symbol Propagation Matrix

Here, we illustrate the definitions mentioned above. Figure 4.1 shows a schematic of a symbol propagation matrix and packetized power. In this example, we set a directed graph $G = (\tilde{V}, A)$, where $\tilde{V} = \{v_0, v_1, v_2\}$ and $A = \{a_0, a_1\}$, and unit times $\overline{T} = \{\overline{t_0}, \overline{t_1}\}$. As schematically shown in Fig. 4.1(a), we consider a transmission of symbols Σ_m, in which a symbol $\sigma \in \Sigma_m$ is transferred at the link a_0 during the unit time $\overline{t_0}$ and at the

[3]In practical systems, energy can be dissipated at links and in nodes, and symbols may not be able to keep constant energy between nodes. These can become noise of power packetization, which is one of future work of this dissertation.

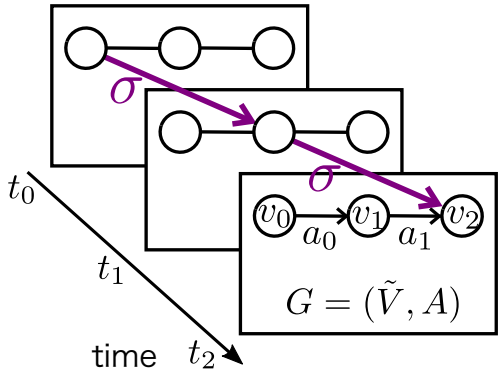

(a) A schematic diagram of symbol propagation. A symbol $\sigma \in \Sigma_m$ is transferred at the link a_0 during the unit time $\overline{t_0}$ and at the link a_1 during the unit time $\overline{t_1}$.

	a_0	a_1
$\overline{t_0}$	(σ, f)	$\sigma_\emptyset$
$\overline{t_1}$	$\sigma_\emptyset$	(σ, f)

(b) Symbol propagation matrix shown as a table.

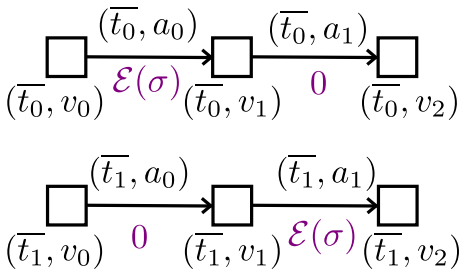

(c) Packetized power as network flow on $\hat{G} = (\overline{T} \times \tilde{V}, \overline{T} \times A)$.

Figure 4.1: Schematic of a symbol propagation matrix and packetized power. We set a directed graph $G = (\tilde{V}, A)$, where $\tilde{V} = \{v_0, v_1, v_2\}$ and $A = \{a_0, a_1\}$, and unit times $\overline{T} = \{\overline{t_0}, \overline{t_1}\}$.

link a_1 during the unit time $\overline{t_1}$. Then, the symbol propagation matrix is determined as shown in Fig. 4.1(b).

In this example, the graph $\hat{G} = (\overline{T} \times \tilde{V}, \overline{T} \times A)$ with spatio-temporal structure is defined as shown in Fig. 4.1(c). Then, packetized power u_m, which is represented by the

cell Σ_m, is introduced as a network flow on this graph. Here, we have $u_m(\overline{t_0}, a_0) = \mathcal{E}(\sigma)$, $u_m(\overline{t_0}, a_1) = 0$, $u_m(\overline{t_1}, a_0) = 0$, and $u_m(\overline{t_1}, a_1) = \mathcal{E}(\sigma)$. The boundary ∂u_m is equal to the change of stored energy corresponding to Σ_m. For example, we have $-\partial u_m(\overline{t_0}, v_1) = \mathcal{E}(\sigma)$ as the "strain", i.e. as the spatial difference of the packetized power u_m, and this value is equal to the increment of the stored energy in v_1 during the unit time $\overline{t_0} = [t_0, t_1)$.

4.2 Power Packet Transferability

To meet supply and demand, i.e. to represent given energies at sources and destinations with symbols, it is necessary to select a symbol at each link $a \in A$ during each unit time $\bar{t} \in \overline{T}$. Here, different choices lead to different transferability, that is the possibility to represent the given energies by transmission of symbols. In this section, we develop a framework to select packetized power in terms of transferability as a network flow problem. To make the problem solvable, we focus on a single cell $\Sigma \in \{\Sigma_m\}_{m=0}^{M-1}$. Besides, we set that $\mathcal{E}(\Sigma)$ to be successive integers $\{1, 2, \cdots\}$, that is, we consider integer flow $u : \overline{T} \times A \to \mathbb{Z}$. Because power packet is a unit of power, it is natural to consider integer flow.

4.2.1 Features of Packetized Power Contributing to Transferability

In networks, packetized power appears as:

V1: supplied energy from sources and supplied energy to destinations,

V2: transferred energy at each link during each unit time,

V3: change of stored energy in each router.

In terms of transferability, V1 needs to satisfy the given energies at sources and destinations, while V2 and V3 need to be small. As for V2, because power is given by the density of power packets at each links, transferred energy at links should be small to utilize limited density of packets during each unit time. In addition, by minimizing the summation of transferred energy, we can obtain the network flow in which energy is

supplied to each destination from sources placed near the destination. As for V3, change of stored energy in routers should be suppressed to keep symbol's energy controllable with density modulation of power packets between routers.

Thus, we select the features of packetized power $u : \overline{T} \times A \to \mathbb{Z}$ contributing to transferability as V1, V2, and V3. V2 is a value of the network flow $u(\bar{t}, a)$ $((\bar{t}, a) \in \overline{T} \times A)$, while V1 and V3 are calculated from the values of the boundary $\partial u(\bar{t}, v)$ $((\bar{t}, v) \in \overline{T} \times \tilde{V})$. V1 and V3 include time integral, such as total supplied energy from source $s \in V_{\mathrm{S}}$, i.e. $\sum_{n=0}^{N-1} \partial u(\overline{t_n}, s)$.

We introduce a cost function of the network flow problem as the summation of costs on these values. Because our features include not only values of network flow but also values of boundary and its integral, it is impossible to formulate the problem as the conventional minimum cost flow problem on the spatio-temporal graph $\hat{G}(\overline{T} \times \tilde{V}, \overline{T} \times A)$. Thus, in the next section, we provide the formulation using M-convex Submodular Flow Problem [62], which is the generalization of the minimum cost flow problem.

4.2.2 Formulation as M-convex Submodular Flow Problem

Now, we formulate the optimization problem to provide transferable packetized power. Here, M-convex submodular flow problem [62] is described on the graph $G(\overline{T} \times \tilde{V}, \overline{T} \times A)$ by univariate discrete convex functions[4] $f_{(\bar{t},a)} : \mathbb{Z} \to \mathbb{R} \cup \{\infty\}$ $((\bar{t}, a) \in \overline{T} \times A)$ and a M-convex function $f : \mathbb{Z}^{\overline{T} \times \tilde{V}} \to \mathbb{R} \cup \{\infty\}$ as

$$\text{Minimize} \qquad \Gamma(u) = \sum_{(\bar{t},a) \in \overline{T} \times A} f_{(\bar{t},a)}(u(\bar{t}, a)) + f(\partial u) \tag{4.9}$$

$$\text{subject to} \qquad u(\bar{t}, a) \in \operatorname{dom} f_{(\bar{t},a)} \qquad ((\bar{t}, a) \in \overline{T} \times A), \tag{4.10}$$

$$\partial u \in \operatorname{dom} f, \tag{4.11}$$

$$u(\bar{t}, a) \in \mathbb{Z} \qquad ((\bar{t}, a) \in \overline{T} \times A). \tag{4.12}$$

[4] A function $\phi : \mathbb{Z} \to \mathbb{R} \cup \{\infty\}$ is called a univariate discrete convex function if we have

$$\phi(x-1) + \phi(x+1) \geq 2\phi(x) \text{ for all } x \in \mathbb{Z} \tag{4.8}$$

and $\operatorname{dom} \phi \neq \emptyset$ [62]. Note that, if a function $\phi : \mathbb{R} \to \mathbb{R} \cup \{\infty\}$ is convex, ϕ satisfies Eq. (4.8).

The variable to be optimized is the network flow $u : \overline{T} \times A \to \mathbb{Z}$. Eq. (4.10) denotes capacity constraints of links, because $f_{(\bar{t},a)}$ is convex, and hence dom $f_{(\bar{t},a)}$ is an interval. Therefore, we can set an upper capacity $\hat{c} : \overline{T} \times A \to \mathbb{R} \cup \{+\infty\}$ and a lower capacity $\check{c} : \overline{T} \times A \to \mathbb{R} \cup \{-\infty\}$ where it is assumed that $\hat{c}(\bar{t}, a) \geq \check{c}(\bar{t}, a)$ for each $(\bar{t}, a) \in \overline{T} \times A$ by defining cost functions $f_{(\bar{t},a)}$ whose domain is equal to the interval $[\check{c}(\bar{t}, a), \hat{c}(\bar{t}, a)]$ $((\bar{t}, a) \in \overline{T} \times A)$.

Then, we introduce the cost function of the boundary as the summation of the costs on V1 and V3. To this end, we prove in Sect. 4.2.3 that, for a laminar family[5] $\mathcal{T}$ of subsets of $\overline{T} \times \tilde{V}$ and univariate discrete convex functions $f_X : \mathbb{Z} \to \mathbb{R} \cup \{+\infty\}$ indexed by $X \in \mathcal{T}$, the function defined by

$$f(\Delta u) = \begin{cases} \sum_{X \in \mathcal{T}} f_X(\Delta u(X)) & (\Delta u(\overline{T} \times \tilde{V}) = 0), \\ +\infty & (\text{otherwise}), \end{cases} \tag{4.14}$$

is an M-convex function. Here, we use the notation $\Delta u(X) = \sum_{(\bar{t},v) \in X} \Delta u(\bar{t}, v)$ for $\Delta u \in \mathbb{Z}^{\overline{T} \times \tilde{V}}$ and $X \subset \overline{T} \times \tilde{V}$. In Eq. (4.14), we can set costs on V1 and V3 by setting a laminar family $\mathcal{T}$ and univariate discrete convex functions $\{f_X\}_{X \in \mathcal{T}}$. For example, we can treat total supplied energy $\sum_{n=0}^{N-1} \partial u(\overline{t_n}, s)$ at source $s \in V_{\mathrm{S}}$ by including $\overline{T} \times \{s\}$ in $\mathcal{T}$. We take the laminar family $\mathcal{T}$ as a disjoint union of a laminar family $\mathcal{T}_{\mathrm{S,D}}$ of subsets of $\overline{T} \times (V_{\mathrm{S}} \cup V_{\mathrm{D}})$ and laminar families $\mathcal{T}_v$ of subsets of $\overline{T} \times \{v\}$ $(v \in V)$.

To sum up, we introduce the cost function Γ of packetized power u as

$$\Gamma(u) = \sum_{X \in \mathcal{T}_{\mathrm{S,D}}} f_X(\partial u(X)) + \sum_{(\bar{t},a) \in \overline{T} \times A} f_{(\bar{t},a)}(u(\bar{t}, a)) + \sum_{v \in V} \sum_{X \in \mathcal{T}_v} f_X(\partial u(X)). \tag{4.15}$$

The first, second, and third term in the right-hand side of Eq. (4.15) corresponds to the costs of V1, V2, and V3, respectively.

[5]By a laminar family, we mean a nonempty family $\mathcal{T}$ such that [62]

$$X, Y \in \mathcal{T} \Rightarrow X \cap Y = \emptyset \text{ or } X \subset Y \text{ or } X \supset Y. \tag{4.13}$$

4.2.3 Proof of the M-convexity of the Function f in Eq. (4.14)

In general, a laminar convex function has $\mathrm{M}^\natural$-convexity [62]. The following corollary shows that, if a laminar convex function is restricted to the hyper-plane, the function has M-convexity. From this corollary, we can confirm that the function f in Eq. (4.14) has M-convexity. This is proved referring to the Note 9.31. in [62] with a slight modification.

Corollary 4.1. *For a finite set V, a laminar family $\mathcal{T}$ of subsets of V, univariate discrete convex functions f_X $(X \in \mathcal{T})$, and an integer $r \in \mathbb{Z}$, a function $f : \mathbb{Z}^V \to \mathbb{R}$ is defined by*

$$f(x) = \begin{cases} \sum_{X \in \mathcal{T}} f_X(x(X)) & (x(V) = r), \\ +\infty & (\textit{otherwise}). \end{cases} \tag{4.16}$$

Then, f has M-convexity.

Proof of Corollary 4.1 Without loss of generality, we assume that $\emptyset \in \mathcal{T}$, $V \in \mathcal{T}$, and every singleton set belongs to $\mathcal{T}$. We represent $\mathcal{T}$ by a directed tree $G = (U, A; S, T)$ with root u_0, where $U = \{u_X \mid X \in \mathcal{T}\} \cup \{u_0\}$, $A = \{a_X \mid X \in \mathcal{T}\}$, $S = \{u_0\}$, $T = \{u_{\{v\}} \mid v \in V\}$, and $\partial^- a_X = u_X$ and $\partial^+ a_X = u_{\hat{X}}$ for $X \in \mathcal{T}$, where $\hat{X}$ denotes the smallest member of $\mathcal{T}$ that properly contains X (and $\hat{V} = 0$ by convention). We associate the given function f_X with arc a_X for $X \in \mathcal{T}$. We define a M-convex function $f' : \mathbb{Z}^S \to \mathbb{R}$ by

$$f'(x) = \begin{cases} 0 & (x = r), \\ \infty & (\text{otherwise}). \end{cases} \tag{4.17}$$

Then, f is the result of flow type transformation:

$$f(y) = \inf_{\xi, x} \left\{ f(x) + \sum_{X \in \mathcal{T}} f_X(\xi(a)) \;\middle|\; \partial\xi = (x, -y, \mathbf{0}), \right.$$
$$\left. \xi \in \mathbb{Z}^A, (x, -y, \mathbf{0}) \in \mathbb{Z}^S \times \mathbb{Z}^T \times \mathbb{Z}^{V \setminus (S \cup T)} \right\} \quad (y \in \mathbb{Z}^T). \tag{4.18}$$

Therefore, from Theorem 9.27. in [62], f has M-convexity. □

4.3 Examples

In this section, we verify that the formulation in Sect. 4.2 provides reasonable packetized power. Here, the power packet transferability is discussed through the following M-convex submodular flow problem:

$$\text{Minimize} \quad \Gamma(u) = \sum_{V' \in \mathcal{T}_{V_\mathrm{S} \cup V_\mathrm{D}}} f_{V'}(\partial u(\overline{T} \times V')) + \sum_{(\bar{t},a) \in \overline{T} \times A} \beta(a) \left| u(\bar{t}, a) \right| \tag{4.19}$$

$$\text{subject to} \quad \check{c}(a) \leq u(\bar{t}, a) \leq \hat{c}(a) \qquad ((\bar{t}, a) \in \overline{T} \times A), \tag{4.20}$$

$$\partial u(\bar{t}, v) = 0 \qquad ((\bar{t}, v) \in \overline{T} \times V), \tag{4.21}$$

$$u(\bar{t}, a) \in \mathbb{Z} \qquad ((\bar{t}, a) \in \overline{T} \times A), \tag{4.22}$$

where $\mathcal{T}_{V_\mathrm{S} \cup V_\mathrm{D}}$ is a laminar family of $V_\mathrm{S} \cup V_\mathrm{D}$. This problem is a special case in which we set the followings:

- Total supplied energy is the only concern at sources and destinations, i.e. $\mathcal{T}_{S,D}$ is set to be $\{\overline{T} \times V' \mid V' \in \mathcal{T}_{V_\mathrm{S} \cup V_\mathrm{D}}\}$.
- Cost functions $f_{(\bar{t},a)}$ are defined by the absolute value with domain $[\check{c}(a), \hat{c}(a)]$ $((\bar{t}, a) \in \overline{T} \times A)$. The coefficients $\beta(a)$ $(a \in A)$ are positive real numbers. Here, $f_{(\bar{t},a)}$ does not depend on unit times $\overline{T}$.
- Boundary of flow is set to be zero at routers V in Eq. (4.21) in order to transfer power without strain. Note that, because of this constraint, we have $\partial u(\{\bar{t}\} \times V_\mathrm{S}) = -\partial u(\{\bar{t}\} \times V_\mathrm{D})$ $(\bar{t} \in \overline{T})$ for a feasible flow u.

In the following, we investigate the aforementioned problem with a mesh graph as an example. The network structure is shown in Fig. 4.2, where $V = \{0, \cdots, 8\}$, $V_\mathrm{S} = \{\mathrm{s}_1, \mathrm{s}_2\}$, $V_\mathrm{D} = \{\mathrm{d}_1, \mathrm{d}_2\}$, and $A = \{0, 1, \cdots, 15\}$. For links between routers $a \in \{0, 1, \cdots, 11\}$, we set $\beta(a) = 1$, $\check{c}(a) = -1$, and $\hat{c}(a) = 1$. This capacity constraint implies $u(\bar{t}, a) \in \{-1, 0, 1\}$ $(\bar{t} \in \overline{T}, a \in \{0, 1, \cdots, 11\})$. For the other links $a \in \{12, 13, 14, 15\}$, we set $\beta(a) = 0$, $\check{c}(a) = -\infty$, and $\hat{c}(a) = \infty$, and hence we have $u(\bar{t}, a) \in \mathbb{Z}$ $(\bar{t} \in \overline{T})$. For the supplied energy of sources and destinations, three settings are considered here: (i) energy is given at each source and each destination by $U_1 : V_\mathrm{S} \cup V_\mathrm{D} \to \mathbb{Z}$, (ii) energy is given at each destination by $U_2 : V_\mathrm{D} \to \mathbb{Z}_{\geq 0}$, and (iii)

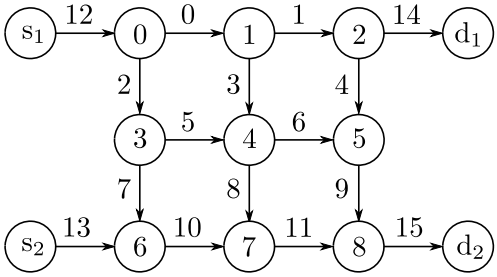

Figure 4.2: Network structure given as a mesh graph. For links between routers $a \in \{0, 1, \cdots, 11\}$, we set $\beta(a) = 1$, $\check{c}(a) = -1$ and $\hat{c}(a) = 1$, which imply $u(\bar{t}, a) \in \{-1, 0, 1\}$ ($\bar{t} \in \overline{T}$). For the other links $a \in \{12, 13, 14, 15\}$, we set $\beta(a) = 0$, $\check{c}(a) = -\infty$ and $\hat{c}(a) = \infty$, which imply $u(\bar{t}, a) \in \mathbb{Z}$ ($\bar{t} \in \overline{T}$).

the total supplied energy is given by $U \in \mathbb{Z}_{\geq 0}$. In the setting (i), U_1 is set to satisfy $\sum_{s \in V_{\mathrm{S}}} U_1(s) = -\sum_{d \in V_{\mathrm{D}}} U_1(d)$ because power is transferred without strain in this example. In the settings (i), (ii), and (iii), the objective functions are defined respectively as:

$$\Gamma_1(u) = \sum_{v \in V_{\mathrm{S}} \cup V_{\mathrm{D}}} 1000 \left| \partial u(\overline{T} \times \{v\}) - U_1(v) \right| + \sum_{(\bar{t}, a) \in \overline{T} \times A} \beta(a) \left| u(\bar{t}, a) \right|, \tag{4.23}$$

$$\Gamma_2(u) = \sum_{v \in V_{\mathrm{D}}} 1000 \left| \partial u(\overline{T} \times \{v\}) + U_2(v) \right| + \sum_{(\bar{t}, a) \in \overline{T} \times A} \beta(a) \left| u(\bar{t}, a) \right|, \tag{4.24}$$

and

$$\Gamma_3(u) = 1000 \left| \partial u(\overline{T} \times V_{\mathrm{D}}) + U \right| + \sum_{(\bar{t}, a) \in \overline{T} \times A} \beta(a) \left| u(\bar{t}, a) \right|. \tag{4.25}$$

In these functions, the coefficients of the first term are set to be 1000. This value is large enough to give priority to representation of the given energy over minimization of energy transferred through links.

Now, this problem is numerically solved by cycle-canceling algorithm [62] as mentioned in Appendix B.1. First, with Γ_1 in the setting (i), we set $N = 1$ and show an optimal flow for each setting of U_1 in Figs. 4.3–4.8. The six optimal flows are named as $\{\alpha_i\}_{i=0}^{5}$. The optimal flows are listed in Tab. 4.1 with their settings and costs $\Gamma_1(u)$. The results confirm the following properties of this problem at $N = 1$:

- By minimizing the cost of V1, given energy U_1 is represented at each source and each destination.

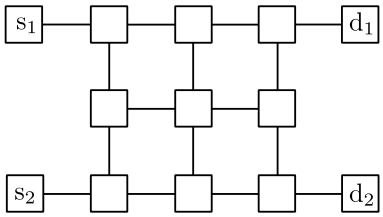

Figure 4.3: An optimal flow in the setting (i) with $N = 1$, $U_1(\mathrm{s}_1) = 0$, $U_1(\mathrm{s}_2) = 0$, $U_1(\mathrm{d}_1) = 0$, and $U_1(\mathrm{d}_2) = 0$, called α_0.

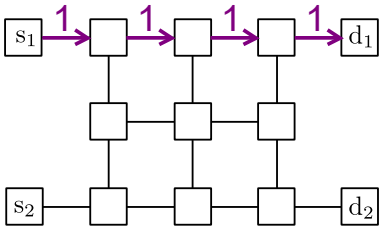

Figure 4.4: An optimal flow in the setting (i) with $N = 1$, $U_1(\mathrm{s}_1) = 1$, $U_1(\mathrm{s}_2) = 0$, $U_1(\mathrm{d}_1) = -1$, and $U_1(\mathrm{d}_2) = 0$, called α_1.

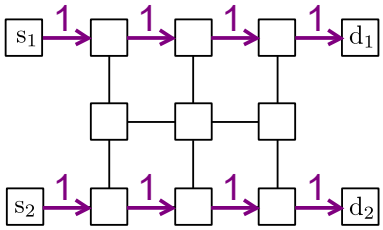

Figure 4.5: An optimal flow in the setting (i) with $N = 1$, $U_1(\mathrm{s}_1) = 1$, $U_1(\mathrm{s}_2) = 1$, $U_1(\mathrm{d}_1) = -1$, and $U_1(\mathrm{d}_2) = -1$, called α_2.

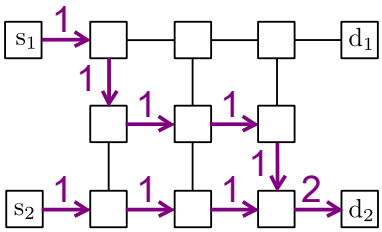

Figure 4.6: An optimal flow in the setting (i) with $N = 1$, $U_1(\mathrm{s}_1) = 1$, $U_1(\mathrm{s}_2) = 1$, $U_1(\mathrm{d}_1) = 0$, and $U_1(\mathrm{d}_2) = -2$, called α_3.

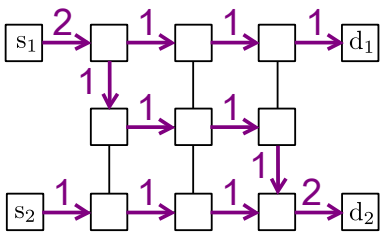

Figure 4.7: An optimal flow in the setting (i) with $N = 1$, $U_1(\mathrm{s}_1) = 2$, $U_1(\mathrm{s}_2) = 1$, $U_1(\mathrm{d}_1) = -1$, and $U_1(\mathrm{d}_2) = -2$, called α_4.

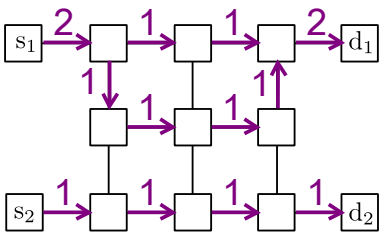

Figure 4.8: An optimal flow in the setting (i) with $N = 1$, $U_1(\mathrm{s}_1) = 2$, $U_1(\mathrm{s}_2) = 1$, $U_1(\mathrm{d}_1) = -2$, and $U_1(\mathrm{d}_2) = -1$, called α_5.

Table 4.1: Optimal flows u in the setting (i) and their cost with various settings of given energy U_1.

N	$U_1(\mathrm{s}_1)$, $U_1(\mathrm{s}_2)$	$U_1(\mathrm{d}_1)$, $U_1(\mathrm{d}_2)$	Cost $\Gamma_1(u)$	An Optimal Flow
1	0, 0	0, 0	0	α_0
1	1, 0	-1, 0	2	α_1
1	1, 1	-1, -1	4	α_2
1	1, 1	0, -2	6	α_3
1	2, 1	-1, -2	8	α_4
1	2, 1	-2, -1	8	α_5

Table 4.2: Optimal flows u in the setting (ii) and their cost with various settings of N and given energy U_2. Here, optimal flows are denoted by the sequence of $\{\alpha_i\}_{i=0}^5$ in time order.

N	$U_2(\mathrm{d}_1)$, $U_2(\mathrm{d}_2)$	Cost $\Gamma_2(u)$	An Optimal Flow
2	3, 3	16	$\alpha_4\alpha_5$
3	3, 3	12	$\alpha_2\alpha_2\alpha_2$
5	3, 3	12	$\alpha_2\alpha_2\alpha_2\alpha_0\alpha_0$
2	5, 2	1016	$\alpha_5\alpha_5$
3	5, 2	18	$\alpha_5\alpha_5\alpha_1$
5	5, 2	14	$\alpha_2\alpha_2\alpha_1\alpha_1\alpha_1$

Table 4.3: Optimal flows u in the setting (iii) and their cost with various settings of N and given energy U. Here, optimal flows are denoted by the sequence of $\{\alpha_i\}_{i=0}^5$ in time order. The settings of N and U correspond to the settings in Tab. 4.2 through the relationship $\sum_{d\in V_\mathrm{D}} U_2(d) = U$.

N	U	Cost $\Gamma_3(u)$	An Optimal Flow
2	6	16	$\alpha_4\alpha_4$
3	6	12	$\alpha_2\alpha_2\alpha_2$
5	6	12	$\alpha_2\alpha_2\alpha_2\alpha_0\alpha_0$
2	7	1016	$\alpha_4\alpha_4$
3	7	16	$\alpha_4\alpha_2\alpha_2$
5	7	14	$\alpha_2\alpha_2\alpha_2\alpha_1\alpha_0$

- By minimizing the cost of V2, energy is transferred with the smallest number of links. Note that, in flow α_2 in Fig. 4.5, the destinations d_1 and d_2 are supplied from the nearest sources, i.e. s_1 for d_1 and s_2 for d_2.

- By imposing the constrain on V3, energy is transferred without strain, i.e. without change of stored energy.

Then, with Γ_2 in the setting (ii) and with Γ_3 in the setting (iii), we solve the problem and list the optimal flows as shown in Tabs. 4.2 and 4.3, respectively. Here, optimal flows are denoted by the sequence of $\{\alpha_i\}_{i=0}^{5}$ in time order. Note that the settings of N and U in Tab. 4.3 correspond to the settings in Tab. 4.2 through the relationship $\sum_{d\in V_{\mathrm{D}}} U_2(d) = U$. In the optimal flows whose costs exceed 1000, the given energy is not represented. Tables 4.2 and 4.3 imply the following properties of this problem:

- The cost of the optimal flow decreases as the number of time step, i.e. N, increases up to a certain point. From N exceeding the point, the cost takes a constant value and α_0, in which symbols are not transferred, is added to the optimal flow.

- The cost of the optimal flow can decrease when the distribution of supplied energy is not specified and the total supplied energy is given. For example, the cost becomes $\Gamma_2(u) = 18$ when we set $N = 3$, $U_2(\mathrm{d}_1) = 5$, and $U_2(\mathrm{d}_2) = 2$ in the setting (ii), while the cost becomes $\Gamma_3(u) = 16$ when we set $N = 3$ and $U = 7$, which is equal to $\sum_{d\in V_{\mathrm{D}}} U_2(d) = 5 + 2$, in the setting (iii).

In other words, more transferable packetized power can be selected if power can be transferred with less temporal and spatial restriction. These properties show that power can be packetized and be controllable while preserving reasonable properties of power.

4.4 Summary

In this chapter, we introduced symbol propagation matrix as a representation of packetized power in networks for a finite duration. Packetized power is described as network flow on a graph with a spatio-temporal structure. Here, power is spatially and temporally transferred in the digitized form as symbols. Then, we considered the

problem of selecting a SPM in terms of transferability, that is, the possibility to represent given energies at sources and destinations for the finite duration. To select packetized power as a network flow problem, we weighted the supplied energy from the sources and the supplied energy to the destinations (V1), transferred energy at each link during each unit time (V2), and change of stored energy in each router (V3). Focusing on a single variety of power flow and considering integer flow, the minimization problem was formulated as M-convex submodular flow problem which is known as generalization of the minimum cost flow problem and is solvable. Finally, the formulation was discussed through examples, and the results show that power can be packetized and be controllable while preserving reasonable properties of power.

Chapter 5

Dynamics of Energy Transfer

This chapter investigates the dynamics of energy transfer with power packets in electrical energy networks based on the conservation of energy. We mainly consider the discrete dynamics of energy transfer in the formulation of symbol propagation matrix discussed in Chapter 4. Here, unlike Chapter 4 in which power flow is globally optimized, symbols to be transmitted are determined by exchanging information between adjacent nodes. In this way, incompleteness of information [65] is considered, and hence symbols are dynamically transferred in a decentralized manner.

In the following sections, we design the operation of nodes in order to match intermittent and spatially distributed supply and demand. In networks, there exist up-stream dispatching of demanded power from destinations to sources and down-stream dispatching of supplied power from sources to destinations. To include numerous sources, destinations, and storage units, the network is designed to separately and individually manage the up-stream dispatching and the down-stream dispatching at the symbol level in a decentralized manner. Here, when symbols are transmitted in a decentralized manner, it is hard to transfer energy without "strain", i.e. without the temporal change of energy stored in each router. Thus, the router's operation is designed to keep stored energy within a given capacity in order to keep symbol's energy controllable with density modulation of power packets between routers. Next, it is numerically verified that supply and demand can be met in the designed network.

At last, we take a glance at corresponding continuous dynamics for future work. Transfer of power packet can be considered as wave propagation by averaging in time.

5.1 Mathematical Representation

Based on the formulation of symbol propagation matrix discussed in Chapter 4, we provide a mathematical representation of the discrete dynamics. The set of symbols Σ_{T} and their energies $\mathcal{E} : \Sigma_{\mathrm{T}} \to \mathbb{R}_{>0}$ are given to the network. The symbols have a partition $\{\Sigma_m\}_{m=0,1,\cdots,M-1}$, whose cell represents a distinct power flow. The network structure is given as a directed graph $G = (\tilde{V}, A)$, where $\tilde{V}$ is a disjoint union of the set of routers V, sources V_{S}, and destinations V_{D}, and A is the set of links. We set that network is synchronized and introduce unit times $\overline{T} = \{\overline{t_0}, \overline{t_1}, \cdots, \overline{t_{N-1}}\}$ and their boundaries $T = \{t_0, t_1, \cdots, t_N\}$, where N is a positive integer, $\overline{t_n} := [t_n, t_{n+1})$, and $t_0 < t_1 < \cdots < t_N$.

We focus on a single cell $\Sigma \in \{\Sigma_m\}_{m=0}^{M-1}$ and consider packetized power with

$$SPM : \overline{T} \times A \to \Sigma \times \{\mathrm{f}, \mathrm{b}\} \cup \{\sigma_\emptyset\}. \tag{5.1}$$

Then, we define packetized power

$$u : \overline{T} \times A \to \mathbb{R} \tag{5.2}$$

and energy[1]

$$U : T \times \tilde{V} \to \mathbb{R}. \tag{5.3}$$

Here, we define energy U at each time $t \in T$ in each node $v \in \tilde{V}$. For each node $v \in \tilde{V}$, we choose zero of the energy at the initial time, setting $U(t_0, v) = 0$ $(v \in \tilde{V})$. Note that $U(t_n, v)$ becomes negative if the node v supplies positive energy to the adjacent nodes during $[t_0, t_n)$. In the consideration of discrete dynamics, we assume that, if energy is kept within a given capacity in each router, symbols can always bring energy between nodes with density modulation of power packets.

Now, we consider the discrete dynamics. Here, we assume the conservation of energy; more precisely, we assume that all energy exchanges in each node $v \in \tilde{V}$ are represented with symbols transferred through the adjacent links $a \in \delta^+ v \cup \delta^- v$. Then, we obtain the

[1]In each router, energy is stored in the storage unit corresponding to the cell Σ.

equation of continuity:

$$U(t_{n+1}, v) - U(t_n, v) + \partial u(\overline{t_n}, v) = 0 \quad (v \in \tilde{V}, n \in \{0, \cdots, N-1\}). \tag{5.4}$$

Eq. (5.4) shows that, for each node $v \in \tilde{V}$, the spatial difference of power $\partial u(\overline{t_n}, v)$ is equal to the temporal change of stored energy $-U(t_{n+1}, v) + U(t_n, v)$. From Eq. (5.4), we find that energy $U(t_{n+1}, \cdot)$ is determined by $U(t_n, \cdot)$ and $u(\overline{t_n}, \cdot)$. In addition, the packetized power $u(\overline{t_n}, \cdot)$ is determined from $SPM(\overline{t_n}, \cdot)$ as

$$u(\overline{t_n}, a) = \begin{cases} \mathcal{E}(\sigma) & (SPM(\overline{t_n}, a) = (\sigma, \mathrm{f})), \\ -\mathcal{E}(\sigma) & (SPM(\overline{t_n}, a) = (\sigma, \mathrm{b})), \\ 0 & (SPM(\overline{t_n}, a) = \sigma_\emptyset). \end{cases} \tag{5.5}$$

Therefore, the discrete dynamics is described by operation of selecting symbols to be transferred during a unit time $\overline{t_n} = [t_n, t_{n+1}) \in \overline{T}$, i.e. $SPM(\overline{t_n}, \cdot)$, at the time t_n. When each node selects symbols by exchanging information between adjacent nodes, packetized power and energy are spatially and temporally developed.

5.2 Design Framework of Networks

In this and the next section, the operation of nodes is designed to meet supply and demand. In the design, at each time $t_n \in T$, each node selects symbols to be transferred during the unit time $\overline{t_n} \in \overline{T}$ by exchanging information between adjacent nodes. Then, packetized power and energy are spatially and temporally developed as mentioned above.

This section presents design framework of networks. To include numerous sources, destinations, and storage units, the network is designed to separately and individually manage the up-stream dispatching of demand and the down-stream dispatching of supply at the symbol level in a decentralized manner. Because it is hard to transfer energy without storing it in a decentralized manner, we also consider the router's operation to keep stored energy within a given capacity. The operation of nodes is specifically designed in the next section.

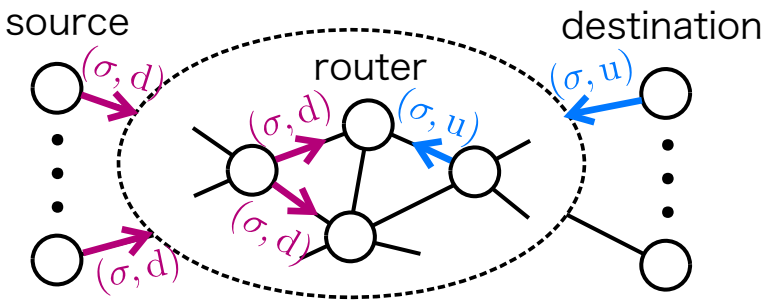

Figure 5.1: A schematic of up-stream requests and down-stream requests in networks. Up-stream requests bring up-stream dispatching of demanded power from destinations to sources, while down-stream requests bring down-stream dispatching of supplied power from sources to destinations.

5.2.1 Up-stream Request and Down-stream Request

We consider the router's operation to manage the up-stream dispatching of demand and the down-stream dispatching of supply in a decentralized manner. In our design, each node selects symbols by exchanging requests of symbols, denoted by

$$\Sigma \times \{\mathrm{u}, \mathrm{d}\}, \tag{5.6}$$

between adjacent nodes. Here, $(\sigma, \mathrm{u}) \in \Sigma \times \{\mathrm{u}\}$ denotes an up-stream request to get the symbol σ from the adjacent node and $(\sigma, \mathrm{d}) \in \Sigma \times \{\mathrm{d}\}$ denotes a down-stream request to give the symbol σ to the adjacent node. If the up-stream request $(\sigma, \mathrm{u}) \in \Sigma \times \{\mathrm{u}\}$ is accepted by an adjacent node, the negative energy $-\mathcal{E}(\sigma)$ is transferred to the adjacent node. If the down-stream request $(\sigma, \mathrm{d}) \in \Sigma \times \{\mathrm{u}\}$ is accepted by an adjacent node, the positive energy $\mathcal{E}(\sigma)$ is transferred to the adjacent node.

In networks, as shown in Fig. 5.1, up-stream requests $\Sigma \times \{\mathrm{u}\}$ are generated at destinations and bring up-stream dispatching of demanded power to sources, while down-stream requests $\Sigma \times \{\mathrm{d}\}$ are generated at sources and bring down-stream dispatching of supplied power to destinations. Then, the network function to match supply and demand is given as the router's operation of matching the up-stream requests and the down-stream requests at the symbol level.

5.2.2 Capacity of Energy

As a capacity of energy, we set a condition of router's operation:

Condition:

For a router $v \in V$, energy satisfies

$$U_{\min}(v) \leq U(t_n, v) \leq U_{\max}(v) \quad (n \in \{1, \cdots, N\}), \tag{5.7}$$

where $U_{\max} : V \to \mathbb{Z}$ and $U_{\min} : V \to \mathbb{Z}$ denote the upper limit and the lower limit respectively, which satisfy $U_{\min}(v) < 0 < U_{\max}(v)$.

For each router $v \in V$, the lower limit $U_{\min}(v)$ restricts the acceptance of up-stream requests, while the upper limit $U_{\max}(v)$ restricts the acceptance of down-stream requests. At a time t_n, a router $v \in V$ can not accept an up-stream request (σ, u) if $U(t_n, v) - \mathcal{E}(\sigma) < U_{\min}(v)$ and can not accept a down-stream request (σ, d) if $U(t_n, v) + \mathcal{E}(\sigma) > U_{\max}(v)$. The condition is introduced to keep symbol's energy controllable with density modulation of power packets between routers.

5.3 Operation of Nodes

Here, the operation of nodes is specifically designed.

5.3.1 Procedure of Selecting Symbols

We present the procedure of selecting symbols to be transferred. Transferred symbols $SPM(\overline{t_n}, \cdot)$ are determined between adjacent nodes at time t_n in two steps in a synchronized manner: in the first step, each node selects requests and exchanges it; in the second step, each node decides whether to accept the received requests. In the following, each step is described in detail.

Step 1 (Selection and Exchange of Requests):

Each node $v \in \tilde{V}$ selects a request which is sent through each adjacent link $a \in \delta^+ v \cup \delta^- v$, as

$$req_v^{\mathrm{tx}} : \delta^+ v \cup \delta^- v \to \Sigma \times \{\mathrm{u}, \mathrm{d}\} \cup \{\sigma_\emptyset\}, \tag{5.8}$$

where $req_v^{\mathrm{tx}}(a) = \sigma_\emptyset$ denotes that there is no request for the link a. Note that an element of $\Sigma \times \{\mathrm{u}, \mathrm{d}\} \cup \{\sigma_\emptyset\}$ is selected at each boundary node of link $a \in A$ in the network. Here, we assume that the requests from both boundary nodes are exchanged without errors at each link. For convenience, we introduce a map defined by

$$req_v^{\mathrm{rx}} : \delta^+ v \cup \delta^- v \ni a \mapsto \begin{cases} req_{\partial^+ a}^{\mathrm{tx}}(a) & (v = \partial^- a), \\ req_{\partial^- a}^{\mathrm{tx}}(a) & (v = \partial^+ a), \end{cases} \tag{5.9}$$

for $v \in \tilde{V}$ as a representation of received requests at node v.

Step 2 (Acceptance of Requests) :

Each node $v \in \tilde{V}$ decides whether to accept the received requests req_v^{rx}. More precisely, the node v selects links, at which requested symbols are accepted to be transferred, as

$$acc_v \subset (req_v^{\mathrm{rx}})^{-1}(\Sigma \times \{\mathrm{u}, \mathrm{d}\}) \in 2^A. \tag{5.10}$$

When deciding whether to accept a received request, each node avoids conflicts between a sent request and the received request through each link. To be specific, the decision rule is designed to satisfy that, for each link $a \in A$ such that $a \in acc_{\partial^+ a} \cap acc_{\partial^- a}$, $\{req_{\partial^+ a}^{\mathrm{rx}}(a), req_{\partial^- a}^{\mathrm{rx}}(a)\} \in \{\{(\sigma, \mathrm{u}), (\sigma, \mathrm{d})\} \mid \sigma \in \Sigma\}$ holds.

Note that, although a router can request a single symbol through multiple links, the symbol can not be copied, and hence can not be transferred through multiple links, as a result of the conservation of energy. This is a significant difference from the packet-switching communication networks, in which flooding of packets is available [5]. In our design, a single symbol is requested at a single link. Then, we assume that, if a request of a symbol is accepted in the second step, the symbol is always transferred. In this way, $SPM(\overline{t_n}, \cdot)$ is determined by the selection of req_v^{tx} and acc_v at each node $v \in \tilde{V}$.

5.3.2 Direction of Symbols

Here, we set a direction of symbols at each node in networks. For each symbol $\sigma \in \Sigma$, a router $v \in V$ has a set of links through which the router can send an up-stream request (σ, u), denoted as $RT_\sigma^{\mathrm{u}}(v) \subset \delta^+ v \cup \delta^- v$, and a set of links through which the router can

send a down-stream request (σ, d), denotes as $RT^{\mathrm{d}}_{\sigma}(v) \subset \delta^{+}v \cup \delta^{-}v$. It is assumed that $RT^{\mathrm{u}}_{\sigma}(v)$ and $RT^{\mathrm{d}}_{\sigma}(v)$ are set to be compatible in the network; more precisely, for $v \in V$ and $\sigma \in \Sigma$, we assume $\partial^{\pm}a \in RT^{\mathrm{u}}_{\sigma}(v) \Leftrightarrow \partial^{\mp}a \in RT^{\mathrm{d}}_{\sigma}(v)$ for all $a \in A$.

For simplicity, we assume that sources and destinations have only one adjacent node and the adjacent node is a router. To be specific, we assume that $\delta^{-}s = \emptyset$ and $\delta^{+}s = \{a\}$, where $\partial^{-}a \in V$, for $s \in V_{\mathrm{S}}$, and that $\delta^{+}d = \emptyset$ and $\partial^{-}d = \{a\}$, where $\partial^{+}a \in V$, for $d \in V_{\mathrm{D}}$.

5.3.3 Network with Single Symbol

Now, a network design is presented. For simplicity, we set $\Sigma = \{\sigma\}$ and $\mathcal{E}(\sigma) = \{1\}$. Then, we consider integer flow $u : \overline{T} \times A \to \{-1, 0, 1\}$ with the upper limit $\hat{c}(a) = 1$ and the lower limit $\check{c}(a) = -1$ for each link $a \in A$. The energy is an integer function $U : T \times \tilde{V} \to \mathbb{Z}$. In our design, each router requests symbols in such a way that energy stored in the router becomes zero. When a router receives requests, it accepts the requests while keeping the stored energy within the capacity as shown in Eq. (5.7). As for supply and demand, an up-stream request is generated at each time with probability $p_d \in [0, 1]$ at each destination $d \in V_{\mathrm{D}}$, while a down-stream request is generated at each time with probability $p_s \in [0, 1]$ at each source $s \in V_{\mathrm{S}}$.

Below, the node's operation is presented at routers, sources, and destinations according to the procedure described in Sect. 5.3.1.

Operation of Router

The operation of a router $v \in V$ is presented at time $t_n \in T$.

Step 1 (Selection of req^{tx}_v):

If $U(t_n, v) > 0$, the router randomly chooses links up to $U(t_n, v)$ from $RT^{\mathrm{d}}_{\sigma}(v)$ and requests (σ, d) through the each chosen link. If $U(t_n, v) < 0$, the router randomly chooses links up to $|U(t_n, v)|$ from $RT^{\mathrm{u}}_{\sigma}(v)$ and requests (σ, u) through the each chosen link.

Step 2 (Selection of acc_v):

The router accepts the received requests req^{rx}_v at the following links included in $(req^{\mathrm{rx}}_v)^{-1}(\Sigma \times \{\mathrm{u}, \mathrm{d}\})$:

- The links $a \in (req_v^{\mathrm{rx}})^{-1}(\Sigma \times \{\mathrm{u}, \mathrm{d}\})$ which satisfy $\{req_v^{\mathrm{rx}}(a), req_v^{\mathrm{tx}}(a)\} = \{(\sigma, \mathrm{u}), (\sigma, \mathrm{d})\}$;
- Randomly chosen links up to $U(t_n, v) - U_{\min}(v)$ from the links $a \in (req_v^{\mathrm{rx}})^{-1}(\Sigma \times \{\mathrm{u}, \mathrm{d}\})$ which satisfy $req_v^{\mathrm{rx}}(a) = (\sigma, \mathrm{u})$ and $req_v^{\mathrm{tx}}(a) = \sigma_\emptyset$;
- Randomly chosen links up to $U_{\max}(v) - U(t_n, v)$ from the links $a \in (req_v^{\mathrm{rx}})^{-1}(\Sigma \times \{\mathrm{u}, \mathrm{d}\})$ which satisfy $req_v^{\mathrm{rx}}(a) = (\sigma, \mathrm{d})$ and $req_v^{\mathrm{tx}}(a) = \sigma_\emptyset$.

Operation of Source

The operation of a source $s \in V_{\mathrm{S}}$ is presented at time $t_n \in T$. Note that the source s has only one adjacent link, denoted as a.

Step 1 (Selection of req_s^{tx}):

The source s requests (σ, d) with probability p_s.

Step 2 (Selection of acc_s):

The source s accepts the received request $req_s^{\mathrm{rx}}(a)$ only if the received request is an up-stream request, i.e. $req_s^{\mathrm{rx}}(a) = (\sigma, \mathrm{u})$, and the source s sends a down-stream request in Step 1, i.e. $req_s^{\mathrm{tx}}(a) = (\sigma, \mathrm{d})$.

Operation of Destination

The operation of a destination $d \in V_{\mathrm{D}}$ is presented at time $t_n \in T$. Note that the destination d has only one adjacent link, denoted as a.

Step 1 (Selection of req_d^{tx}):

The destination d requests (σ, u) with probability p_d.

Step 2 (Selection of acc_d):

The destination d accepts the received request $req_d^{\mathrm{rx}}(a)$ only if the received request is a down-stream request, i.e. $req_d^{\mathrm{rx}}(a) = (\sigma, \mathrm{d})$, and the destination d sends an up-stream request in Step 1, i.e. $req_s^{\mathrm{tx}}(a) = (\sigma, \mathrm{u})$.

5.4 Numerical Verification

In this section, we numerically verify the network presented in Sect. 5.3.3. The network structure is shown in Fig. 5.2, where $V = \{0, 1, \cdots, 8\}$, $V_{\mathrm{S}} = \{\mathrm{s}_1, \mathrm{s}_2\}$, $V_{\mathrm{D}} =$

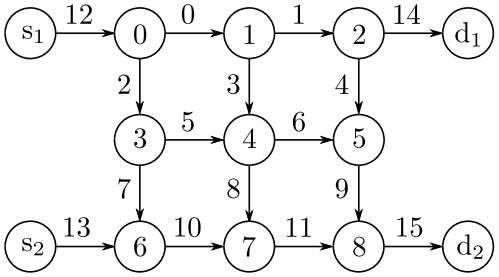

Figure 5.2: Network structure given as a mesh graph. This graph is same as the graph in Fig. 4.2 in Chapter 4.

Table 5.1: Direction of down-stream requests RT_σ^{d} at each router $v \in V$.

$v \in V$	$RT_\sigma^{\mathrm{d}}(v)$
0	{0, 2}
1	{1, 3}
2	{4, 14}
3	{2, 5, 7}
4	{3, 6, 8}
5	{4, 9}
6	{7, 10}
7	{8, 11}
8	{9, 15}

$\{\mathrm{d}_1, \mathrm{d}_2\}$, and $A = \{0, 1, \cdots, 15\}$. Symbols are transferred by $N = 100$ steps. The upper limit and the lower limit of energy in each router $v \in V$ are set as $U_{\max}(v) = 3$ and $U_{\min}(v) = -3$ respectively. Then, at each router $v \in V$, we have $U(t_n, v) \in \{-3, -2, -1, 0, 1, 2, 3\}$ for $t_n \in T$. The direction of symbols is shown in Tab. 5.1 as $RT_\sigma^{\mathrm{d}}(v)$ for each router $v \in V$. RT_σ^{d} forbids symbols to move in the left direction in Fig. 5.2.

Then, we calculate the total supplied energy from sources $-U(t_{100}, \mathrm{s}_1)$, $-U(t_{100}, \mathrm{s}_2)$ and to destinations $U(t_{100}, \mathrm{d}_1)$, $U(t_{100}, \mathrm{d}_2)$ with various settings of p_{s_1}, p_{s_2}, p_{d_1}, and p_{d_2}. The energies are calculated as an average of 100,000 trials.

First, we consider the case in which the up-stream requests and the down-stream requests are balanced, i.e. $p_{\mathrm{s}_1} + p_{\mathrm{s}_2} = p_{\mathrm{d}_1} + p_{\mathrm{d}_2}$ holds. The result is shown in Tab. 5.2. From the result of the average value, we can find that almost all of up-stream requests and down-stream requests are satisfied in the network.

Then, we consider the case in which up-stream requests are sent from the destinations more frequently than down-stream requests of the sources, i.e. $p_{\mathrm{s}_1} + p_{\mathrm{s}_2} < p_{\mathrm{d}_1} + p_{\mathrm{d}_2}$ holds (see Tab. 5.2). From the result of the average value, we can find that almost all of

Table 5.2: $U(t_{100}, v)$ $(v \in V_{\mathrm{S}} \cup V_{\mathrm{D}})$ in the case of $p_{\mathrm{s}_1} + p_{\mathrm{s}_2} = p_{\mathrm{d}_1} + p_{\mathrm{d}_2}$. The value of $U(t_{100}, v)$ is represented as average(standard deviation).

$v \in V_{\mathrm{S}} \cup V_{\mathrm{D}}$	s_1	s_2	d_1	d_2
p_v	1.00	1.00	1.00	1.00
$U(t_{100}, v)$	-100(0.0)	-100(0.0)	100(0.0)	100(0.0)
p_v	1.00	0.10	0.10	1.00
$U(t_{100}, v)$	-100(0.1)	-10(3.0)	10(3.0)	100(0.1)
p_v	0.50	0.50	0.70	0.30
$U(t_{100}, v)$	-50(5.0)	-50(4.9)	70(4.5)	30(4.6)

Table 5.3: $U(t_{100}, v)$ $(v \in V_{\mathrm{S}} \cup V_{\mathrm{D}})$ in the case of $p_{\mathrm{s}_1} + p_{\mathrm{s}_2} < p_{\mathrm{d}_1} + p_{\mathrm{d}_2}$. The value of $U(t_{100}, v)$ is represented as average(standard deviation).

$v \in V_{\mathrm{S}} \cup V_{\mathrm{D}}$	s_1	s_2	d_1	d_2
p_v	0.30	0.30	0.70	0.30
$U(t_{100}, v)$	-30(4.6)	-30(4.6)	56(5.7)	27(3.8)
p_v	0.60	0.00	0.70	0.30
$U(t_{100}, v)$	-60(4.9)	0(0.0)	63(4.0)	21(3.5)
p_v	0.00	0.60	0.70	0.30
$U(t_{100}, v)$	0(0.0)	-60(4.9)	52(5.8)	30(4.4)

down-stream requests are satisfied but some up-stream requests are not satisfied. For example, in the case of $p_{\mathrm{s}_1} = 0.30$, $p_{\mathrm{s}_2} = 0.30$, $p_{\mathrm{d}_1} = 0.70$, and $p_{\mathrm{d}_2} = 0.30$, d_1 and d_2 will send up-stream requests 70 times and 30 times respectively in average, but the averages of the supplied energies are $U(t_{100}, \mathrm{d}_1) = 56 < 70$ and $U(t_{100}, \mathrm{d}_2) = 27 < 30$. This seems to be a natural result because of the conservation of energy.

5.5 Discussion on Continuous Dynamics

At last, we take a glance at the corresponding continuous dynamics for future work. In this section, we consider power packet transfer as wave propagation by averaging in time. The wave propagation is considered in a series of inductor-coupled resonator.

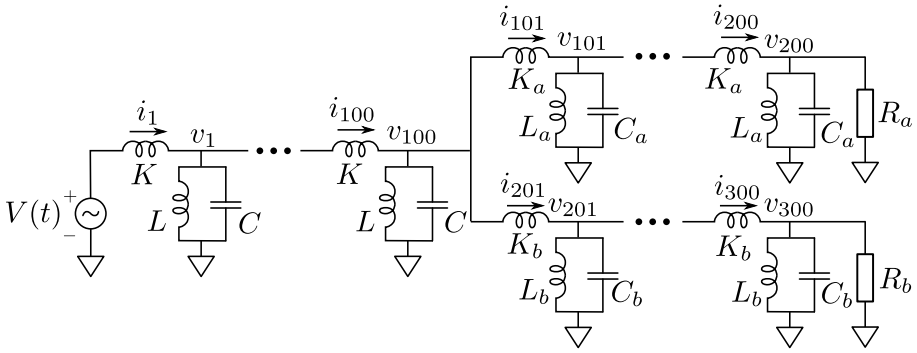

Figure 5.3: A series of inductor-coupled resonator with branch.

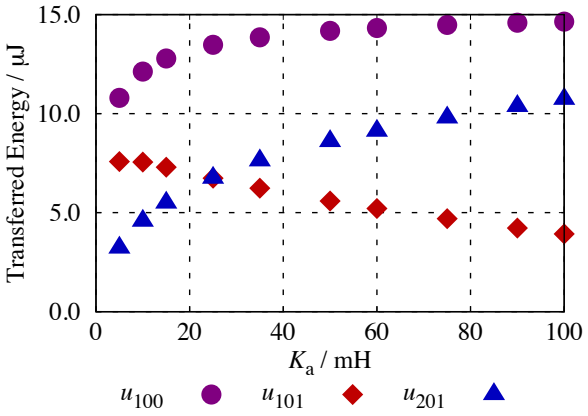

Figure 5.4: The relationship between K_a and energy transferred at the branch point.

This is the model of the Schrödinger equation, in which energy stored in each resonator corresponds to the probability distribution in quantum mechanics, while power flow corresponds to the probability flux in quantum mechanics [66, 67].

Figure 5.3 shows a series of inductor-coupled resonator with branch. Each branch line has uniform circuit parameters. In this circuit, we investigate energy transferred at the branch point. The voltage source generates a sinusoidal wave with a Gaussian envelope, $V(t) = \mathrm{e}^{-(t-\tau)^2(\Delta\omega)^2} \sin \omega_c t$. Here, we set $\tau = 20$ ms, $\Delta\omega = 100$ Hz, and $\omega_c = 11$ kHz. Circuit parameters are set as $L = L_a = L_b = 10$ mH, $C = C_a = C_b = 1$ μF, $K = K_b = 25$ mH, and $R_a = R_b = 100$ Ω.

With this setting, a transient analysis is performed using a circuit simulator called

Ngspice [68] referring to [67]. We evaluate transferred energy at the branch point as

$$u_n = \int_{0\ \mathrm{ms}}^{85\ \mathrm{ms}} v_n i_n \mathrm{d}t \quad (n \in \{100, 101, 201\}). \tag{5.11}$$

The integral interval is set to neglect the reflected wave from the each end of the loads. The relationship between the value of K_a and transferred energies u_{100}, u_{101}, and u_{201} are shown in Fig. 5.4. Figure 5.4 demonstrates that proportion of energy transferred toward each end of the load changes with varying the circuit impedance K_a. The result implies that we could adjust the transferred energy by changing circuit impedance in the time domain as average.

5.6 Summary

In this chapter, we investigated the dynamics of energy transfer with power packets in networks based on the conservation of energy. We mainly considered discrete dynamics in the formulation of the symbol propagation matrix introduced in Chapter 4. First, we mathematically represented the discrete dynamics of packetized power and energy stored in each node. The packetized power and the stored energy satisfy the equation of continuity. The discrete dynamics are described by the operation of selecting symbols to be transmitted. Then, we presented the design framework of networks and specifically the design of node's operation. The network was designed to separately and individually manage the up-stream dispatching of required power from destinations and the down-stream dispatching of supplied power from sources at the symbol level. Here, symbols to be transmitted were determined by exchanging information between adjacent nodes in a decentralized manner. The router's operation was designed to keep stored energy within a given capacity. It is numerically verified that supply and demand can be met in the designed network.

Finally, we took a glance at the corresponding continuous dynamics for future work. Here, power packet transfer is considered as wave propagation by averaging in time. The numerical result implies that we could adjust the transferred energy by changing circuit impedance in the time domain as average.

Chapter 6

Conclusion and Future Work

This dissertation addressed the design of electrical energy networks based on power packetization. We defined power packet as a unit of electric power and mathematically established the packet-centric framework in which power is digitized and quantized. As a concluding chapter, we now summarize the contributions of this dissertation and discuss future directions.

6.1 Summary

In Chapter 2, we presented two studies on router's operations in the physical layer before considering power packetization in networks. In the first study, we investigated the reception of information tags at the receiving router under asynchronous conditions. By analyzing the asynchronous sampling at the receiving router, we clarified the effect of detection errors on the density of power packets. In the second study, we investigated the up-stream dispatching of power at a router with the density modulation of power packets. We analyzed it by the averaging method and numerically verified that it can be realized if energy stored in the router is kept at a constant level.

In Chapters 3, 4, and 5, we presented the packet-centric framework of energy transfer in networks. Power packet is a unit of electric power transferred by a pulse with an information tag. In Shannon's information theory, messages are represented by symbol sequences in a digitized manner. Referring to this formulation, we introduced symbol in power packetization as a minimum unit of power transferred by a tagged pulse. Then,

power packetization is a simultaneous representation of messages and energy with symbol sequences.

In Chapter 3, energy representation is considered with a set of symbol sequences, which represent energy as the total amount of energy of symbols. First, we clarified the condition for existence of energy representation. This shows the limit on accuracy with which all sufficiently large energy can be represented. Then, we theoretically proved an asymptotic property. This asymptotic property shows that, as the represented energy becomes infinite, the frequency of occurrences of a symbol in almost all sequences can be approximated by the probability determined from the energy of symbols. At last, this property was numerically verified in representation of finite energy. As theoretical limits of communication are given in information theory by asymptotic properties with the length of codewords increasing to infinity, this asymptotic property has a potential to provide design principles for representing given energy with symbol sequences in power packet dispatching networks.

In Chapter 4, we considered packetized power in networks for a finite duration. Symbol propagation matrix (SPM) was introduced as a representation of packetized power, in which symbols are transferred at links during unit times. Packetized power is described as network flow in a spatio-temporal structure. Then, we considered the problem of selecting a SPM in terms of transferability, that is, the possibility to represent given energies at sources and destinations for the finite duration. To select packetized power as a network flow problem, we weighted the supplied energy from the sources and the supplied energy to the destinations (V1), transferred energy at each link during each unit time (V2), change of stored energy in each router (V3). This problem was formulated as M-convex submodular flow problem, which is known as the generalization of the minimum cost flow problem and is solvable. At last, the formulation was discussed through examples, and the results show that power can be packetized and be controllable while preserving reasonable properties of power.

In Chapter 5, based on the formulation of the symbol propagation matrix, we considered the discrete dynamics of energy transfer by designing the operation of nodes. Here, unlike Chapter 4 in which power flow was globally optimized, symbols to be transmitted were determined by exchanging information between adjacent nodes. The network was designed to separately and individually manage the up-stream dispatching of required

power from destinations and the down-stream dispatching of supplied power from sources at the symbol level in a decentralized manner. The router's operation was designed to keep stored energy within a given capacity. It is numerically verified that supply and demand can be met in the designed network.

Finally, in Chapter 5, we took a glance at the corresponding continuous dynamics for future work. Power packet transfer can be considered as wave propagation by averaging in time. The numerical result implies that we could adjust the transferred energy by changing circuit impedance in the time domain as average.

6.2 Discussion and Future Work

Defining the power packet as a unit of electric power, we have established the packet-centric framework in which power is digitized and quantized. This framework is completely different from the circuit theory, in which power is handled in a continuous manner and is governed by Kirchhoff laws and Tellegen's theorem [6]. Instead of connecting multiple sources in parallel to a single bus, we addressed to design a novel electrical energy network, which processes power according to the number of power packets in a digitized manner. The author believes that this approach enables us to meet supply and demand among numerous sources, destinations, and storage units, and to save a significant amount of energy by utilizing potential energy sources (e.g. regenerative energy from all motors in a robot) whose energy would otherwise be dissipated as heat. It is a challenge to design the circulatory system of the machine based on power packetization and to integrate energy and information, being related to cybernetics which deals with control and communication in the animal and the machine [12].

In closing, we arrange some future directions and possible extensions of this packet-centric framework.

When we introduced symbols in the power packetization, we assumed that power is quantized, i.e. that the energy of each symbol is uniquely determined as a positive real number. As mentioned in Chapter 3, a load can be treated as resistive with PFC circuits, and hence power can be discussed in real numbers without lack of generality. On the other hand, in information theory, sampling theorem generally ensures that a continuous band-limited signal can be represented as a sum of orthogonal functions, and

hence as a discrete-time signal [1, 3]. In power packetization, it will be an interesting future research topic to find a condition for generally ensuring power quantization[1].

If energy stored in each router is not kept within a given capacity, we may not be able to control energy of symbols with density modulation of power packets between routers. For example, in Sect. 2.2, it was numerically shown that sufficient power can not be supplied from a router if energy stored in the router decreases. Then, it would be hard to quantize power. It is also an interesting future research topic to consider power packetization in transient states such as charging up of the router's storage. One approach to handle the transient states is to consider power packet transfer as wave propagation by averaging in time as in Sect. 5.5.

In this dissertation, the packet-centric framework was considered based on the conservation of energy. Especially in Chapters 4 and 5, it was assumed that all energy exchanges in each node are represented with symbols transferred through the adjacent links, and hence we obtained the equation of continuity. In practical systems, energy can be dissipated at links and in nodes, and symbols may not be able to have constant energy between nodes. These can become "noise" of power packetization, which causes a change of energy. On the other hand, information theory demonstrates that it is possible to send information at the channel capacity through a noisy channel with arbitrarily small error by proper encoding [1]. In power packetization, coping with "noise" is another future direction.

In networks, energy is transferred with time division multiplexing (TDM) at links and stored in the corresponding storage unit in routers. Thus, power flow is distinguished by using the information tag as an index. Considering multiple kinds of power flows, we can introduce a resource allocation problem of assigning a density of each flow at links[2].

[1]We should note the differences between energy transfer and information transfer. Especially, power is expressed with a product of a variable and its covariable, which are voltage difference and current in electrical network, force and velocity in mechanics, and so on. In addition, energy of a single symbol can be transferred in a variety of ways during a unit time, while the variety itself carries information.

[2]This problem can be formulated in the framework of the symbol propagation matrix introduced in Chapter 4.

Appendix A

Derivations in Chapter 2

A.1 Derivation of Eq. (2.2)

Eq. (2.2) is derived as

$$\begin{aligned} T_{\mathrm{c}}\langle\tau\rangle_{\overline{\mathrm{c}}} &= -\tau - T_{\mathrm{c}}\lfloor -\tau/T_{\mathrm{c}}\rfloor \\ &= T_{\mathrm{c}}\lceil\tau/T_{\mathrm{c}}\rceil - \tau \\ &= T_{\mathrm{c}}\min\{j \mid j \in \mathbb{Z} \wedge j \geq \tau/T_{\mathrm{c}}\} - \tau \\ &= \min\{T_{\mathrm{c}}j - \tau \mid j \in \mathbb{Z} \wedge T_{\mathrm{c}}j \geq \tau\}. \end{aligned} \tag{A.1}$$

A.2 Derivation of Eq. (2.3)

For $\tau \in \mathbb{R}$, we have

$$\begin{aligned} &|[\tau, T_{\mathrm{b}} + \tau) \cap T_{\mathrm{c}}\mathbb{Z}| \\ &\quad= |\{j \in \mathbb{Z} \mid 0 \leq T_{\mathrm{c}}j - \tau < T_{\mathrm{b}}\}| \\ &\quad= |\{j' \in \mathbb{Z} \mid j' \geq 0 \wedge T_{\mathrm{c}}\langle\tau\rangle_{\overline{\mathrm{c}}} + T_{\mathrm{c}}j' < T_{\mathrm{b}}\}| \\ &\quad= |\{j' \in \mathbb{Z} \mid 0 \leq j' < T_{\mathrm{b}}/T_{\mathrm{c}} - \langle\tau\rangle_{\overline{\mathrm{c}}}\}| \\ &\quad= \lceil T_{\mathrm{b}}/T_{\mathrm{c}} - \langle\tau\rangle_{\overline{\mathrm{c}}}\rceil \\ &\quad= \lfloor T_{\mathrm{b}}/T_{\mathrm{c}}\rfloor + \lceil\langle T_{\mathrm{b}}/T_{\mathrm{c}}\rangle - \langle\tau\rangle_{\overline{\mathrm{c}}}\rceil \end{aligned}$$

$$= \begin{cases} \lfloor T_{\rm b}/T_{\rm c} \rfloor & \langle \tau \rangle_{\overline{c}} \geq \langle T_{\rm b}/T_{\rm c} \rangle \,, \\ \lfloor T_{\rm b}/T_{\rm c} \rfloor + 1 & \langle \tau \rangle_{\overline{c}} < \langle T_{\rm b}/T_{\rm c} \rangle \,. \end{cases} \tag{A.2}$$

In addition, we have

$$\begin{aligned} & \langle T_{\rm b} k + \tau_i \rangle_{\overline{c}} \\ &= \langle -\tau_i/T_{\rm c} - k T_{\rm b}/T_{\rm c} \rangle \\ &= \langle -\tau_i/T_{\rm c} - k T_{\rm b}/T_{\rm c} - \lfloor -\tau_i/T_{\rm c} \rfloor - k \lfloor T_{\rm b}/T_{\rm c} \rfloor \rangle \\ &= \langle \langle \tau_i \rangle_{\overline{c}} - k \langle T_{\rm b}/T_{\rm c} \rangle \rangle \,. \end{aligned} \tag{A.3}$$

This completes the derivation of Eq. (2.3).

A.3 Derivation of Eqs. (2.4) and (2.6)

First, we derive Eq. (2.4). From Eq. (2.3), the set of symbols sampled $\lfloor T_{\rm b}/T_{\rm c} \rfloor$ times is represented as

$$\begin{aligned} & \{k \in \{0, 1, \cdots, K_i - 1\} \mid \langle \langle \tau_i \rangle_{\overline{c}} - k \langle T_{\rm b}/T_{\rm c} \rangle \rangle \geq \langle T_{\rm b}/T_{\rm c} \rangle \} \\ &= \{k \in \{0, \cdots, K_i - 1\} \mid \exists l \in \mathbb{Z} \text{ s.t.} \\ &\qquad \langle T_{\rm b}/T_{\rm c} \rangle - k + l \leq \langle \tau_i \rangle_{\overline{c}} - k \langle T_{\rm b}/T_{\rm c} \rangle < 1 - k + l \} \\ &= \{k \in \{0, \cdots, K_i - 1\} \mid \exists l \in \mathbb{Z} \text{ s.t. } \iota_l(\langle \tau_i \rangle_{\overline{c}}) = k \}. \end{aligned} \tag{A.4}$$

Because we have $\iota_{-1}(\phi) < 0 \leq \iota_0(\phi)$ and $\iota_{l+1}(\phi) \geq \iota_l(\phi) + 1$, this set is equal to the set in Eq. (2.4). This completes the derivation of Eq. (2.4).

Then, assuming $\langle T_{\rm b}/T_{\rm c} \rangle \neq 0$ holds, we derive Eq. (2.6). From Eq. (2.3), the set of symbols sampled $\lfloor T_{\rm b}/T_{\rm c} \rfloor + 1$ times is represented as

$$\begin{aligned} & \{k \in \{0, 1, \cdots, K_i - 1\} \mid \langle \langle \tau_i \rangle_{\overline{c}} - k \langle T_{\rm b}/T_{\rm c} \rangle \rangle < \langle T_{\rm b}/T_{\rm c} \rangle \} \\ &= \{k \in \{0, \cdots, K_i - 1\} \mid \exists l \in \mathbb{Z} \text{ s.t.} \\ &\qquad -l \leq \langle \tau_i \rangle_{\overline{c}} - k \langle T_{\rm b}/T_{\rm c} \rangle < -l + \langle T_{\rm b}/T_{\rm c} \rangle \} \\ &= \{k \in \{0, \cdots, K_i - 1\} \mid \exists l \in \mathbb{Z} \text{ s.t. } \kappa_l(\langle \tau_i \rangle_{\overline{c}}) = k \}. \end{aligned} \tag{A.5}$$

Because we have $\kappa_{-1}(\phi) < 0 \leq \kappa_0(\phi)$ and $\kappa_{l+1}(\phi) \geq \kappa_l(\phi) + 1$, this set is equal to the set in Eq. (2.6). This completes the derivation of Eq. (2.6).

Appendix B

Algorithms for M-convex Submodular Flow Problems

B.1 Cycle-canceling Algorithm

In this section, we provide cycle-canceling algorithm [62] for the M-convex submodular flow problem presented in Eqs. (4.9)–(4.12). For a feasible flow $u : \overline{T} \times A \to \mathbb{Z}$, we define an auxiliary network as follows. Let $G_u = (\overline{T} \times \tilde{V}, A_u)$ be a directed graph with vertex set $\overline{T} \times \tilde{V}$ and arc set $A_u = A_u^* \cup B_u^* \cup C_u$ consisting of three disjoint parts:

$$A_u^* = \{(\bar{t}, a) \mid (\bar{t}, a) \in \overline{T} \times A, u(\bar{t}, a) + 1 \leq \hat{c}(\bar{t}, a)\}, \tag{B.1}$$

$$B_u^* = \{(\bar{t}, a)_{\mathrm{r}} \mid (\bar{t}, a) \in \overline{T} \times A, u(\bar{t}, a) - 1 \geq \check{c}(\bar{t}, a)\}$$
$$((\bar{t}, a)_{\mathrm{r}} : \text{reorientation of } (\bar{t}, a)), \tag{B.2}$$

$$C_u = \{(\mu, \nu) \mid \mu, \nu \in \overline{T} \times \tilde{V}, \mu \neq \nu, \partial u - (\chi_\mu - \chi_\nu) \in \operatorname{dom} f\}. \tag{B.3}$$

We define a function $l_u : A_u \to \mathbb{R}$, representing arc lengths, by

$$l_u(b) = \begin{cases} f_{(\bar{t},a)}(u(\bar{t}, a) + 1) - f_{(\bar{t},a)}(u(\bar{t}, a)) & (b = (\bar{t}, a) \in A_u^*), \\ f_{(\bar{t},a)}(u(\bar{t}, a) - 1) - f_{(\bar{t},a)}(u(\bar{t}, a)) & (b = (\bar{t}, a)_{\mathrm{r}} \in B_u^*), \\ f(\partial u - \chi_\mu + \chi_\nu) - f(\partial u) & (b = (\mu, \nu) \in C_u). \end{cases} \tag{B.4}$$

Here, χ_μ denotes the μ-th unit vector. We refer to (G_u, l_u) as the auxiliary network. We call a directed cycle of negative length a negative cycle. In Sect. 4.3, we use the following algorithm to solve M-convex submodular flow problem presented in Eqs. (4.9)–(4.12):

1° Find a feasible integer flow u.

2° If (G_u, l_u) has no negative cycle, then stop (u is an optimal flow).

3° Let Q be a negative cycle with the smallest number of arcs[1].

4° Modify u as

$$u(\bar{t}, a) \leftarrow \begin{cases} u(\bar{t}, a) + 1 & ((\bar{t}, a) \in Q \cup A_u^*), \\ u(\bar{t}, a) - 1 & ((\bar{t}, a)_{\mathrm{r}} \in Q \cup B_u^*), \\ u(\bar{t}, a) & (\text{otherwise}), \end{cases} \tag{B.5}$$

and go to 2°.

B.2 Negative Cycle with the Smallest Number of Arcs

We use a variant of the standard shortest-path algorithm [64] to find a negative cycle with the smallest number of arcs of a network (G, l), where $G = (V, A)$ is a directed graph and $l : A \to \mathbb{R}$ represents arc length. It is enough to consider a simple graph[2] $G' = (V, A')$, where $A' = \{(u, v) \mid \exists a \in A \text{ s.t. } \partial^+ a = u, \partial^- a = v\}$. The arc length of G' is denoted as $l : V \times V \to \mathbb{R}$ and is defined by

$$l(u, v) = \begin{cases} \min\{l(a) \mid \partial^+ a = u, \partial^- a = v\} & (\exists a \in A \text{ s.t. } \partial^+ a = u, \partial^- a = v), \\ 0 & (u = v), \\ \infty & (\text{otherwise}). \end{cases} \tag{B.6}$$

Then, the algorithm is described as following:

[1] A negative cycle having the smallest number of arcs can be found by a variant of the standard shortest-path algorithm explained in Appendix B.2.

[2] A graph without parallel arcs and selfloops.

1° For $u, v \in V$, put $p_{uv}^{(1)} \leftarrow l(u,v)$, $q_{uv}^{(1)} \leftarrow u$, $h \leftarrow 1$.

2° While $p_{vv}^{(h)} \geq 0$ for all $v \in V$ and $h < |V|$, repeat (I) and (II):

I. For $u, v \in V$, put

$$p_{uv}^{(h+1)} \leftarrow \min_{w \in V}\{p_{uw}^{(h)} + p_{wv}^{(1)}\}, \tag{B.7}$$

and

$$q_{uv}^{(h+1)} \leftarrow \arg\min_{w \in V}\{p_{uw}^{(h)} + p_{wv}^{(1)}\}. \tag{B.8}$$

II. Put $h \leftarrow h + 1$.

In the algorithm, $p_{uv}^{(h)}$ is equal to the length of a shortest path from u to v with at most h arcs. If $p_{uv}^{(h-1)} \neq p_{uv}^{(h)}$ for some $u, v \in V$ and $h \in \{2, 3, \cdots, |V|\}$, there exists a sequence of vertices $(v_j)_{j=0}^{h}$ such that $v_0 = u$, $v_h = v$, $v_{j-1} = q_{uv_j}^{(j)}$ for all $j \in \{1, 2, \cdots, h\}$, and the path $(v_0, \cdots, v_{h-1}, v_h) = (u, \cdots, q_{uq_{uv}^{(h-1)}}^{(h-2)}, q_{uv}^{(h-1)}, v)$ is the shortest path from u to v with at most h arcs. Therefore, if $p_{vv}^{(h)} < 0$ for some $v \in V$ at some $1 < h \leq |V|$ in the algorithm, the path $(v, \cdots, q_{vq_{vv}}^{(h-2)}, q_{vv}^{(h-1)}, v)$ is the negative cycle with the smallest number of arcs.

Bibliography

[1] C. E. Shannon, "A mathematical theory of communication," *The Bell System Technical Journal*, vol. 27, pp. 379–423 and 623–656, July and October 1948.

[2] J. Massey, "Information theory: the copernican system of communications," *IEEE Communications Magazine*, vol. 22, no. 12, pp. 26–28, December 1984.

[3] C. E. Shannon, "Communication in the presence of noise," *Proceedings of the IRE*, vol. 37, no. 1, pp. 10–21, January 1949.

[4] L. Kleinrock, "An early history of the Internet [history of communications]," *IEEE Communications Magazine*, vol. 48, no. 8, pp. 26–36, August 2010.

[5] A. S. Tanenbaum and D. J. Wetherall, *Computer Networks*, 5th ed. USA: Prentice Hall, 2011, chapter 1, 5.

[6] C. A. Desoer and E. S. Kuh, *Basic Circuit Theory*. USA: McGraw-Hill, 1991, chapter 9.

[7] G. Oster, A. Perelson, and A. Katchalsky, "Network thermodynamics," *Nature*, vol. 234, pp. 393–399, December 1971.

[8] I. Csiszár and J. Körner, *Information Theory: Coding Theorems for Discrete Memoryless Systems*, 2nd ed. UK: Cambridge University Press, 2011, chapter 2, 4.

[9] L. R. Varshney, "Transporting information and energy simultaneously," in *Proc. 2008 IEEE International Symposium on Information Theory*, July 2008, pp. 1612–1616.

[10] P. Grover and A. Sahai, "Shannon meets Tesla: wireless information and power transfer," in *Proc. 2010 IEEE International Symposium on Information Theory*, June 2010, pp. 2363–2367.

[11] R. Zhang and C. K. Ho, "MIMO broadcasting for simultaneous wireless information and power transfer," *IEEE Transactions on Wireless Communications*, vol. 12, no. 5, pp. 1989–2001, May 2013.

[12] N. Wiener, *Cybernetics: Or Control and Communication in the Animal and the Machine*. USA: John Wiley & Sons, 1948.

[13] A. L. Fradkov, *Cybernetical Physics: From Control of Chaos to Quantum Control*, ser. Understanding Complex Systems. Berlin: Springer, 2007, pp. 5–10.

[14] T. Takuno, M. Koyama, and T. Hikihara, "In-home power distribution systems by circuit switching and power packet dispatching," in *Proc. 2010 1st IEEE International Conference on Smart Grid Communications*, Gaithersburg, MD, USA, October 2010, pp. 427–430.

[15] T. Takuno, "High frequency switching of SiC transistors and its application to in-home power distribution," *Ph.D. dissertation, Department of Electrical Engineering, Kyoto University*, 2012.

[16] S. F. Tie and C. W. Tan, "A review of energy sources and energy management system in electric vehicles," *Renewable and Sustainable Energy Reviews*, vol. 20, pp. 82–102, 2013.

[17] P. G. Pereirinha and J. P. Trovão, "Multiple energy sources hybridization: the future of electric vehicles?" in *New Generation of Electric Vehicles*, Z. Stevic, Ed. InTech Press, 2012, chapter 8.

[18] M. Sinnett, "787 no-bleed systems: saving fuel and enhancing operational efficiencies," *Boeing Aero Magazine*, vol. 4, pp. 6–11, 2007.

[19] B. Sarlioglu and C. T. Morris, "More electric aircraft: review, challenges, and opportunities for commercial transport aircraft," *IEEE Transactions on Transportation Electrification*, vol. 1, no. 1, pp. 54–64, June 2015.

[20] S. Seok, A. Wang, M. Y. M. Chuah, D. J. Hyun, J. Lee, D. M. Otten, J. H. Lang, and S. Kim, "Design principles for energy-efficient legged locomotion and implementation on the MIT Cheetah Robot," *IEEE/ASME Transactions on Mechatronics*, vol. 20, no. 3, pp. 1117–1129, June 2015.

[21] A. J. Wood, B. F. Wollenberg, and G. B. Sheblé, *Power Generation, Operation, and Control*. USA: John Wiley & Sons, 2013, chapter 1.

[22] H. Farhangi, "The path of the smart grid," *IEEE Power and Energy Magazine*, vol. 8, no. 1, pp. 18–28, January 2010.

[23] M. Inoue, T. Higuma, Y. Ito, N. Kushiro, and H. Kubota, "Network architecture for home energy management system," *IEEE Transactions on Consumer Electronics*, vol. 49, no. 3, pp. 606–613, August 2003.

[24] N. Kushiro, S. Suzuki, M. Nakata, H. Takahara, and M. Inoue, "Integrated residential gateway controller for home energy management system," *IEEE Transactions on Consumer Electronics*, vol. 49, no. 3, pp. 629–636, August 2003.

[25] K. Sakai and Y. Okabe, "Quality-aware energy routing toward on-demand home energy networking: (position paper)," in *Proc. 2011 IEEE Consumer Communications and Networking Conference*, Las Vegas, NV, USA, January 2011, pp. 1041–1044.

[26] T. Maeda, H. Nakano, N. Morimoto, K. Sakai, and Y. Okabe, "Design and implementation of an on-demand home power management system based on a hierarchical protocol," in *Proc. 2015 IEEE 39th Annual Computer Software and Applications Conference*, vol. 3, July 2015, pp. 188–193.

[27] T. Yoshihisa, N. Fujita, and M. Tsukamoto, "A rule generation method for electrical appliances management systems with home EoD," in *Proc. the 1st IEEE Global Conference on Consumer Electronics 2012*, Tokyo, Japan, October 2012, pp. 248–250.

[28] J. Toyoda and H. Saitoh, "Proposal of an open-electric-energy-network (OEEN) to realize cooperative operations of IOU and IPP," in *Proc. 1998 International*

Conference on Energy Management and Power Delivery, vol. 1, Singapore, March 1998, pp. 218–222.

[29] J. Inoue and Y. Fujii, "Proposal of an innovative electric power distribution system based on packet power transactions," *IEEJ Transactions on Power and Energy*, vol. 131, no. 2, pp. 143–150, 2011, (in Japanese).

[30] M. M. He, E. M. Reutzel, X. Jiang, R. H. Katz, S. R. Sanders, D. E. Culler, and K. Lutz, "An architecture for local energy generation, distribution, and sharing," in *Proc. 2008 IEEE Energy 2030 Conference*, November 2008, pp. 1–6.

[31] E. Gelenbe, "Energy packet networks: adaptive energy management for the cloud," in *Proc. 2nd International Workshop on Cloud Computing Platforms*, Bern, Switzerland, April 2012.

[32] R. Rojas-Cessa, Y. Xu, and H. Grebel, "Management of a smart grid with controlled-delivery of discrete power levels," in *Proc. 2013 IEEE International Conference on Smart Grid Communications (SmartGridComm)*, October 2013, pp. 1–6.

[33] B. P. Stalling, T. Clemmer, H. A. Mantooth, R. Motte, H. Xu, T. Price, and R. Dougal, "Design and evaluation of a universal power router for residential applications," in *Proc. 2012 IEEE Energy Conversion Congress and Exposition (ECCE)*, September 2012, pp. 587–594.

[34] T. Funaki, J. C. Balda, J. Junghans, A. S. Kashyap, H. A. Mantooth, F. Barlow, T. Kimoto, and T. Hikihara, "Power conversion with SiC devices at extremely high ambient temperatures," *IEEE Transactions on Power Electronics*, vol. 22, no. 4, pp. 1321–1329, July 2007.

[35] J. Millán, P. Godignon, X. Perpiñà, A. Pérez-Tomás, and J. Rebollo, "A survey of wide bandgap power semiconductor devices," *IEEE Transactions on Power Electronics*, vol. 29, no. 5, pp. 2155–2163, May 2014.

[36] T. Takuno, T. Hikihara, T. Tsuno, and S. Hatsukawa, "HF gate drive circuit for a normally-on SiC JFET with inherent safety," in *Proc. 13th European Conference on Power Electronics and Applications*, Barcelona, Spain, September 2009, pp. 1–4.

[37] K. Nagaoka, K. Chikamatsu, A. Yamaguchi, K. Nakahara, and T. Hikihara, "High-speed gate drive circuit for SiC MOSFET by GaN HEMT," *IEICE Electronics Express*, vol. 12, no. 11, pp. 1–8, May 2015.

[38] T. Takuno, Y. Kitamori, R. Takahashi, and T. Hikihara, "AC power routing system in home based on demand and supply utilizing distributed power sources," *Energies*, vol. 4, no. 5, pp. 717–726, 2011.

[39] R. Takahashi, Y. Kitamori, and T. Hikihara, "AC power local network with multiple power routers," *Energies*, vol. 6, no. 12, pp. 6293–6303, 2013.

[40] A. Kordonis, R. Takahashi, D. Nishihara, and T. Hikihara, "The three-phase power router and its operation with matrix converter toward smart-grid applications," *Energies*, vol. 8, no. 4, pp. 3034–3046, 2015.

[41] R. Takahashi, T. Takuno, and T. Hikihara, "Estimation of power packet transfer properties on indoor power line channel," *Energies*, vol. 5, no. 7, pp. 2141–2149, 2012.

[42] R. Takahashi, K. Tashiro, and T. Hikihara, "Router for power packet distribution network: design and experimental verification," *IEEE Transactions on Smart Grid*, vol. 6, no. 2, pp. 618–626, March 2015.

[43] Y. Zhou, R. Takahashi, N. Fujii, and T. Hikihara, "Power packet dispatching with second-order clock synchronization," *International Journal of Circuit Theory and Applications*, vol. 44, no. 3, pp. 729–743, March 2016.

[44] Y. Zhou, "Power packet dispatching based on synchronization with features on safety," *Ph.D. dissertation, Department of Electrical Engineering, Kyoto University*, 2015.

[45] N. Fujii, R. Takahashi, and T. Hikihara, "Networked power packet dispatching system for multi-path routing," in *Proc. 2014 IEEE/SICE International Symposium on System Integration*, December 2014, pp. 357–362.

[46] R. Takahashi, S. Azuma, and T. Hikihara, "Power regulation with predictive dynamic quantizer in power packet dispatching system," *IEEE Transactions on Industrial Electronics*, vol. 63, no. 12, pp. 7653–7661, December 2016.

[47] S. Mochiyama, R. Takahashi, and T. Hikihara, "Trajectory control of manipulator fed by power packets," *International Journal of Circuit Theory and Applications*, 2016.

[48] J. Bialek, "Tracing the flow of electricity," *IEE Proceedings - Generation, Transmission and Distribution*, vol. 143, no. 4, pp. 313–320, July 1996.

[49] S. W. Golomb, J. R. Davey, I. S. Reed, H. L. V. Trees, and J. J. Stiffler, "Synchronization," *IEEE Transactions on Communications Systems*, vol. 11, no. 4, pp. 481–491, December 1963.

[50] H. Mercier, V. K. Bhargava, and V. Tarokh, "A survey of error-correcting codes for channels with symbol synchronization errors," *IEEE Communications Surveys & Tutorials*, vol. 12, no. 1, pp. 87–96, First Quarter 2010.

[51] E. Zehnder, *Lectures on Dynamical Systems: Hamiltonian Vector Fields and Symplectic Capacities*, ser. EMS Textbooks in Mathematics. European Mathematical Society, 2010, chapter 1, pp. 5–14.

[52] J. G. Kassakian, M. F. Schlecht, and G. C. Verghese, *Principles of Power Electronics*. USA: Addison-Wesley, 1991, pp. 261–274.

[53] S. Savari, "A probabilistic approach to some asymptotics in noiseless communication," *IEEE Transactions on Information Theory*, vol. 46, no. 4, pp. 1246–1262, July 2000.

[54] M. Smorodinsky, "The capacity of a general noiseless channel and its connection with Hausdorff dimension," *Proceedings of the American Mathematical Society*, vol. 19, no. 6, pp. 1247–1254, December 1968.

[55] I. Csiszár, "Simple proofs of some theorems on noiseless channels," *Information and Control*, vol. 14, no. 3, pp. 285–298, March 1969.

[56] T. Uyematsu, *Gendai Shannon Riron*. Japan: Baifukan, 1998, chapter 2, (in Japanese).

[57] G. Dueck and J. Körner, "Reliability function of a discrete memoryless channel at rates above capacity," *IEEE Transactions on Information Theory*, vol. 25, no. 1, pp. 82–85, January 1979.

[58] R. M. Krause, "Channels which transmit letters of unequal duration," *Information and Control*, vol. 5, no. 1, pp. 13–24, March 1962.

[59] T. Han and K. Kobayashi, "Exponential-type error probabilities for multiterminal hypothesis testing," *IEEE Transactions on Information Theory*, vol. 35, no. 1, pp. 2–14, January 1989.

[60] F. Perbet, A. Maki, and B. Stenger, "Correlated probabilistic trajectories for pedestrian motion detection," in *Proc. 2009 IEEE 12th International Conference on Computer Vision*, September 2009, pp. 1647–1654.

[61] A. Maki, F. Perbet, B. Stenger, and R. Cipolla, "Detecting bipedal motion from correlated probabilistic trajectories," *Pattern Recognition Letters*, vol. 34, no. 15, pp. 1808–1818, 2013.

[62] K. Murota, *Discrete Convex Analysis*, ser. SIAM Monographs on Discrete Mathematics and Applications. USA: Society for Industrial and Applied Mathematics, 2003.

[63] M. Iri, *Network Flow, Transportation and Scheduling: Theory and Algorithms*, ser. Mathematics in Science and Engineering. USA: Academic Press, 1969, vol. 57, pp. 28–37.

[64] M. Iri, S. Fujishige, and T. Oyama, *Graphs, Networks, and Matroids*. Japan: Sangyo-Tosho, 1986, (in Japanese).

[65] H. Yuasa, "Network thermodynamics: the theory for an integration of physics and system engineering," *Systems, control and information*, vol. 43, no. 9, pp. 473–479, September 1999, (in Japanese).

[66] M. Kitano, *Fundamentals of Quantum Mechanics*. Japan: Kyoritsu Shuppan, 2010, chapter 10, (in Japanese).

[67] T. Nakanishi, "Coupled-resonator-based metamaterials emulating quantum systems," *Ph.D. dissertation, Department of Electronic Science and Engineering, Kyoto University*, 2016.

[68] http://ngspice.sourceforge.net/.

List of Publications

Journal Articles

1. S. Nawata, R. Takahashi, and T. Hikihara, "An asymptotic property of energy representation with power packet," *IEICE Transactions on Fundamentals of Electronics, Communications and Computer Sciences*, vol.J97-A, no.9, pp.584–592, September 2014, (in Japanese).

2. S. Nawata, R. Takahashi, and T. Hikihara, "Up-stream dispatching of power by density of power packet", *IEICE Transactions on Fundamentals of Electronics, Communications and Computer Sciences*, vol.E99-A, no.12, pp.2581–2584, December 2016.

3. S. Nawata, R. Takahashi, and T. Hikihara, "Design possibility for covert power packet transfer using asynchronous sampling," submitted for publication.

4. S. Nawata, A. Maki, and T. Hikihara, "Power packet transferability via probabilistic symbol propagation," in preparation.

5. S. Nawata, A. Maki, and T. Hikihara, "Up-stream dispatching and down-stream dispatching in electrical energy networks based on power packetization," in preparation.

International Conference Proceedings

6. S. Nawata, N. Fujii, Y. Zhou, R. Takahashi, and T. Hikihara, "A theoretical examination of an unexpected transfer of power packets by synchronization failure",

in *Proc. 2014 International Symposium on Nonlinear Theory and its Applications (NOLTA2014)*, Luzern, Switzerland, September 14–18, 2014.

7. T. Hikihara, S. Nawata, and R. Takahashi, "Power packet dispatching and dynamics in network", in *Proc. 24th International Congress of Theoretical and Applied Mechanics (ICTAM2016)*, Montreal Canada, August 21–26, 2016.

Domestic Conference Proceedings

8. T. Hikihara, S. Nawata, and R. Takahashi, "Mathematical model for circuit connection in power packet transmission system," in *Proc. 2012 IEICE General Conference, Okayama*, March 20–23, 2012, (in Japanese).

9. T. Hikihara, S. Nawata, and R. Takahashi, "Dynamical model of power packet transmission system related with circuit connection," in *Proc. 56th Annual Conference of the Institute of Systems, Control and Information Engineers*, Kyoto, May 21–23, 2012, (in Japanese).

10. S. Nawata, R. Takahashi, and T. Hikihara, "A study on energy and entropy of power packet," in *Proc. 57th Annual Conference of the Institute of Systems, Control and Information Engineers*, Hyogo, May 15–17, 2013, (in Japanese).

11. S. Nawata, R. Takahashi, and T. Hikihara, "A study on convexity of energy and entropy relationship in power packet transmission," in *Proc. 26th Workshop on Circuits and Systems*, Hyogo, July 29–30, 2013, (in Japanese).

12. S. Nawata, R. Takahashi, and T. Hikihara, "A study on energy representation with power packet," *The 10th Meeting of the Union of Research Activity Groups, Japan SIAM*, Kyoto, March 19–20, 2014, (in Japanese).

13. S. Nawata, N. Fujii, Y. Zhou, R. Takahashi, and T. Hikihara, "A study on an unexpected transfer of power packets by synchronization failure," in *Proc. 10th Technical Meeting of IEICE Complex Communication Sciences (CCS)*, Osaka, May 19–20, 2014, (in Japanese).

14. S. Nawata, N. Fujii, T. Kajiyama, Y. Zhou, R. Takahashi, and T. Hikihara, "A theoretical study on synchronization of power packet transmission," in *Proc. 58th Annual Conference of the Institute of Systems, Control and Information Engineers*, Kyoto, May 21–23, 2014, (in Japanese).

15. S. Nawata, R. Takahashi, and T. Hikihara, "A study on existence condition of circuit connections for power packet transmission," in *Proc. 13th Technical Meeting of IEICE Complex Communication Sciences (CCS)*, Tokyo, March 5–6, 2015, (in Japanese).

16. S. Nawata, R. Takahashi, and T. Hikihara, "A study on up-stream dispatching of power with power packet," in *Proc. 2016 IEICE General Conference*, Fukuoka, March 15–18, 2016, (in Japanese).

17. S. Nawata, M. Tanimoto, M. Matsushima, A. Maki, and T. Hikihara, "A study on dynamics of energy transfer with power packet: discrete dynamics and continuous dynamics," *IEICE Technical Report*, vol.116, no.285, CCS2016-31, pp.9–12, Kyoto, November 4–5, 2016, (in Japanese).